Atmosphere-Ice-Ocean Boundary Layer Processes and Their **Role in Polar Change**

Theoretical Overview

Miles McPhee
McPhee Research

25 Jun 2012

Atmosphere-Ice-Ocean Boundary Layer Processes
and Their **Role in Polar Change**

Theoretical Overview

Miles McPhee
McPhee Research

25 Jun 2012

1. The changing age (thickness) of sea ice is significantly altering drag characteristics and mobility.

Atmosphere-Ice-Ocean Boundary Layer Processes
and Their **Role in Polar Change**

Theoretical Overview

Miles McPhee

McPhee Research

25 Jun 2012

1. The changing age (thickness) of sea ice is significantly altering drag characteristics and mobility.

2. Lower summer ice concentrations and increased insolation are also affecting mobility, with possible positive feedback.

Atmosphere-Ice-Ocean Boundary Layer Processes
and Their **Role in Polar Change**

Theoretical Overview

Miles McPhee
McPhee Research

25 Jun 2012

1. The changing age (thickness) of sea ice is significantly altering drag characteristics and mobility.

2. Lower summer ice concentrations and increased insolation are also affecting mobility, with possible positive feedback.

3. Increased stratification in the western Arctic is modifying exchanges between the ice/IOBL system and the deeper ocean.

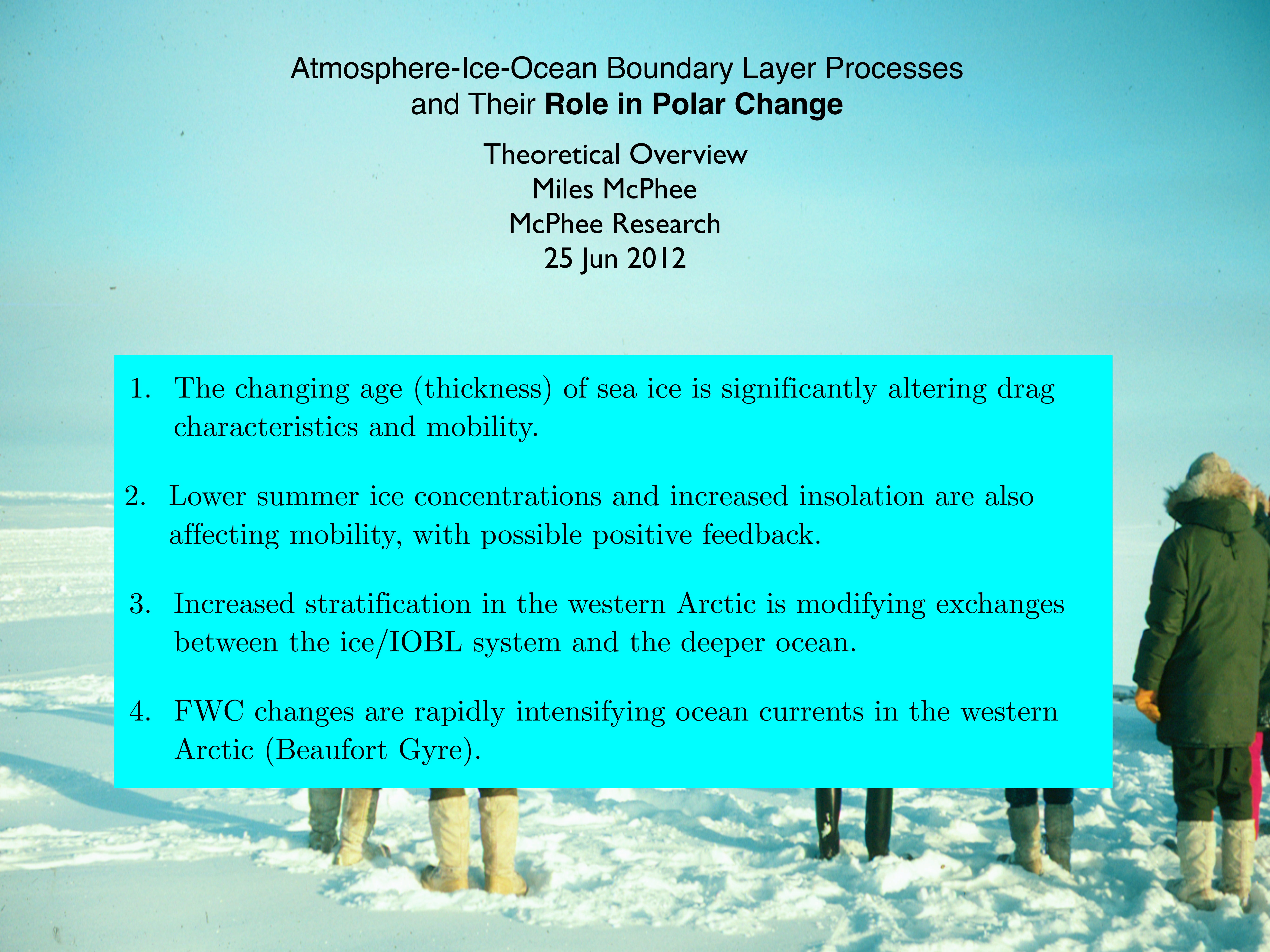

Atmosphere-Ice-Ocean Boundary Layer Processes and Their **Role in Polar Change**

Theoretical Overview
Miles McPhee
McPhee Research
25 Jun 2012

1. The changing age (thickness) of sea ice is significantly altering drag characteristics and mobility.

2. Lower summer ice concentrations and increased insolation are also affecting mobility, with possible positive feedback.

3. Increased stratification in the western Arctic is modifying exchanges between the ice/IOBL system and the deeper ocean.

4. FWC changes are rapidly intensifying ocean currents in the western Arctic (Beaufort Gyre).

Atmosphere-Ice-Ocean Boundary Layer Processes and Their **Role in Polar Change**

Theoretical Overview

Miles McPhee
McPhee Research

25 Jun 2012

1. The changing age (thickness) of sea ice is significantly altering drag characteristics and mobility.

2. Lower summer ice concentrations and increased insolation are also affecting mobility, with possible positive feedback.

3. Increased stratification in the western Arctic is modifying exchanges between the ice/IOBL system and the deeper ocean.

4. FWC changes are rapidly intensifying ocean currents in the western Arctic (Beaufort Gyre).

References: McPhee, 2008, Air-Ice-Ocean Interaction, Springer, ISBN 978-0-387-78334-5 (**AIO**);
McPhee, 2012, Cold Reg. Sci. Tech., 76-77 (Max Coon Issue), 24-36/

$$\frac{\partial \boldsymbol{u}}{\partial t} + \boldsymbol{u} \cdot \nabla \boldsymbol{u} + f\boldsymbol{k} \times \boldsymbol{u} = -\nabla p / \boldsymbol{\rho} - g \frac{\boldsymbol{\rho}'}{\boldsymbol{\rho}} \boldsymbol{k} + \nabla \cdot \underset{\sim}{\boldsymbol{\tau}}$$

$\boldsymbol{\tau}_{ij} = -\left\langle u_i u_j \right\rangle$ is the kinematic Reynolds stress

$$\frac{\partial \boldsymbol{u}}{\partial t} + \boldsymbol{u}\cdot\nabla\boldsymbol{u} + f\boldsymbol{k}\times\boldsymbol{u} = -\nabla p/\boldsymbol{\rho} - g\frac{\boldsymbol{\rho}'}{\boldsymbol{\rho}}\boldsymbol{k} + \nabla\cdot\underset{\sim}{\boldsymbol{\tau}}$$

$\boldsymbol{\tau}_{ij} = -\langle u_i u_j \rangle$ is the kinematic Reynolds stress

Consider velocity relative to the geostrophic velocity:

$$f\boldsymbol{k}\times\boldsymbol{u}_g \equiv -\nabla p/\boldsymbol{\rho} = -g\nabla\boldsymbol{\eta}$$

The steady, horizontally homogeneous boundary layer eqn is:

$$if\hat{u} = \frac{\partial\hat{\boldsymbol{\tau}}}{\partial z}; \qquad \hat{\boldsymbol{\tau}} = -\langle u'w'\rangle - i\langle v'w'\rangle$$

Ekman, 1905

Reynolds stress proportional to velocity gradient: $\hat{\tau} = K\,\partial\hat{u}/\partial z = K\hat{u}_z$

$if\hat{u} = K\hat{u}_{zz};$ bc's: $\hat{u}(z \to -\infty) = 0;$ $\hat{\tau}_0 = K\hat{u}_z(0)$

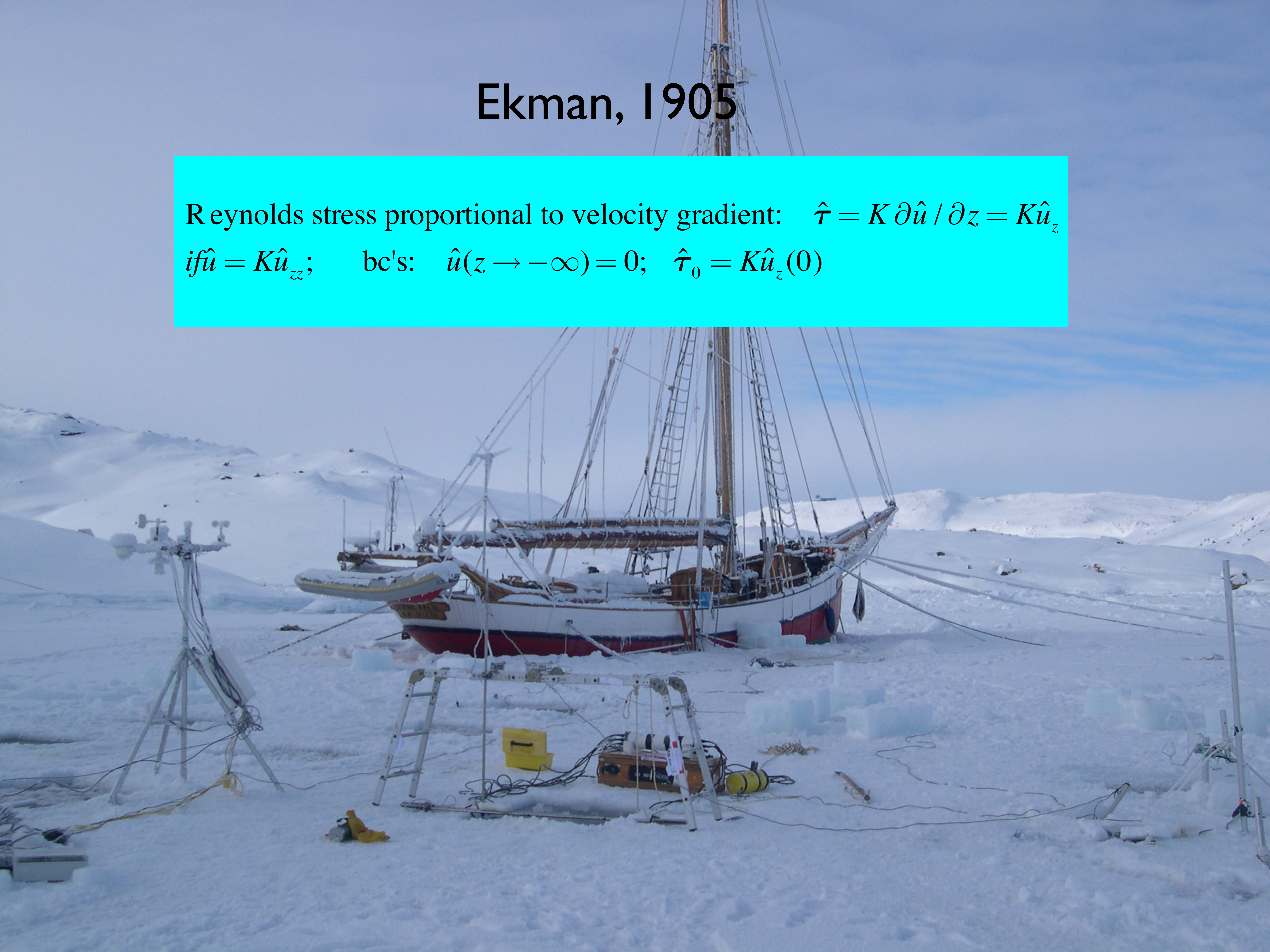

Ekman, 1905

Reynolds stress proportional to velocity gradient: $\hat{\boldsymbol{\tau}} = K\,\partial\hat{u}\,/\,\partial z = K\hat{u}_z$

$if\hat{u} = K\hat{u}_{zz}$; bc's: $\hat{u}(z \to -\infty) = 0$; $\hat{\boldsymbol{\tau}}_0 = K\hat{u}_z(0)$

Solution: $\hat{u}(z) = \left(\frac{-i}{fK}\right)^{1/2} \hat{\boldsymbol{\tau}}_0 e^{\;f/2K}$

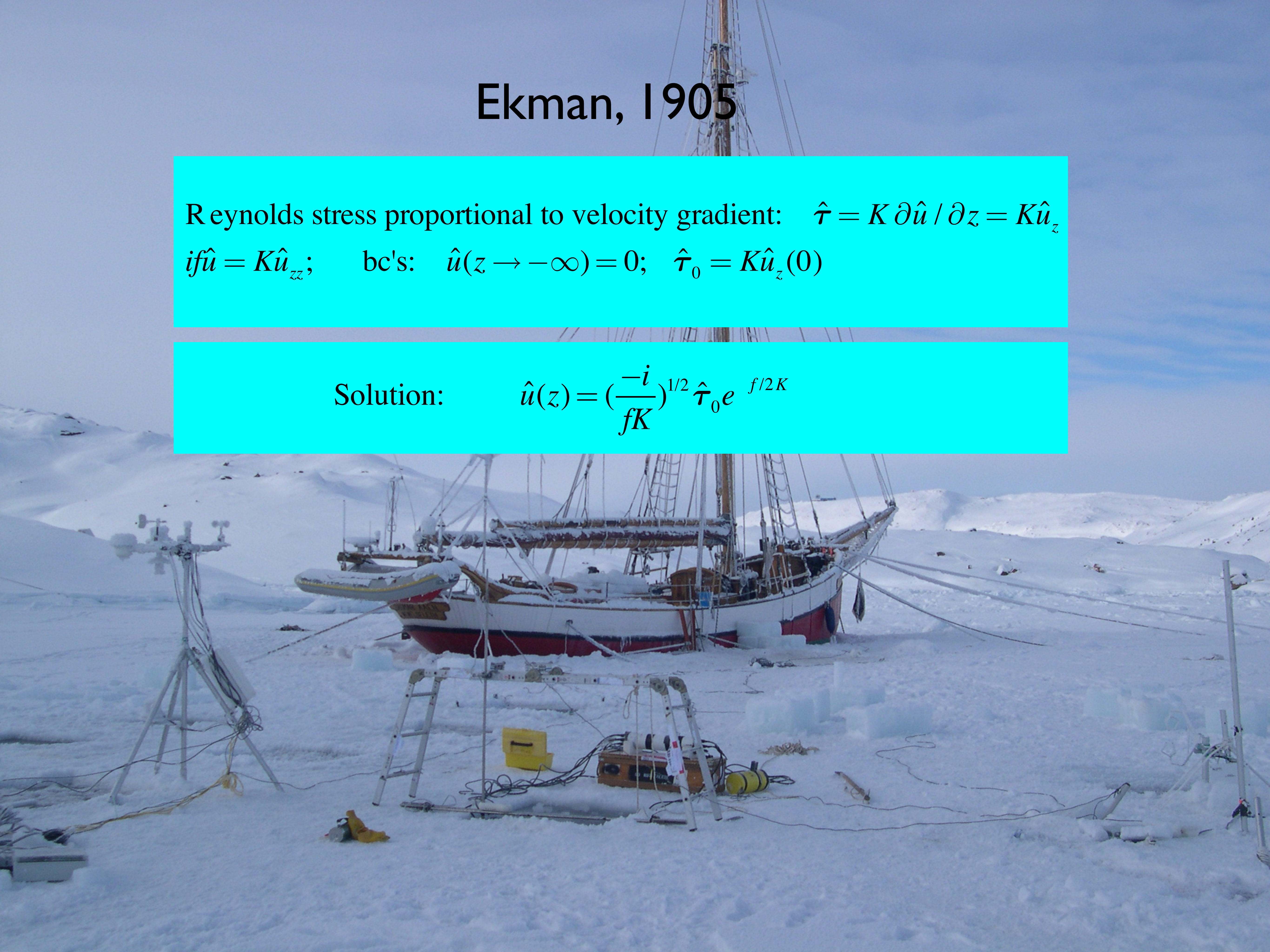

Ekman, 1905

Reynolds stress proportional to velocity gradient: $\hat{\tau} = K\,\partial\hat{u}/\partial z = K\hat{u}_z$

$if\hat{u} = K\hat{u}_{zz}$; bc's: $\hat{u}(z \to -\infty) = 0$; $\hat{\tau}_0 = K\hat{u}_z(0)$

Solution: $\hat{u}(z) = (\frac{-i}{fK})^{1/2}\hat{\tau}_0 e^{\;f/2K}$

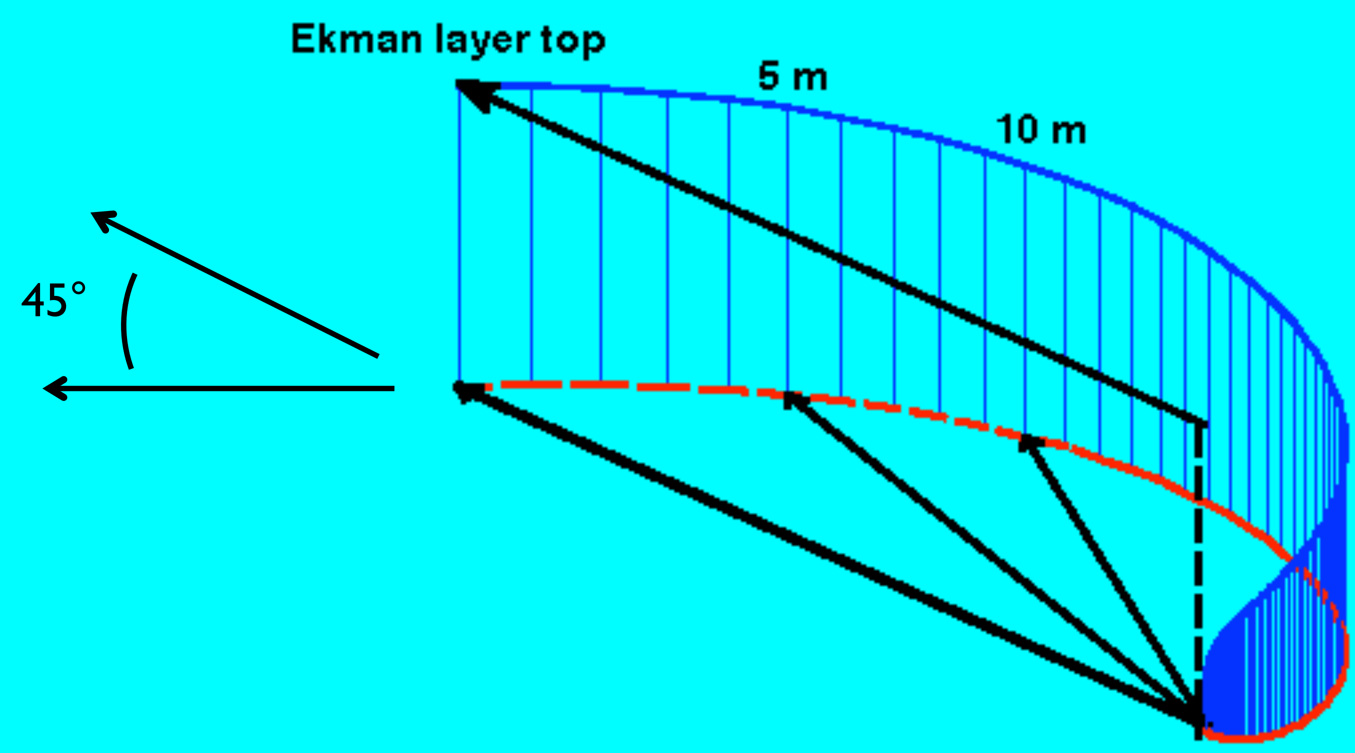

Yes Virginia, there ARE Ekman spirals

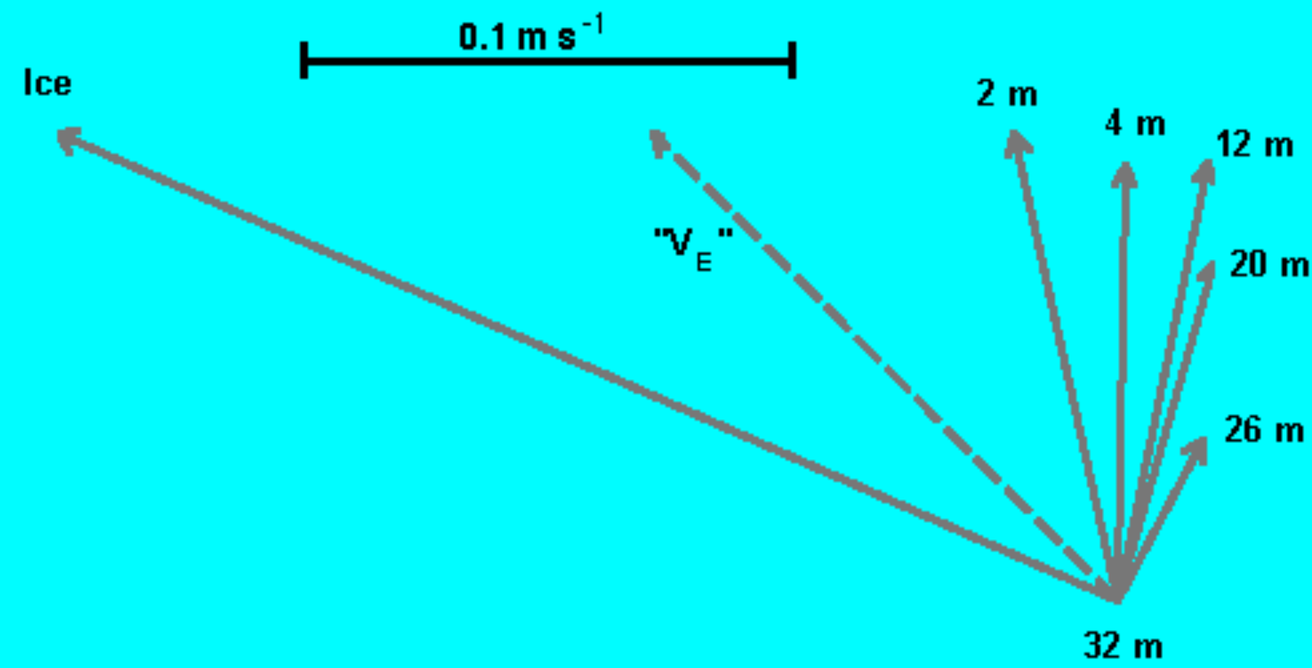

Currents relative to 32 m averaged for 5 h on 12 Apr 1972 during the AIDJEX Pilot

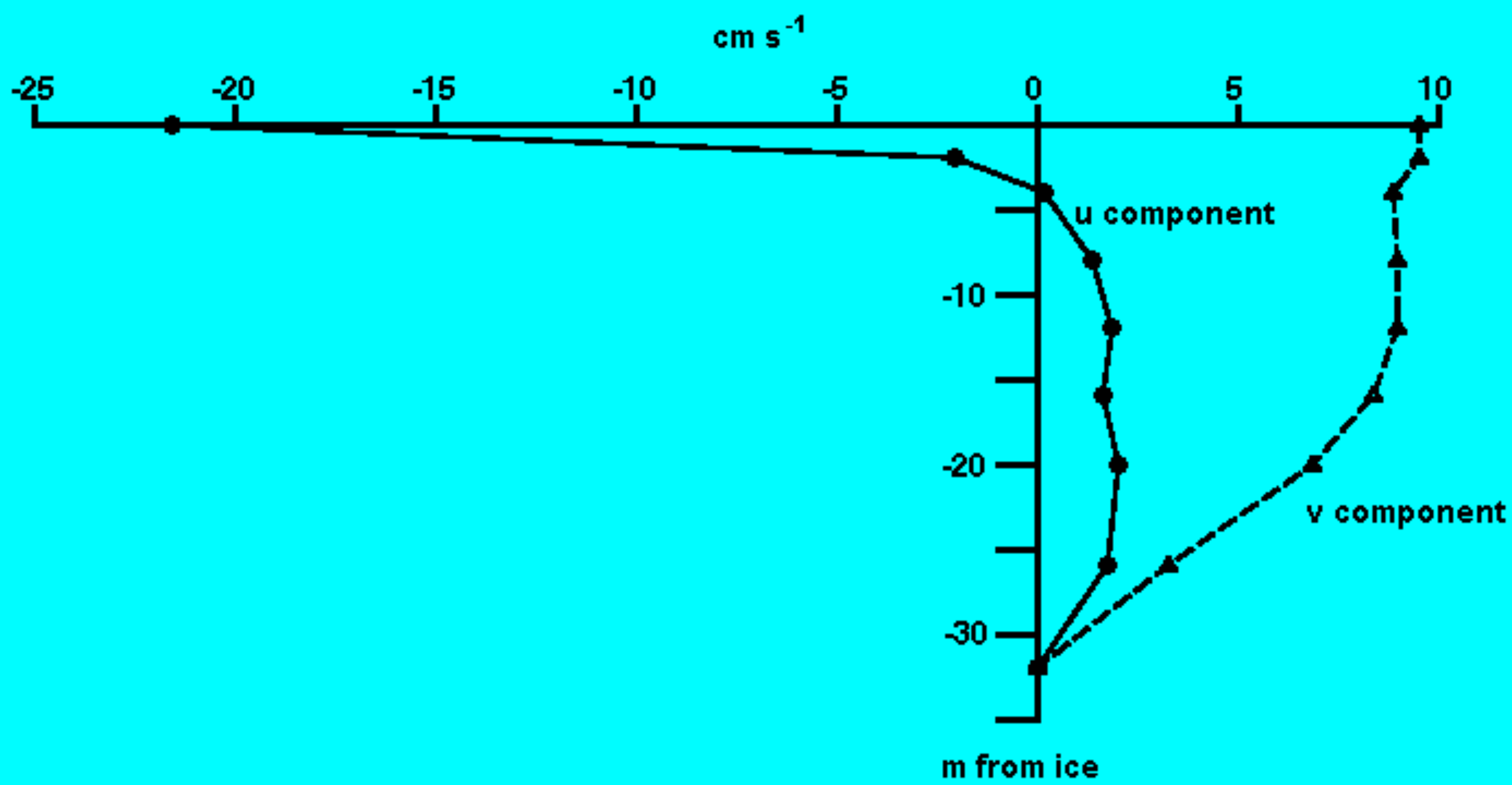

McPhee and Smith, *J. Phys. Oceanogr.*, 1976

Eddy Viscosity

$$\left[\frac{\hat{\tau}}{\partial \hat{u} / \partial z}\right] = \mathrm{L}^2\ \mathrm{T}^{-1} \quad \rightarrow \quad K = u_\varepsilon \lambda$$

u_ε scale velocity, good choice is friction velocity: $\hat{u}_* = \hat{\tau} / \sqrt{\tau}$

λ turbulent length scale for vertical exchange

Eddy Viscosity

$$\left[\frac{\hat{\tau}}{\partial \hat{u} / \partial z} \right] = \mathrm{L}^2\ \mathrm{T}^{-1} \quad \rightarrow \quad K = u_\varepsilon \lambda$$

u_ε scale velocity, good choice is friction velocity: $\hat{u}_* = \hat{\tau} / \sqrt{\tau}$

λ turbulent length scale for vertical exchange

Near a boundary in a neutrally stratified flow, stress is nearly constant and the velocity profile is logarithmic, hence the dimensionless shear is

$$\phi = \frac{\kappa z \hat{u}_z}{\hat{u}_{*0}} = 1$$

In the neutral ***surface layer*** : $\quad u_\varepsilon = u_{*0};\ \ \lambda = \kappa |z| \ \Rightarrow \ K = u_{*0} \kappa |z|$

Eddy Viscosity

$$\left[\frac{\hat{\tau}}{\partial \hat{u}/\partial z}\right] = \mathrm{L}^2\ \mathrm{T}^{-1} \quad \rightarrow \quad K = u_\varepsilon \lambda$$

u_ε scale velocity, good choice is friction velocity: $\hat{u}_* = \hat{\tau} / \sqrt{\tau}$

λ turbulent length scale for vertical exchange

Near a boundary in a neutrally stratified flow, stress is nearly constant and the velocity profile is logarithmic, hence the dimensionless shear is

$$\phi = \frac{\kappa z \hat{u}_z}{\hat{u}_{*0}} = 1$$

In the neutral ***surface layer*** : $\quad u_\varepsilon = u_{*0};\ \ \lambda = \kappa |z| \ \Rightarrow\ K = u_{*0}\kappa |z|$

BUT the surface layer only extends some small fraction of the planetary scale, *~0.05*u_{*0}/f, typically ~5m in the ocean, ~150 m in the atmosphere.

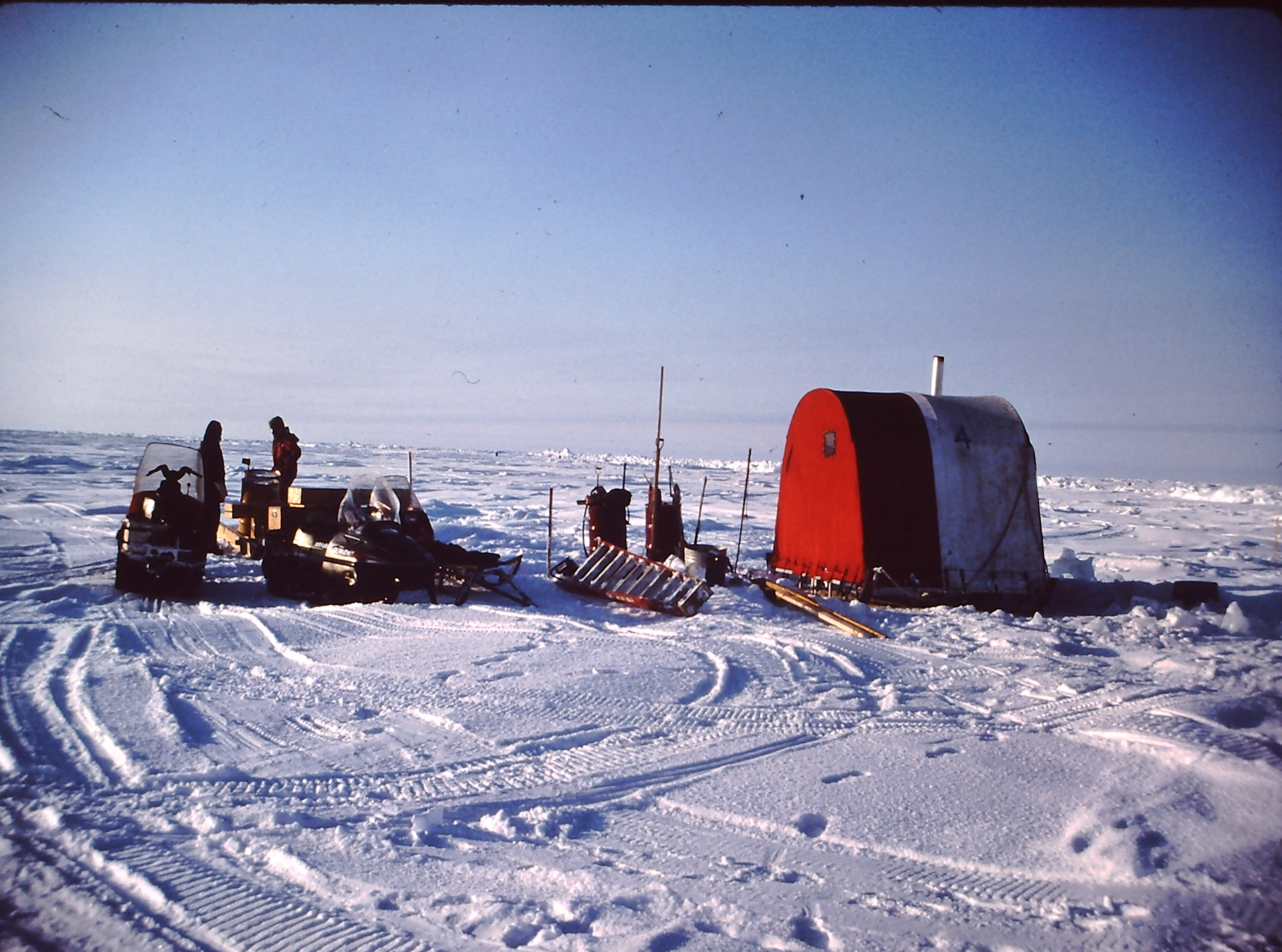

Eddy Viscosity, Mixing Length & the TKE Equation

Steady, horizontally homogeneous, neglect vertical transport terms:

$$P_S + P_b = \varepsilon$$

$$\hat{\tau} \cdot \hat{u}_z - \langle w'b' \rangle = \varepsilon$$

$$P_S = u_*^4 / K = u_*^3 / \lambda$$

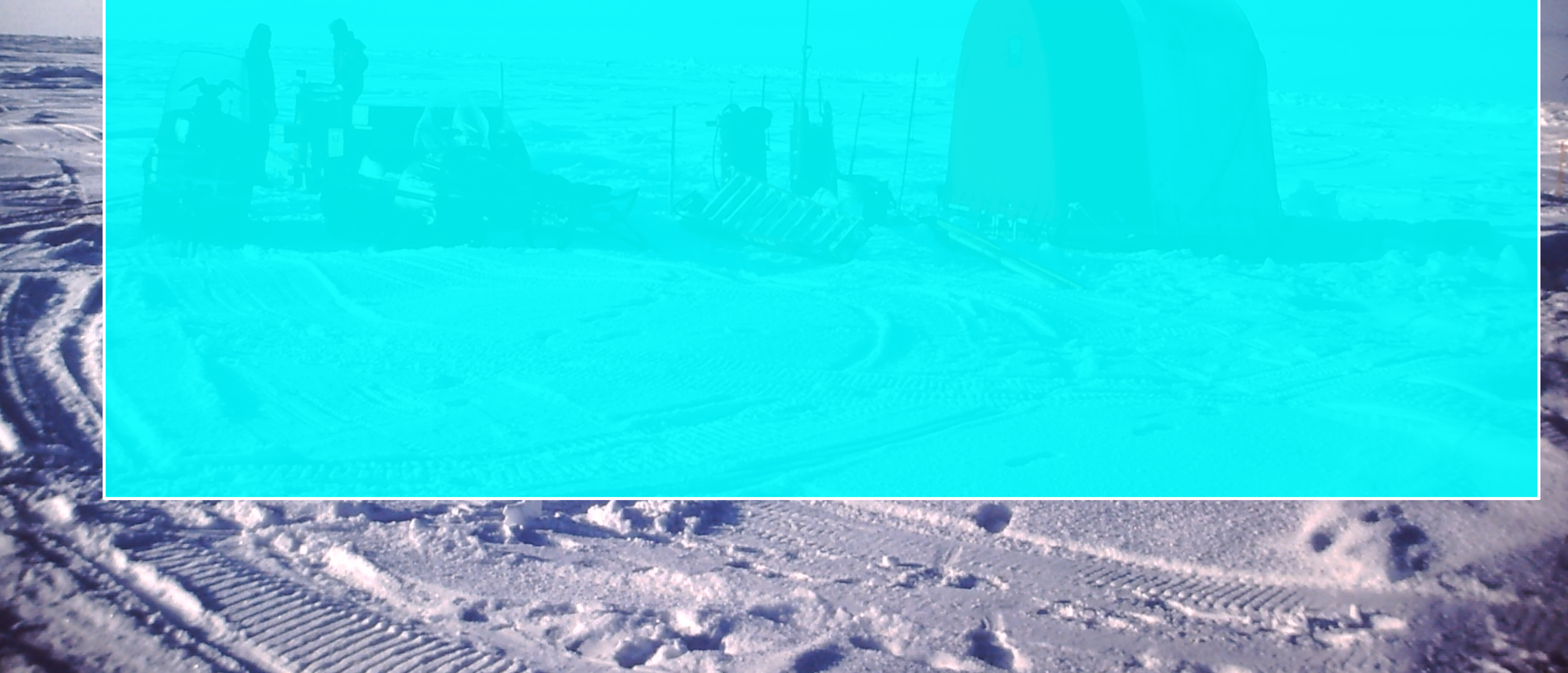

Eddy Viscosity, Mixing Length & the TKE Equation

Steady, horizontally homogeneous, neglect vertical transport terms:

$$P_S + P_b = \varepsilon$$

$$\hat{\tau} \cdot \hat{u}_z - \langle w'b' \rangle = \varepsilon$$

$$P_S = u_*^4 / K = u_*^3 / \lambda$$

In the neutral outer (Ekman) layer, measure ε and $u_* = (\langle u'w' \rangle^2 + \langle v'w' \rangle^2)^{1/4}$ to estimate

$$\boxed{\lambda_\varepsilon = u_*^3 / \varepsilon}$$

Turbulence spectra

Turbulence spectra

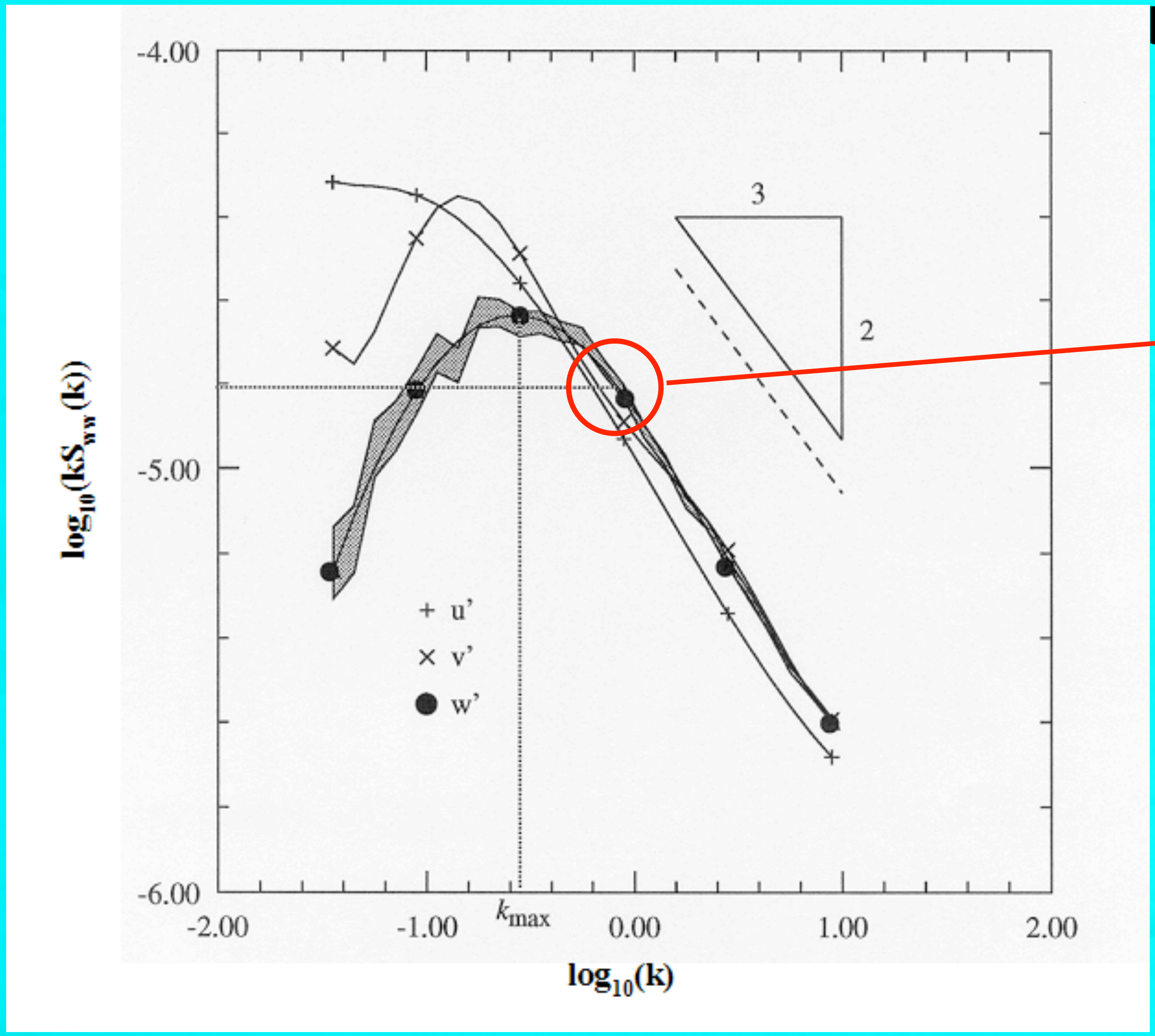

6-h average w variance spectrum at 20 m below the ice during Ice Station Weddell, 1992.

$$S_{ww}(k) = \frac{4\alpha_{\varepsilon}}{3}\varepsilon^{2/3}k^{-5/3}$$

Turbulence spectra

6-h average w variance spectrum at 20 m below the ice during Ice Station Weddell, 1992.

$$S_{ww}(k) = \frac{4\alpha_\varepsilon}{3}\varepsilon^{2/3}k^{-5/3}$$

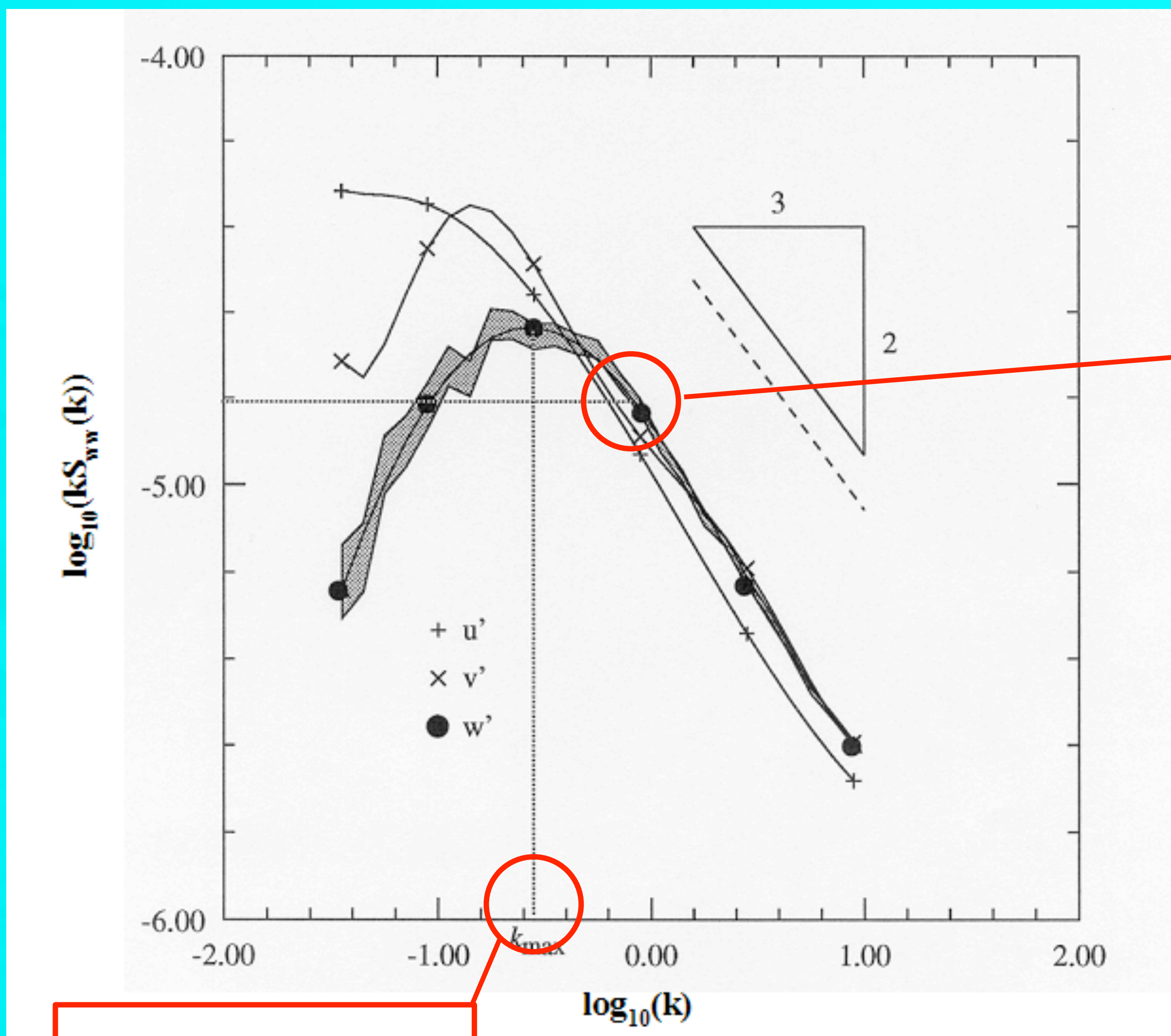

$$\lambda_{\text{peak}} = c_\lambda / k_{\max}$$

Turbulence spectra

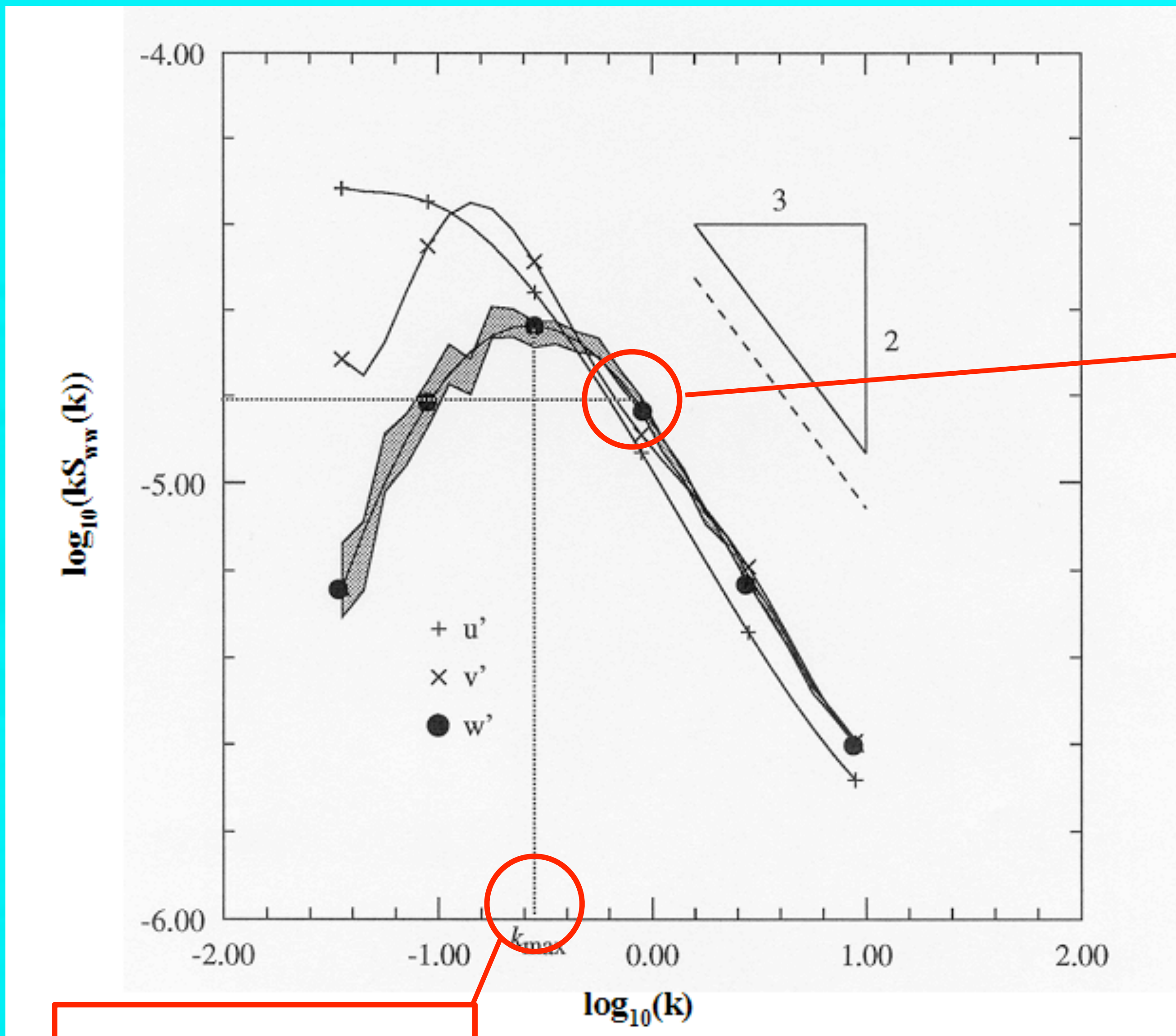

6-h average w variance spectrum at 20 m below the ice during Ice Station Weddell, 1992.

$$\boxed{S_{ww}(k) = \frac{4\alpha_{\varepsilon}}{3}\varepsilon^{2/3}k^{-5/3}}$$

$$\boxed{\lambda_{peak} = c_{\lambda} / k_{max}}$$

Information in the area-preserving vertical velocity spectrum alone (ε, λ_{peak}) provides an estimate of local stress:

$$\boxed{u_{*_{\varepsilon}} = (\varepsilon\lambda_{peak})^{1/3}}$$

$$u_{*(\mathrm{cov})} = (\langle u'w' \rangle^2 + \langle v'w' \rangle^2)^{1/4}$$

$$u_{*(\mathrm{spec})} = (\varepsilon \lambda_{\mathrm{peak}})^{1/3}$$

$$u_{*(\mathrm{cov})} = (\langle u'w'\rangle^2 + \langle v'w'\rangle^2)^{1/4}$$

$$u_{*(\mathrm{spec})} = (\varepsilon \lambda_{\mathrm{peak}})^{1/3}$$

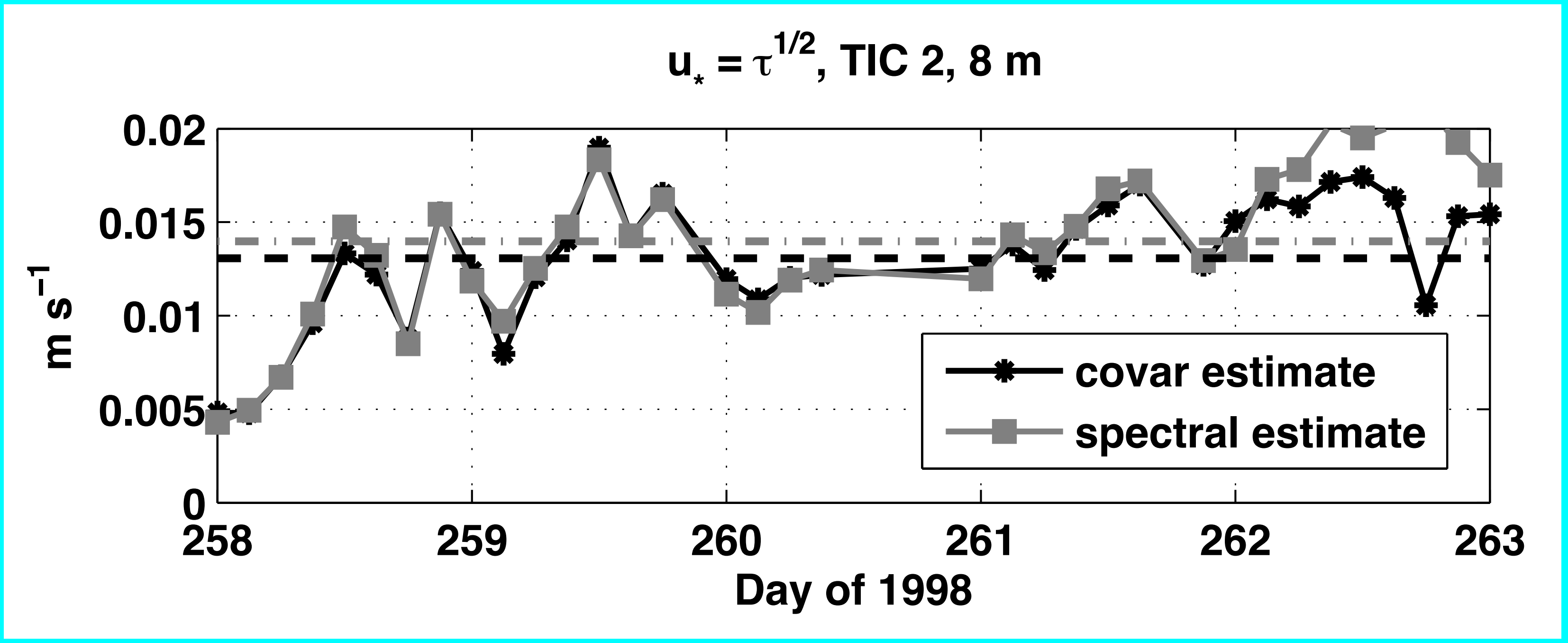

$$u_{*(\mathrm{cov})} = (\langle u'w' \rangle^2 + \langle v'w' \rangle^2)^{1/4}$$

$$u_{*(\mathrm{spec})} = (\varepsilon \lambda_{\mathrm{peak}})^{1/3}$$

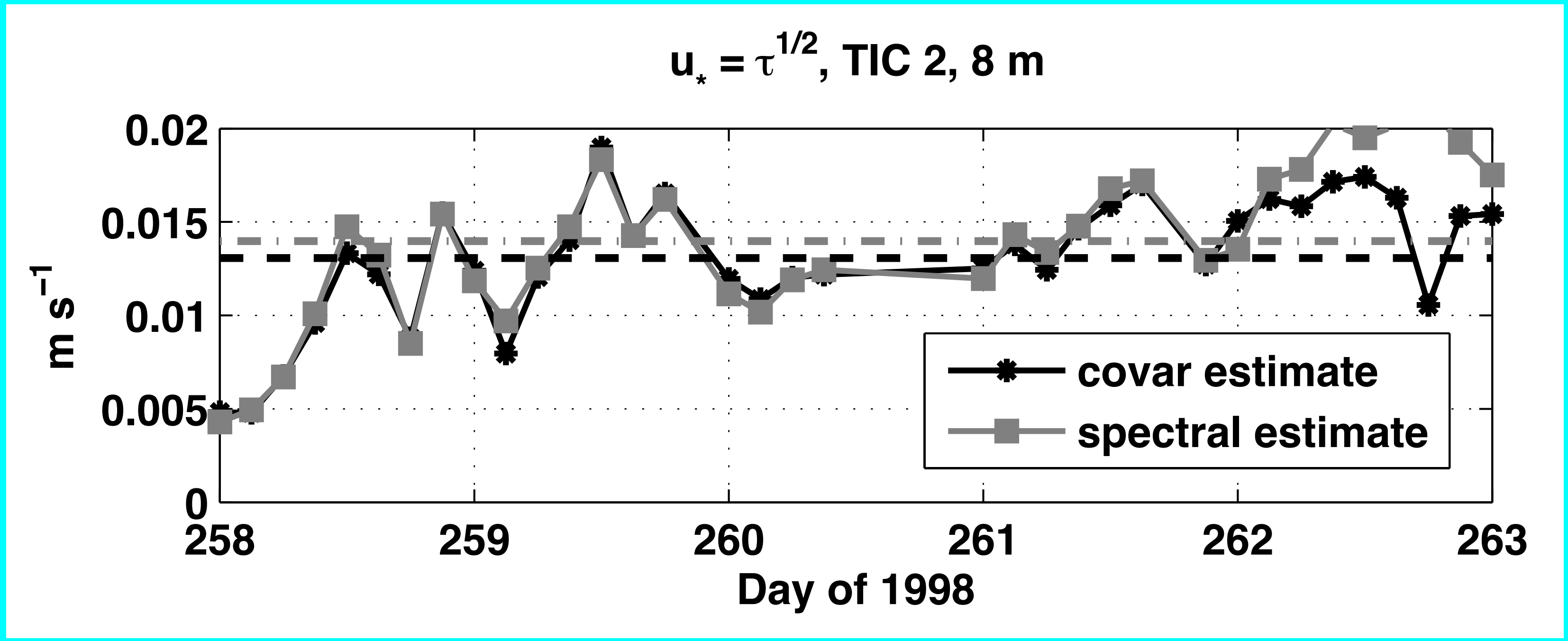

$$\left| \langle w'T' \rangle \frac{\partial T}{\partial z} \right| = \frac{\langle w'T' \rangle^2}{\lambda_T u_*} = \varepsilon_T$$

$$u_{*(\mathrm{cov})} = (\langle u'w' \rangle^2 + \langle v'w' \rangle^2)^{1/4}$$

$$u_{*(\mathrm{spec})} = (\varepsilon \lambda_{\mathrm{peak}})^{1/3}$$

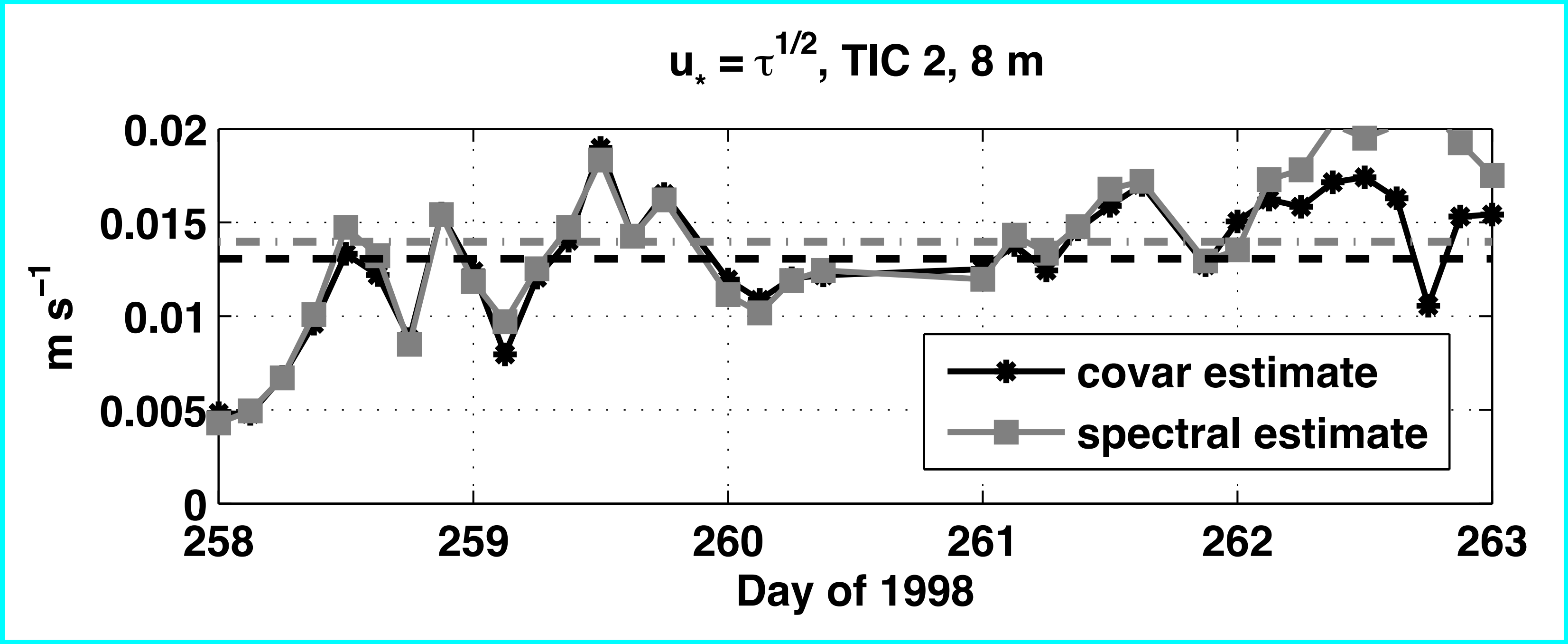

$$\left| \langle w'T' \rangle \frac{\partial T}{\partial z} \right| = \frac{\langle w'T' \rangle^2}{\lambda_T u_*} = \varepsilon_T$$

$$S_{TT}(k) = \alpha_\Theta \varepsilon_T \varepsilon^{-1/3} k^{-5/3}$$

$$u_{*(\mathrm{cov})} = (\langle u'w' \rangle^2 + \langle v'w' \rangle^2)^{1/4}$$

$$u_{*(\mathrm{spec})} = (\varepsilon \lambda_{\mathrm{peak}})^{1/3}$$

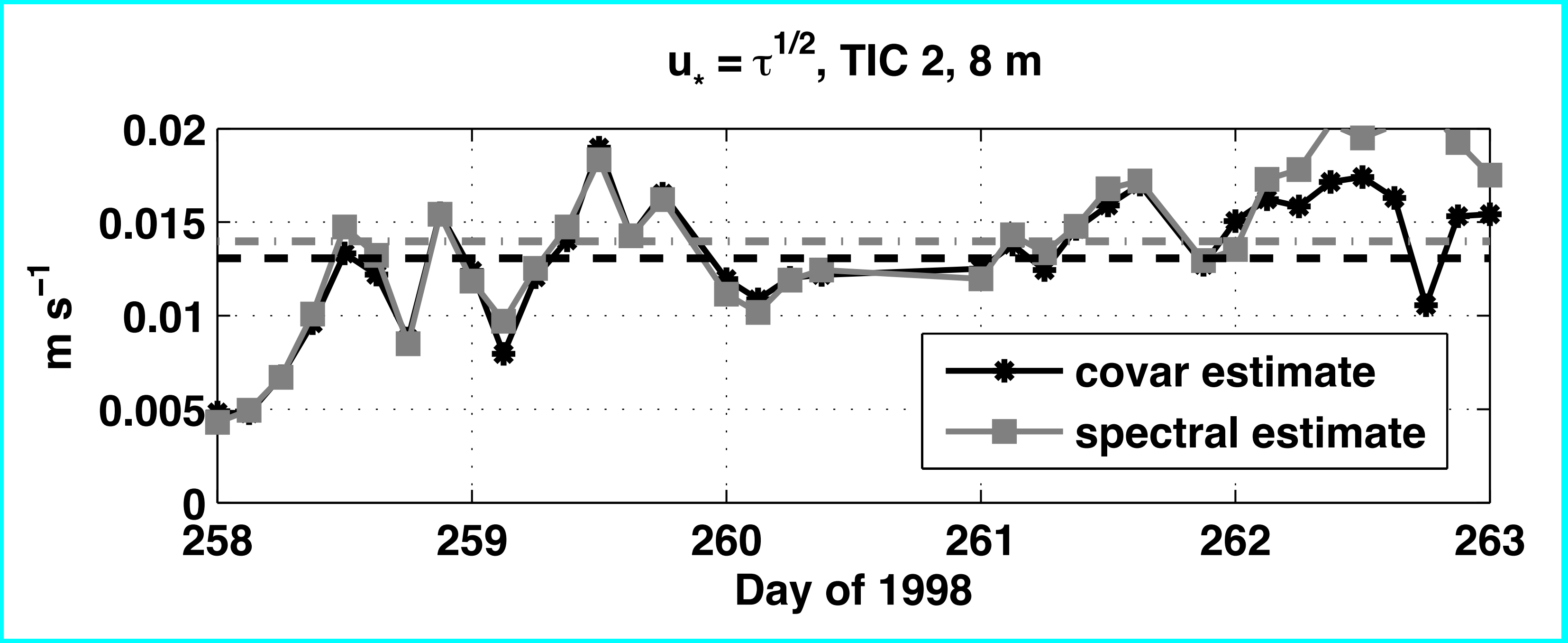

$$\left| \langle w'T' \rangle \frac{\partial T}{\partial z} \right| = \frac{\langle w'T' \rangle^2}{\lambda_T u_*} = \varepsilon_T$$

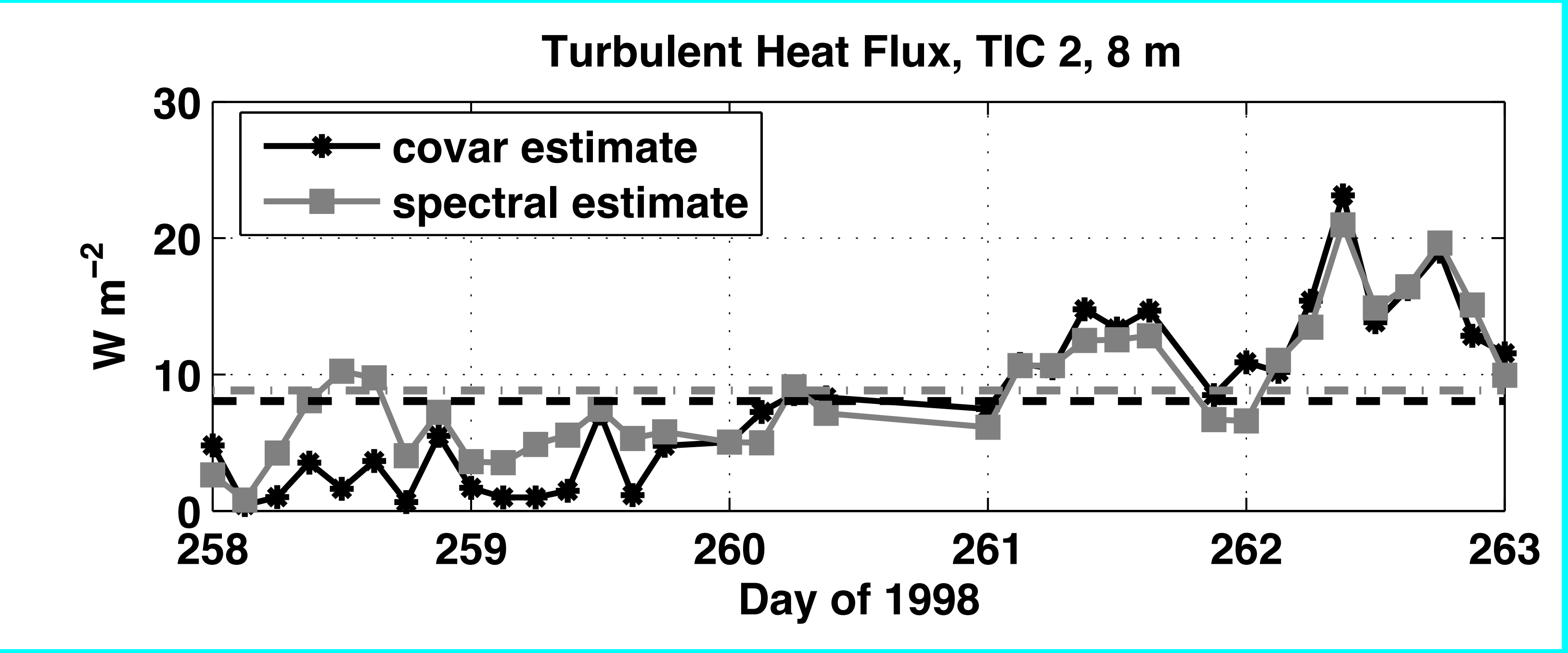

$$S_{TT}(k) = \alpha_{\Theta} \varepsilon_T \varepsilon^{-1/3} k^{-5/3}$$

IOBL Similarity

IOBL Similarity

$$if\hat{u} = \frac{\partial \hat{\tau}}{\partial z} \qquad \rightarrow \quad \hat{\tau} = u_{*0}\hat{u}_{*0}\hat{\mathrm{T}}; \;\; \hat{u} = \hat{u}_{*0}\hat{U}; \;\; z = \zeta u_{*0} / f$$

$$i\hat{U} = \frac{\partial \hat{\mathrm{T}}}{\partial \zeta} \;\; ; \quad 1^{\mathrm{st}} - \text{order closure:} \quad \rightarrow \; \hat{\mathrm{T}} = \frac{fK_m}{u_{*0}^2}\frac{\partial \hat{U}}{\partial \zeta} = K_*\frac{\partial \hat{U}}{\partial \zeta}$$

$$\frac{\partial^2 \hat{\mathrm{T}}}{\partial \zeta^2} - \frac{i}{K_*}\hat{\mathrm{T}} = 0; \;\; \text{Boundary conditions: } \hat{\mathrm{T}}(\zeta \rightarrow -\infty) = 0; \qquad \hat{\mathrm{T}}(\zeta = 0) = \frac{\hat{\tau}_0}{u_{*0}\hat{u}_{*0}} = 1$$

IOBL Similarity

$$if\hat{u} = \frac{\partial \hat{\tau}}{\partial z} \quad \rightarrow \quad \hat{\tau} = u_{*0}\hat{u}_{*0}\hat{\mathrm{T}}; \;\; \hat{u} = \hat{u}_{*0}\hat{U}; \;\; z = \zeta u_{*0} / f$$

$$i\hat{U} = \frac{\partial \hat{\mathrm{T}}}{\partial \zeta} \;\; ; \;\; 1^{\text{st}} - \text{order closure:} \quad \rightarrow \hat{\mathrm{T}} = \frac{fK_m}{u_{*0}^2}\frac{\partial \hat{U}}{\partial \zeta} = K_* \frac{\partial \hat{U}}{\partial \zeta}$$

$$\frac{\partial^2 \hat{\mathrm{T}}}{\partial \zeta^2} - \frac{i}{K_*}\hat{\mathrm{T}} = 0; \;\; \text{Boundary conditions: } \hat{\mathrm{T}}(\zeta \rightarrow -\infty) = 0; \quad \hat{\mathrm{T}}(\zeta = 0) = \frac{\hat{\tau}_0}{u_{*0}\hat{u}_{*0}} = 1$$

$$\boxed{\hat{\mathrm{T}} = e^{\hat{\delta}\zeta}} \qquad (\, \hat{\delta} = \sqrt{i / K_*}\,)$$

IOBL Similarity

$$if\hat{u} = \frac{\partial \hat{\tau}}{\partial z} \quad \rightarrow \quad \hat{\tau} = u_{*0}\hat{u}_{*0}\hat{\mathrm{T}};\ \ \hat{u} = \hat{u}_{*0}\hat{U};\ \ z = \zeta u_{*0}/f$$

$$i\hat{U} = \frac{\partial \hat{\mathrm{T}}}{\partial \zeta}\ ;\quad 1^{\mathrm{st}} - \text{order closure:} \quad \rightarrow\ \hat{\mathrm{T}} = \frac{fK_m}{u_{*0}^2}\frac{\partial \hat{U}}{\partial \zeta} = K_*\frac{\partial \hat{U}}{\partial \zeta}$$

$$\frac{\partial^2 \hat{\mathrm{T}}}{\partial \zeta^2} - \frac{i}{K_*}\hat{\mathrm{T}} = 0;\ \ \text{Boundary conditions: } \hat{\mathrm{T}}(\zeta \rightarrow -\infty) = 0; \quad \hat{\mathrm{T}}(\zeta = 0) = \frac{\hat{\tau}_0}{u_{*0}\hat{u}_{*0}} = 1$$

$$\boxed{\hat{\mathrm{T}} = e^{\hat{\delta}\zeta}} \qquad (\,\hat{\delta} = \sqrt{i/K_*}\,)$$

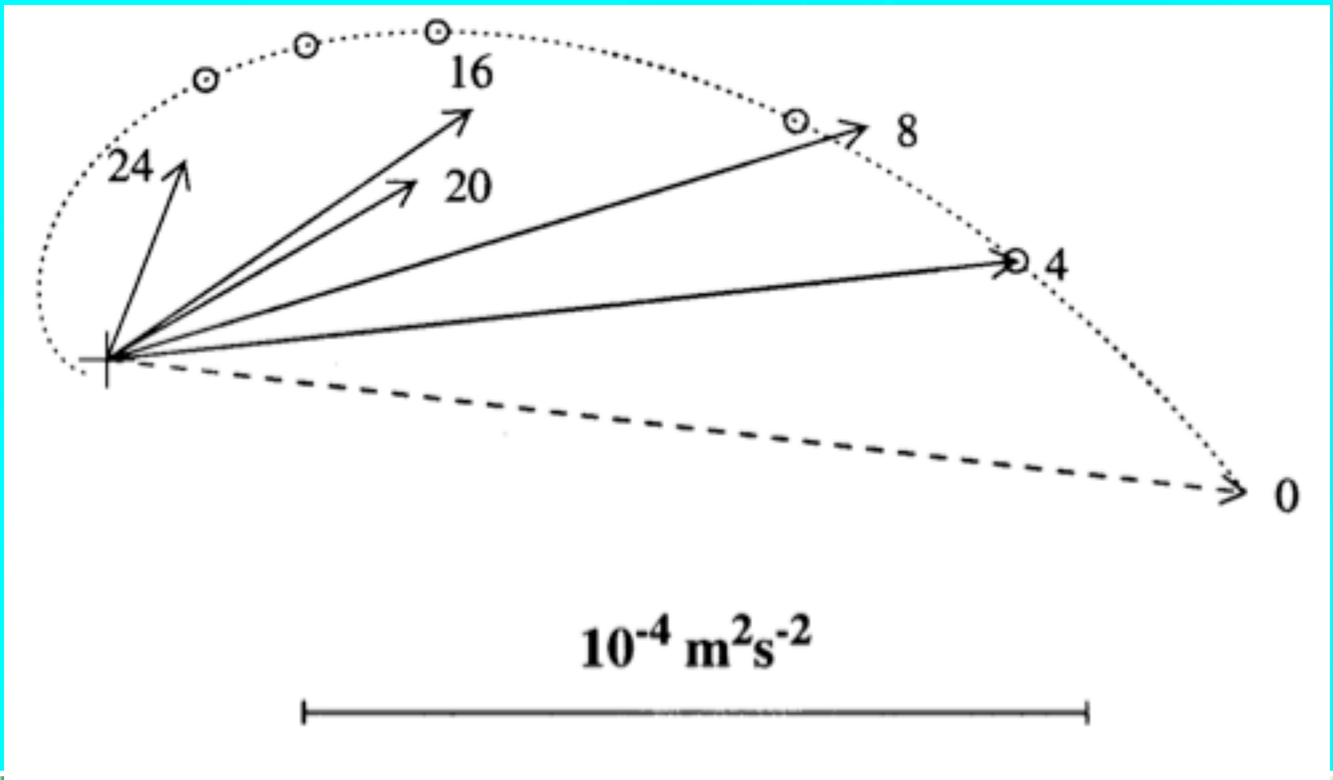

Wind event at Ice Station Weddell (1992)

$$\hat{\tau} = \langle u'w' \rangle + i\langle v'w' \rangle$$

McPhee and Martinson, *Science*.,1994

λ, K measurements

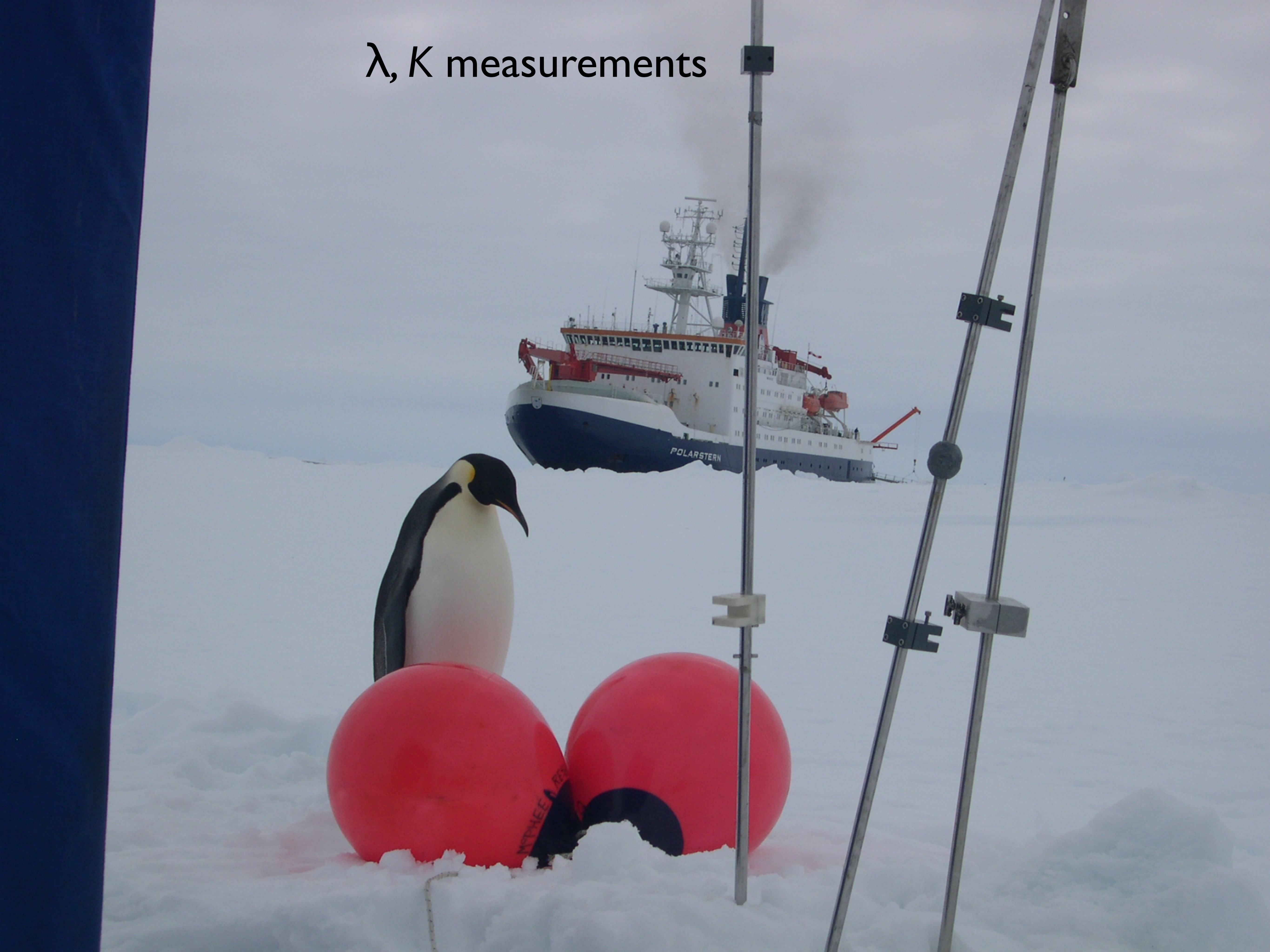

λ, *K* measurements

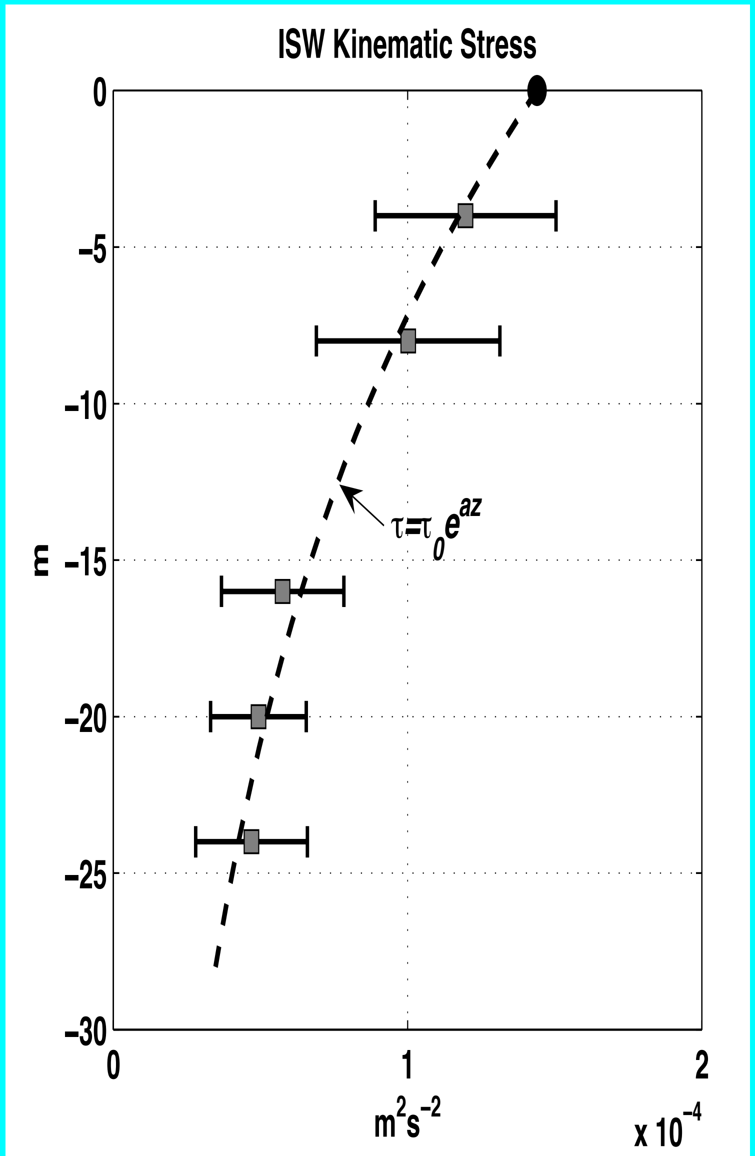

λ, *K* measurements

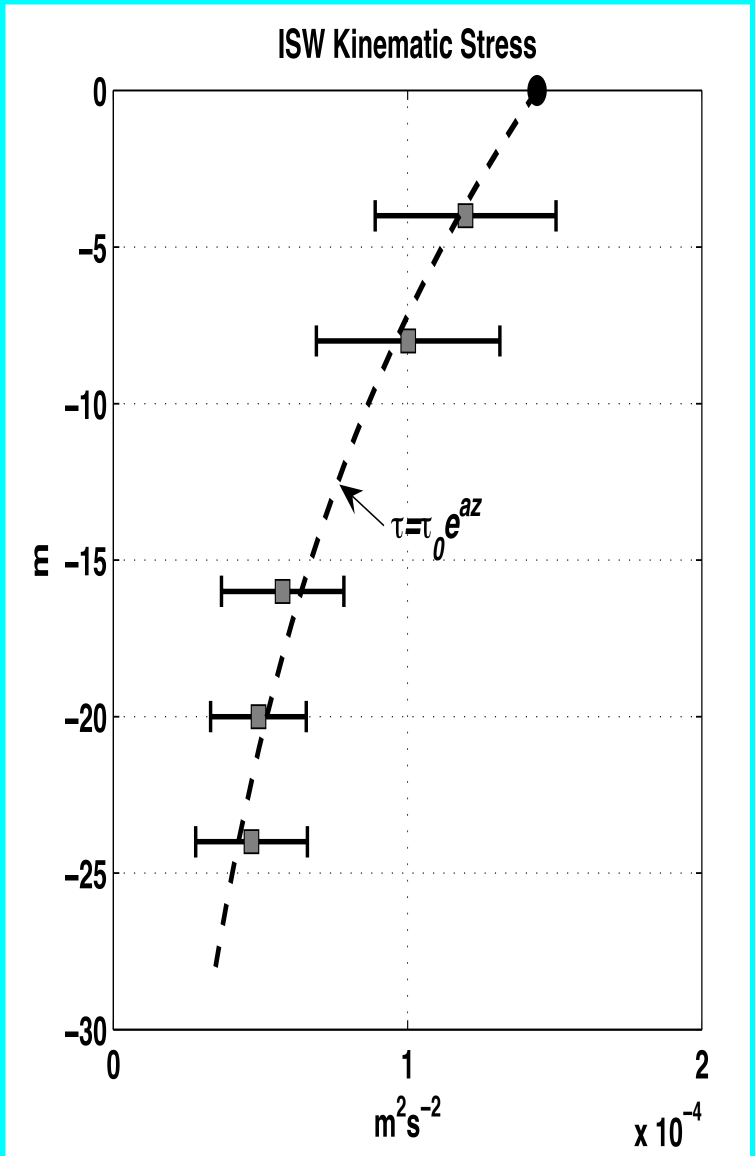

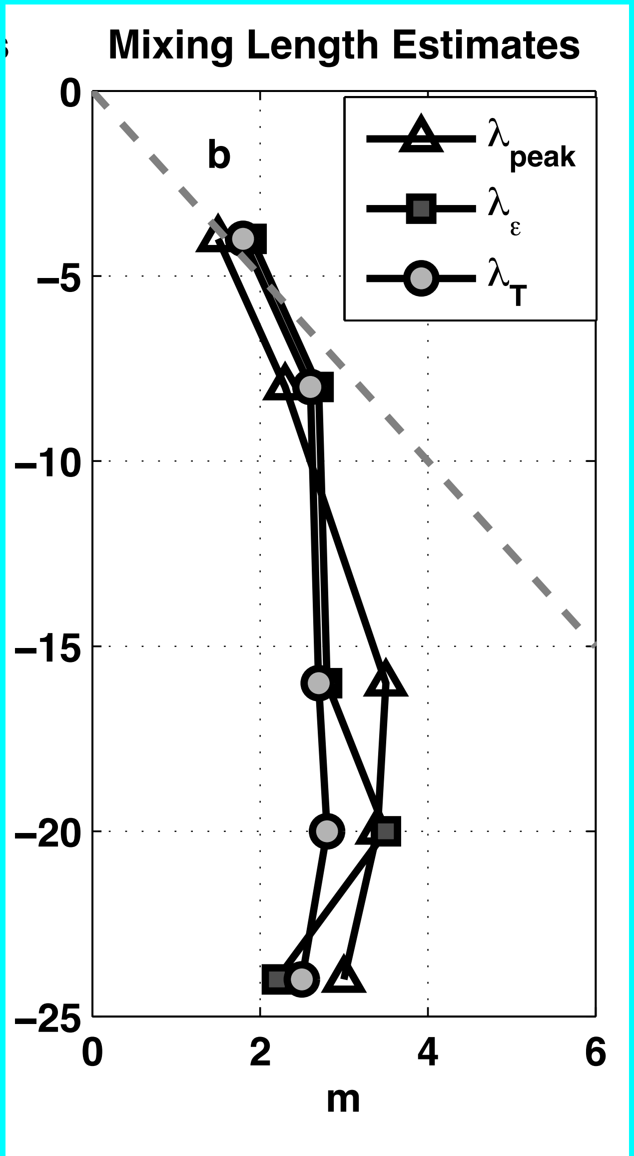

λ, *K* measurements

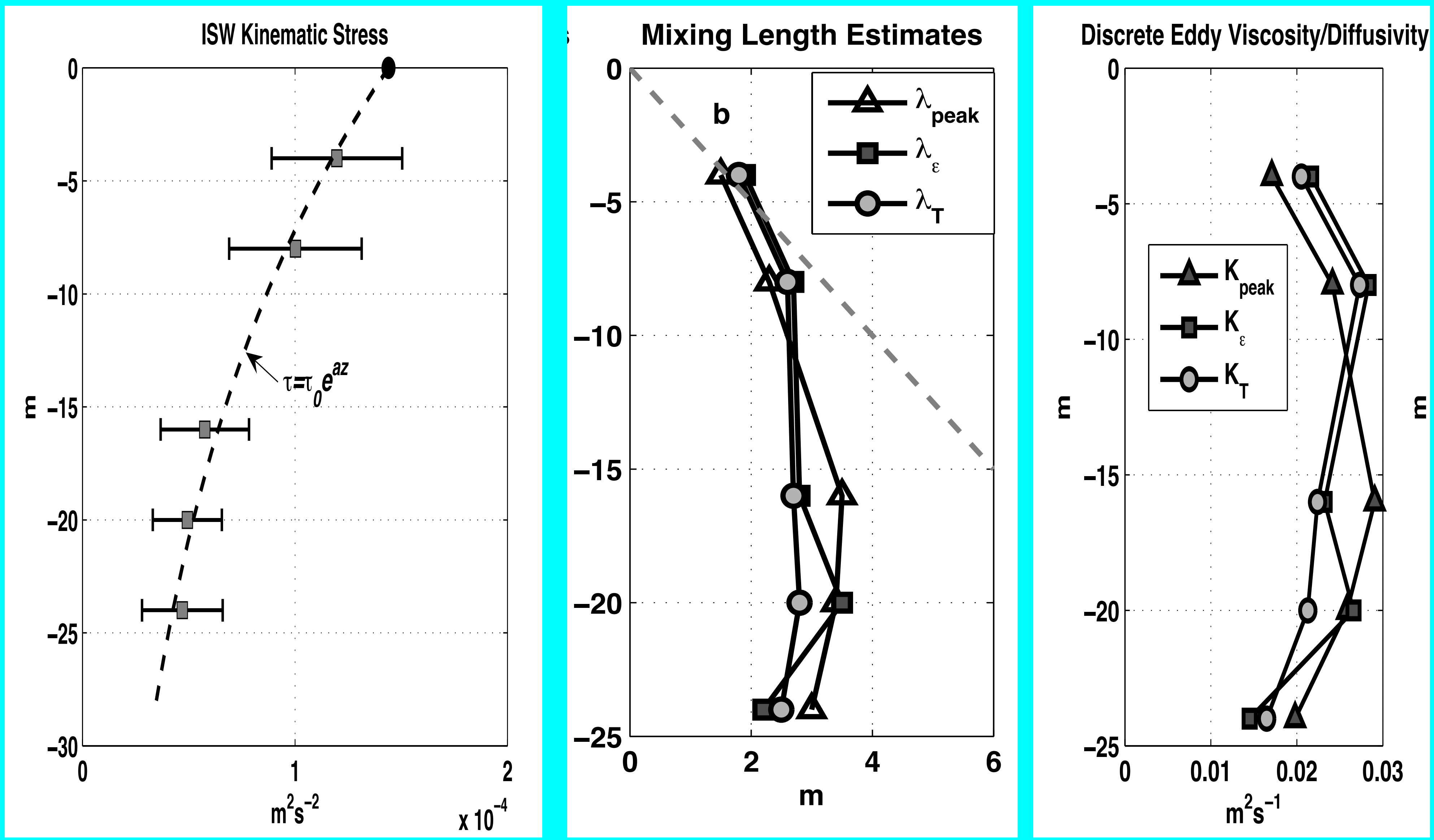

λ, *K* measurements

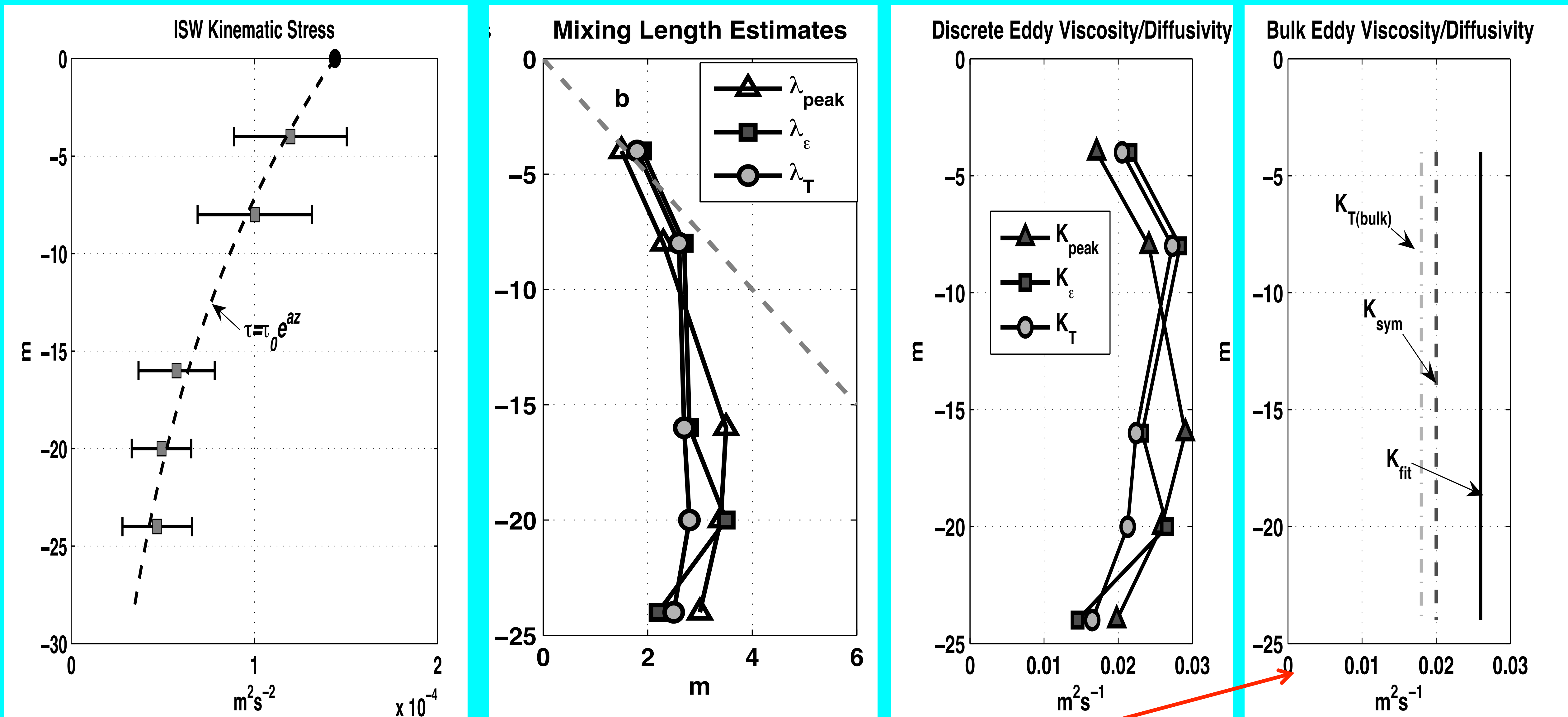

$$K_{\text{fit}} = f/(2a^2)$$ (from the Ekman solution)

$$K_{\text{sim}} = K_* u_{*0}^2 / f$$ (Similarity bulk estimate)

$$K_{\text{T(bulk)}} = \overline{\frac{-\langle w'T'\rangle}{\partial T/\partial z}}$$ (from mean properties in the IOBL)

$K_{T(bulk)}$ estimate

Polar mixed layers make wonderful calibration baths.
Choose a time when turbulent heat flux is about zero
and adjust thermometers to agree

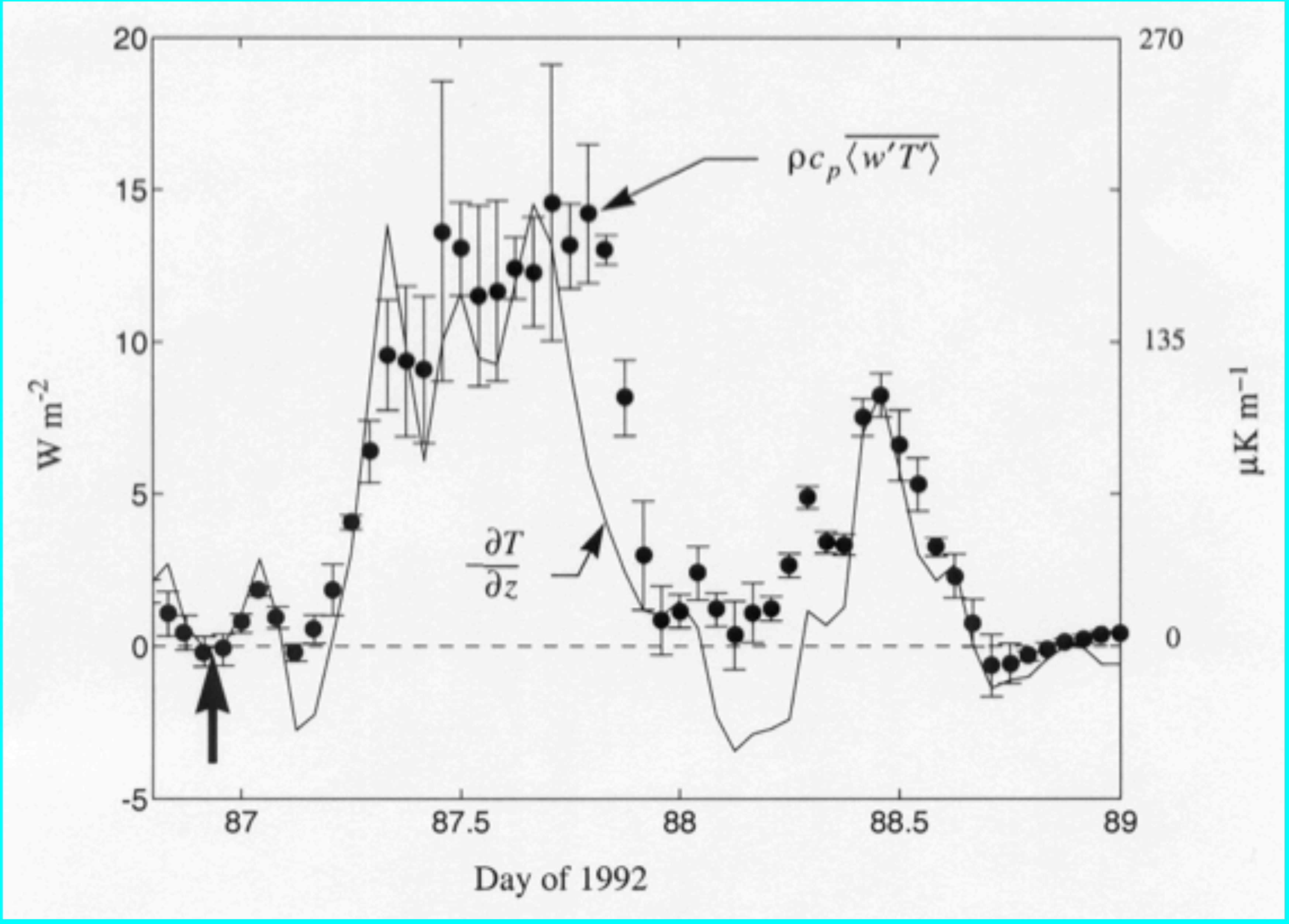

Similarity (continued)

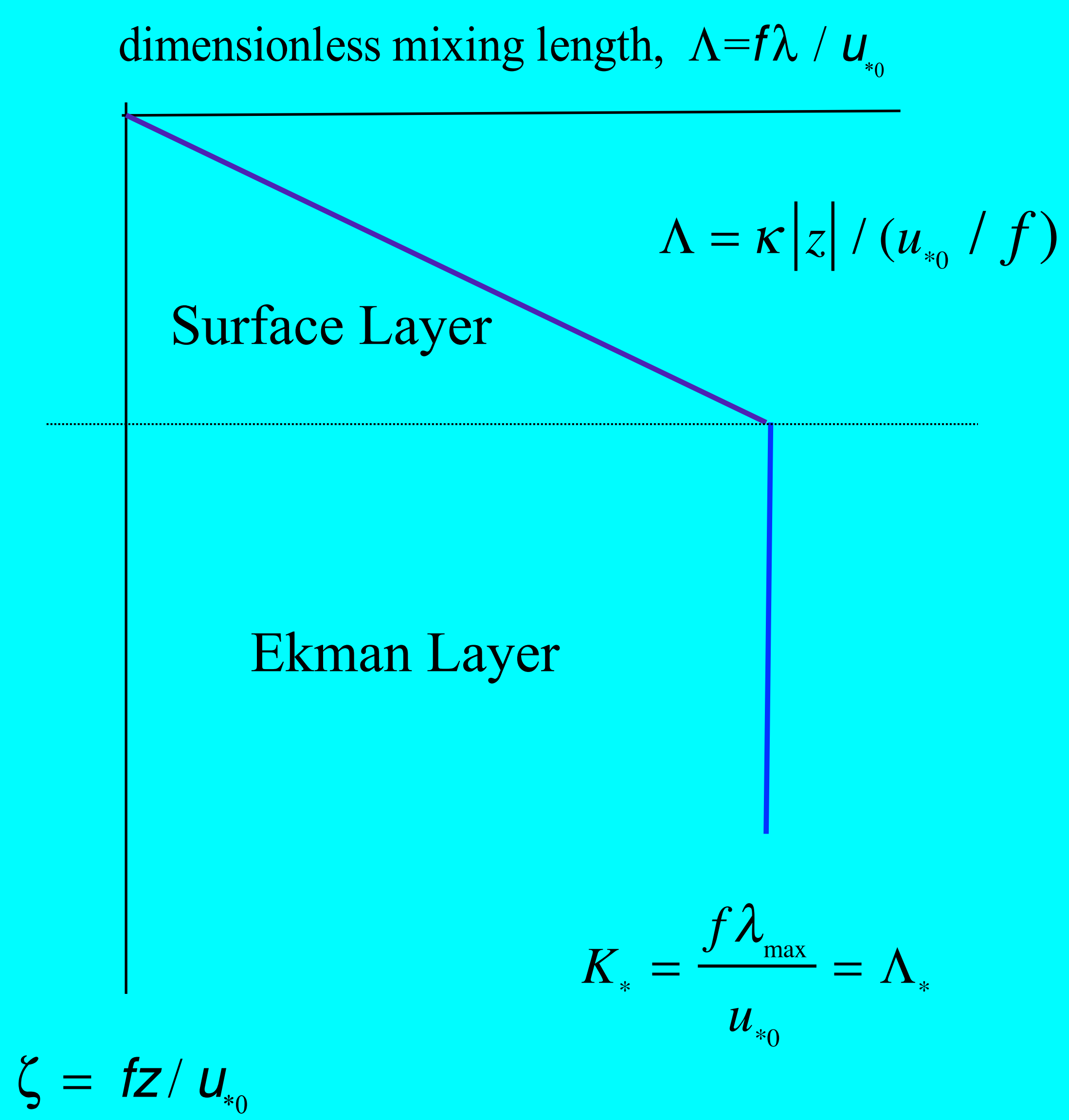

For similarity, K_* is constant in the Ekman layer, and if Λ increases linearly in the surface layer (where $\lambda = \kappa |z|$), the surface layer extent is

$$|z|_{\mathrm{sl}} = \frac{\Lambda_*}{\kappa} u_{*0} / f$$

Similarity (continued)

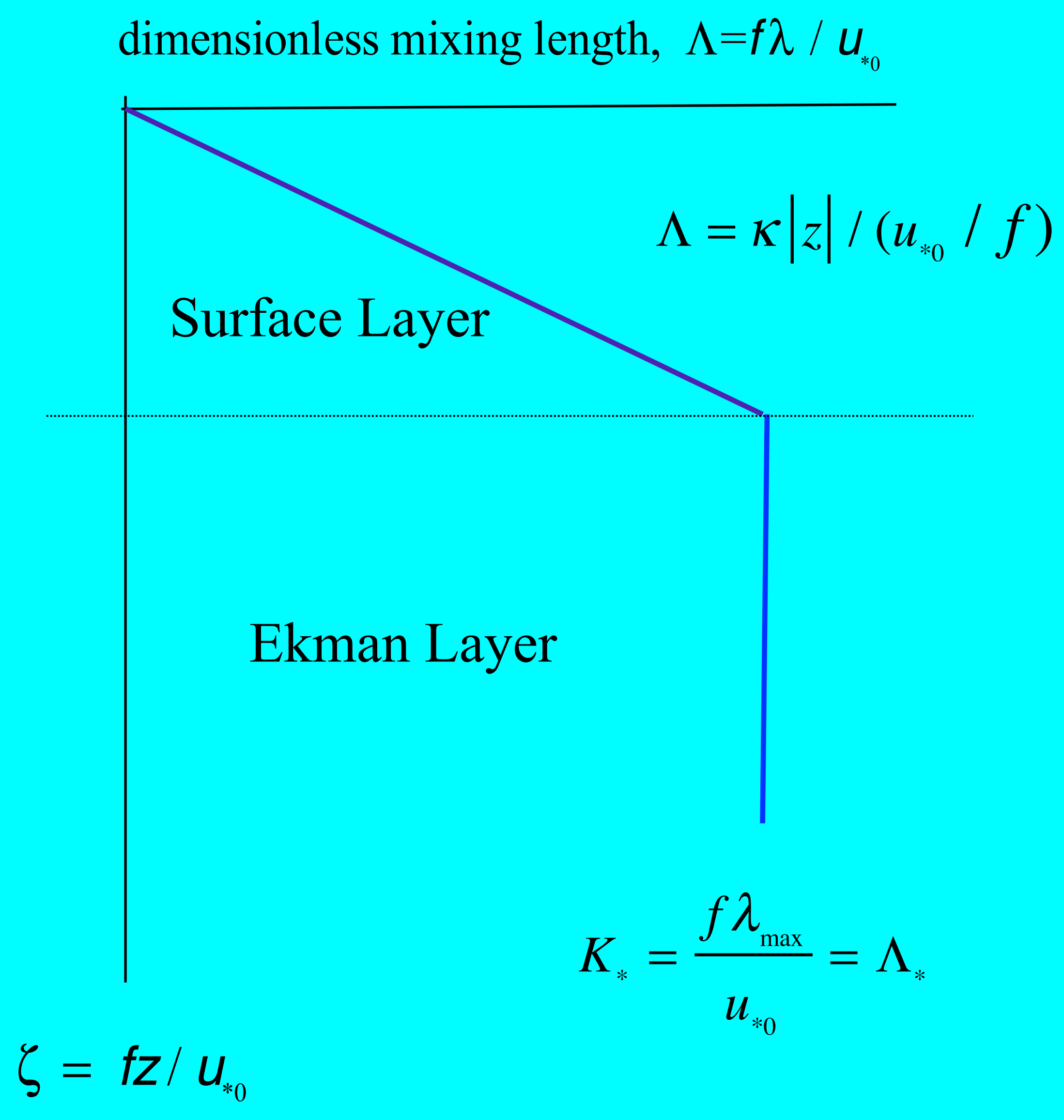

For similarity, K_* is constant in the Ekman layer, and if Λ increases linearly in the surface layer (where $\lambda = \kappa|z|$), the surface layer extent is

$$|z|_{sl} = \frac{\Lambda_*}{\kappa} u_{*0} / f$$

From the LOW, the change in velocity across the surface layer is

$$\frac{\Delta\hat{u}}{\hat{u}_{*0}} = \frac{1}{\kappa}\log\frac{|z_{sl}|}{z_0} = \frac{1}{\kappa}(\log\frac{u_{*0}}{fz_0} + \log\frac{\Lambda_*}{\kappa})$$

Similarity (continued)

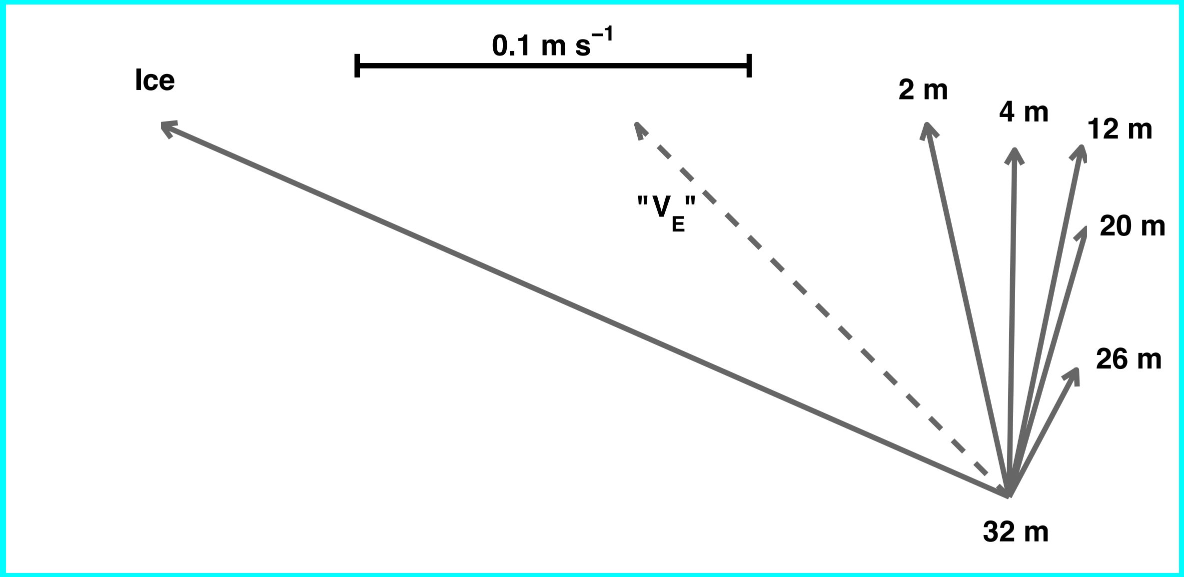

So now we can put together an "inverse drag law:"

$$\frac{\hat{v}_0}{\hat{u}_{*0}} = \frac{\hat{v}_E}{\hat{u}_{*0}} + \frac{\Delta\hat{u}}{\hat{u}_{*0}}$$

$$= \frac{1}{\kappa}\left[\log\frac{u_{*0}}{fz_0} + \log\frac{\Lambda_*}{\kappa} + \frac{1}{\sqrt{2K_*}}(1-i)\right]$$

$$= \frac{1}{\kappa}\left[\log Ro_* - A \mp iB\right]$$

$Ro_* = u_{*0}/(fz_0)$ Surface friction Rossby number

A and B are similarity constants (neutral stability)

Similarity (continued)

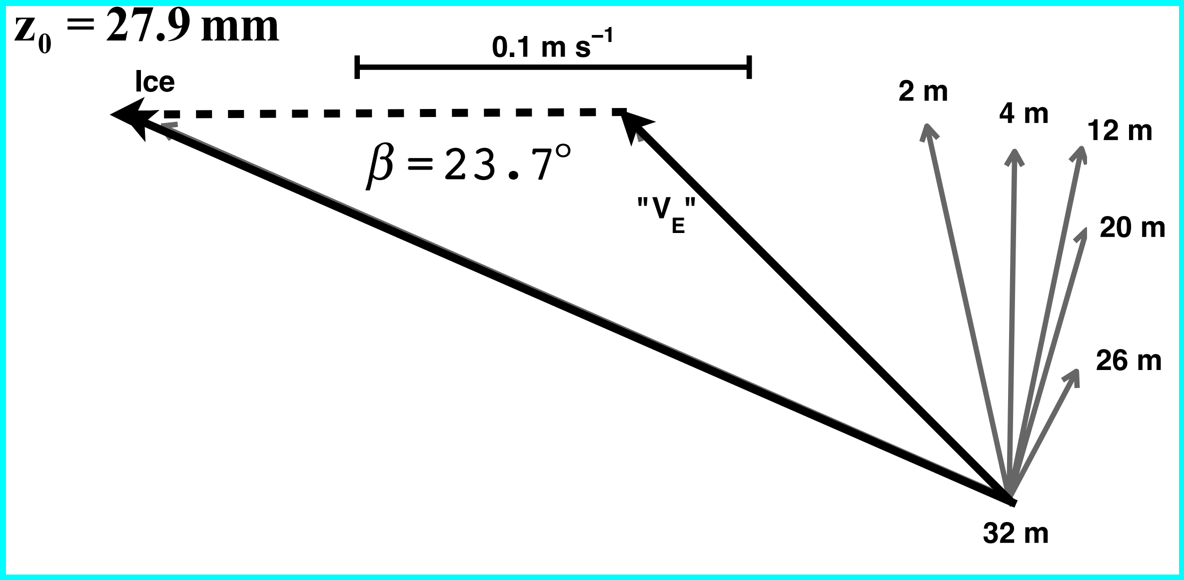

So now we can put together an "inverse drag law:"

$$
\begin{aligned}
\frac{\hat{v}_0}{\hat{u}_{*0}} &= \frac{\hat{v}_E}{\hat{u}_{*0}} + \frac{\Delta \hat{u}}{\hat{u}_{*0}} \\
&= \frac{1}{\kappa}\left[\log \frac{u_{*0}}{f z_0} + \log \frac{\Lambda_*}{\kappa} + \frac{1}{\sqrt{2K_*}}(1-i)\right] \\
&= \frac{1}{\kappa}\left[\log Ro_* - A \mp iB\right]
\end{aligned}
$$

$Ro_* = u_{*0} / (f z_0)$ Surface friction Rossby number

A and B are similarity constants (neutral stability)

Similarity (continued)

So now we can put together an "inverse drag law:"

$$\frac{\hat{v}_0}{\hat{u}_{*0}} = \frac{\hat{v}_E}{\hat{u}_{*0}} + \frac{\Delta\hat{u}}{\hat{u}_{*0}}$$

$$= \frac{1}{\kappa}\left[\log\frac{u_{*0}}{fz_0} + \log\frac{\Lambda_*}{\kappa} + \frac{1}{\sqrt{2K_*}}(1-i)\right]$$

$$= \frac{1}{\kappa}\left[\log Ro_* - A \mp iB\right]$$

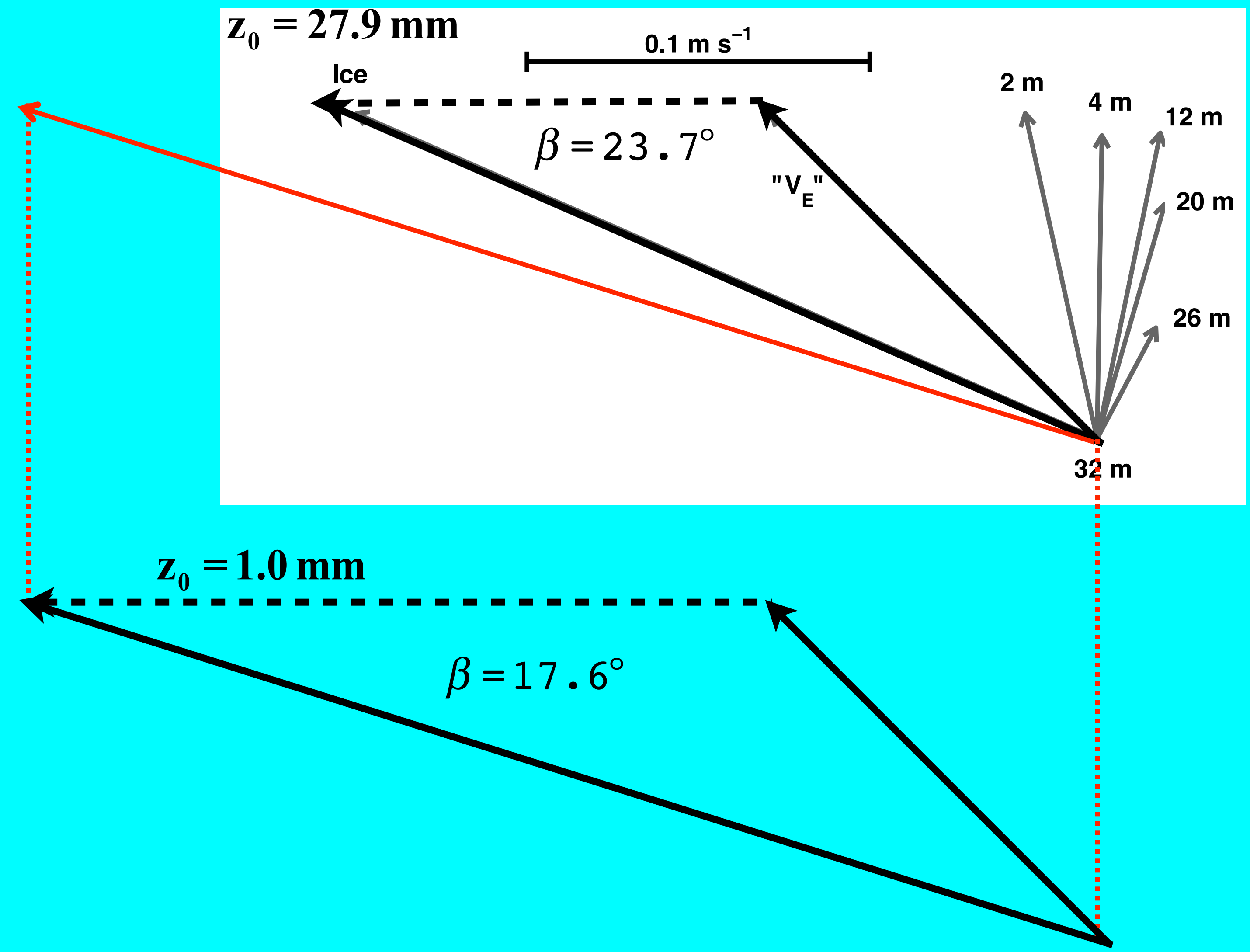

$Ro_* = u_{*0}/(fz_0)$ Surface friction Rossby number

A and B are similarity constants (neutral stability)

Similarity (continued)

$$A = -\log\frac{\Lambda_*}{\kappa} - \frac{\kappa}{\sqrt{2\Lambda_*}} + 1 + \sqrt{\frac{\Lambda_*}{2\kappa^2}} \approx 2.3$$

$$B = -\frac{\kappa}{\sqrt{2\Lambda_*}} + \sqrt{\frac{\Lambda_*}{2\kappa^2}} \approx 2.0$$

for $\Lambda_* = 0.028$

$$\hat{\Gamma} = \frac{\hat{v}_0}{\hat{u}_{*0}} = \frac{1}{\boldsymbol{\kappa}}[\log Ro_* - A - iB]$$

$$c_w = \frac{u_{*0}^2}{v_0^2} = \Gamma^{-2}$$

Similarity (continued)

$$A = -\log\frac{\Lambda_*}{\kappa} - \frac{\kappa}{\sqrt{2\Lambda_*}} + 1 + \sqrt{\frac{\Lambda_*}{2\kappa^2}} \approx 2.3$$

$$B = -\frac{\kappa}{\sqrt{2\Lambda_*}} + \sqrt{\frac{\Lambda_*}{2\kappa^2}} \approx 2.0$$

for $\Lambda_* = 0.028$

$$\hat{\Gamma} = \frac{\hat{v}_0}{\hat{u}_{*0}} = \frac{1}{\kappa}[\log Ro_* - A - iB]$$

$$c_w = \frac{u_{*0}^2}{v_0^2} = \Gamma^{-2}$$

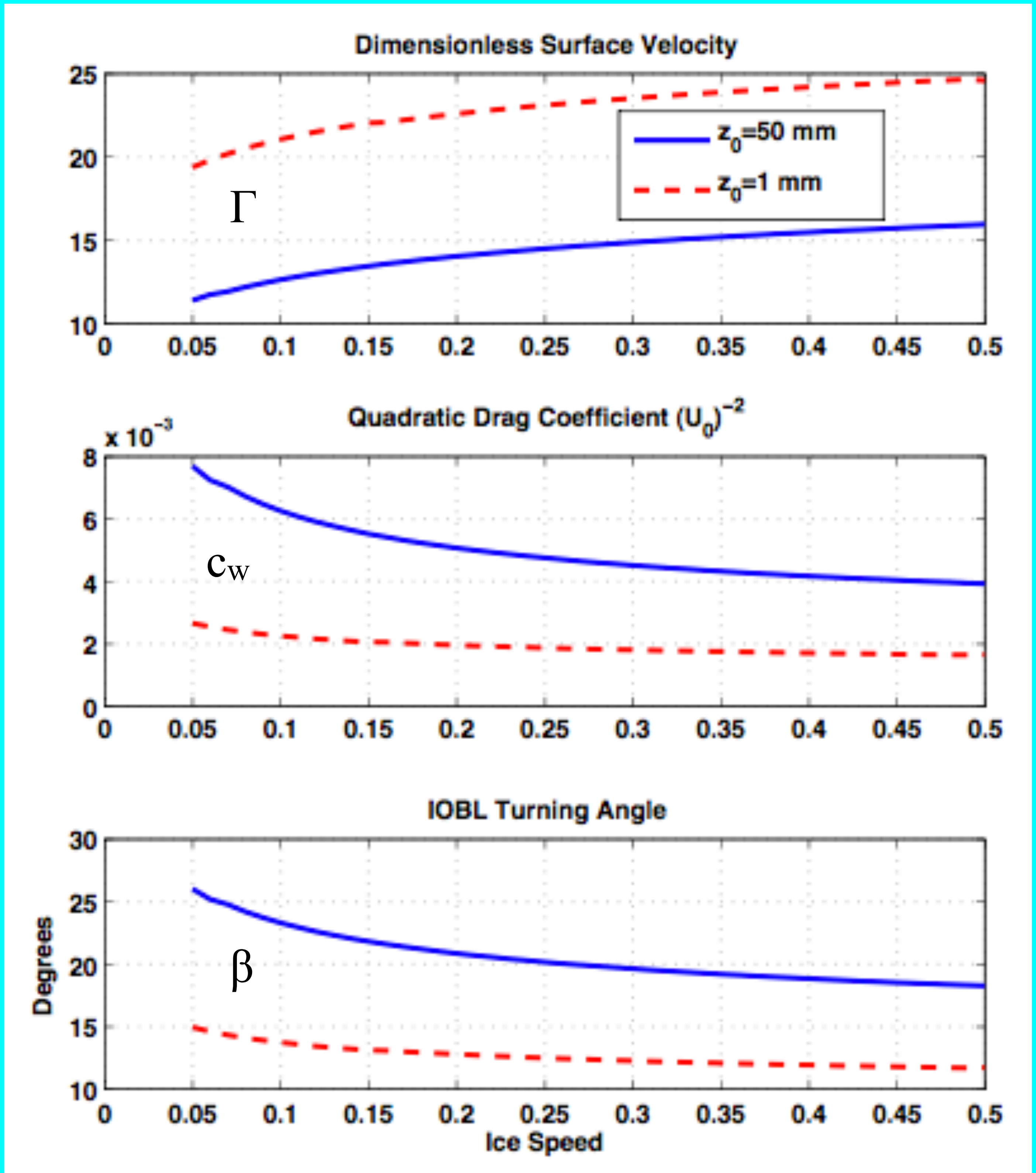

SLTC Roughness Estimates

SLTC Roughness Estimates

Location	z_0	Type	
ISPOL (western Weddell)	40 mm	Multiyear pack ice	McPhee, Deep-Sea Res., 2008, doi;10.1016/j.dsr1012.2007
SHEBA (western Weddell)	49 mm	Multiyear pack ice	McPhee, Air-Ice-Ocean Interaction, 2008
NPEO (North Pole)	90 mm	Multiyear pack ice, highly deformed	Shaw et al., JGR, 2008, doi: 10.1029/2007JC004550
MaudNESS (eastern Weddell)	4 mm	Thin, first year ice	Sirevaag et al., JGR, 2010, doi: 10.1029/2008JC005141

SLTC Roughness Estimates

Location	z_0	Type	
ISPOL (western Weddell)	40 mm	Multiyear pack ice	McPhee, Deep-Sea Res., 2008, doi;10.1016/j.dsr1012.2007
SHEBA (western Weddell)	49 mm	Multiyear pack ice	McPhee, Air-Ice-Ocean Interaction, 2008
NPEO (North Pole)	90 mm	Multiyear pack ice, highly deformed	Shaw et al., JGR, 2008, doi: 10.1029/2007JC004550
MaudNESS (eastern Weddell)	4 mm	Thin, first year ice	Sirevaag et al., JGR, 2010, doi: 10.1029/2008JC005141

Rough guidelines for hydraulic roughness, z_0:

Multiyear pack, identifiable floes:	$40-60$ mm
Highly deformed ice, marginal ice zones:	$80-120$ mm
Thin, first-year ice:	$1-5$ mm
Undeformed fast ice:	$z_{0s} \approx (\nu / u_{*0}) e^2$

(hydraulically smooth, Hinze [1975])

Impact of Stratification

Impact of Stratification

Neutral stratification, 2 length scales (the smaller scale governs):
|z|, and the planetary scale, u_{*0}/f, and associated mixing lengths

$$
\begin{aligned}
\lambda_{\mathrm{sl}} &= \kappa|z|; && |z| < \Lambda_* u_{*0}/(\kappa f) \\
\lambda_{\mathrm{Ek}} &= \Lambda_* u_{*0}/f; && |z| \geq \Lambda_* u_{*0}/(\kappa f)
\end{aligned}
$$

Impact of Stratification

Neutral stratification, 2 length scales (the smaller scale governs):
$|z|$, and the planetary scale, u_{*0}/f, and associated mixing lengths

$$\lambda_{\mathrm{sl}} = \kappa |z|; \qquad |z| < \Lambda_* u_{*0}/(\kappa f)$$
$$\lambda_{\mathrm{Ek}} = \Lambda_* u_{*0}/f; \qquad |z| \geq \Lambda_* u_{*0}/(\kappa f)$$

Melting or freezing at the ice/water interface introduces buoyancy flux, and a third turbulent scale, the Obukhov length:

$$L = \frac{u_{*0}^3}{\kappa \langle w'b' \rangle_0} \qquad \left(\text{where } \langle w'b' \rangle_0 = \frac{g}{\rho} \langle w'\rho' \rangle_0\right)$$

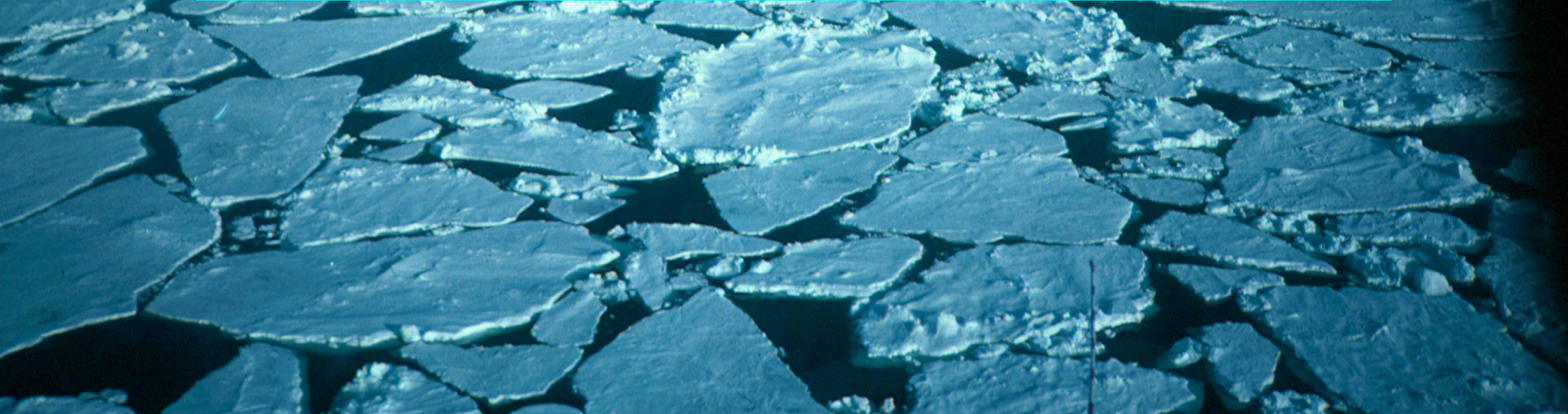

Impact of Stratification

Neutral stratification, 2 length scales (the smaller scale governs): |z|, and the planetary scale, u_{*0}/f, and associated mixing lengths

$$\lambda_{\mathrm{sl}} = \kappa|z|; \qquad |z| < \Lambda_* u_{*0}/(\kappa f)$$
$$\lambda_{\mathrm{Ek}} = \Lambda_* u_{*0}/f; \qquad |z| \geq \Lambda_* u_{*0}/(\kappa f)$$

Melting or freezing at the ice/water interface introduces buoyancy flux, and a third turbulent scale, the Obukhov length:

$$L = \frac{u_{*0}^3}{\kappa\langle w'b'\rangle_0} \qquad \left(\text{where } \langle w'b'\rangle_0 = \frac{g}{\rho}\langle w'\rho'\rangle_0\right)$$

When L is small and positive, buoyancy flux from melting quells turbulence, decreases turbulence scales, and increases shear.

When L is small in magnitude and negative, buoyancy flux from freezing enhances turbulence, increases turbulence scales, and decreases shear.

Stratification (continued)

Stratification (continued)

Consider stabilizing buoyancy flux, either from melting at the boundary, or from an existing density gradient in the IOBL

Dimensionless TKE equation: $1+\frac{P_b}{P_S}=1-R_f=1-\frac{\lambda}{\kappa L}=\frac{\varepsilon\lambda}{u_*^3}$

Stratification (continued)

Consider stabilizing buoyancy flux, either from melting at the boundary, or from an existing density gradient in the IOBL

Dimensionless TKE equation: $$1+\frac{P_b}{P_S}=1-R_f=1-\frac{\lambda}{\kappa L}=\frac{\varepsilon\lambda}{u_*^3}$$

For viable turbulence the flux Richardson number is less than a critical value, $R_c \approx 0.2$

$$R_f=\frac{\langle w'b'\rangle\lambda}{u_*^3}<R_c \quad \Rightarrow \quad \lambda_{\max}<R_c\kappa L$$

AIO, Ch 4

Adymptotes: $\lambda_{\max}\to\Lambda_* u_*/f$ for $L=u_*^3/(\kappa\langle w'b'\rangle)\to\infty$

$\lambda_{\max}\to R_c\kappa L$ for $L\to 0^+$

Stratification (continued)

Consider stabilizing buoyancy flux, either from melting at the boundary, or from an existing density gradient in the IOBL

Dimensionless TKE equation: $1+\dfrac{P_b}{P_S}=1-R_f=1-\dfrac{\lambda}{\kappa L}=\dfrac{\varepsilon\lambda}{u_*^3}$

For viable turbulence the flux Richardson number is less than a critical value, $R_c \approx 0.2$

$$R_f=\frac{\langle w'b'\rangle\lambda}{u_*^3}<R_c \qquad \Rightarrow \qquad \lambda_{\max}<R_c\kappa L$$

Adymptotes: $\lambda_{\max}\to\Lambda_* u_*/f$ for $L= u_*^3\big/\left(\kappa\langle w'b'\rangle\right)\to\infty$

$\lambda_{\max}\to R_c\kappa L$ for $L\to 0^+$

AIO, Ch 4

An expression with these limits:

$$\lambda_{\max}=\eta_*\Lambda_* u_*/f$$

where $\eta_*=\left(1+\dfrac{\Lambda_*\mu_*}{\kappa R_c}\right)^{-1/2}$

and $\mu_*=u_*/(fL)$ is the ratio of the planetary length scale to the Obukhov length

Stratification (continued)

With stable stratification ($\eta_* \leq 1$)

the similarity scales are:

Length: $\eta_* u_* / f$

Velocity: $\hat{u}_* / \eta_*$

Eddy viscosity $(\eta_* u_*)^2 / f$

Kinematic stress: $u_* \hat{u}_* / f$

$$\hat{\Gamma}(Ro_*, \mu_*) = \hat{v}_0 / \hat{u}_{*0}$$

$$= \frac{1}{\kappa}\left[\log Ro_* - A(\mu_*) \mp iB(\mu_*)\right]$$

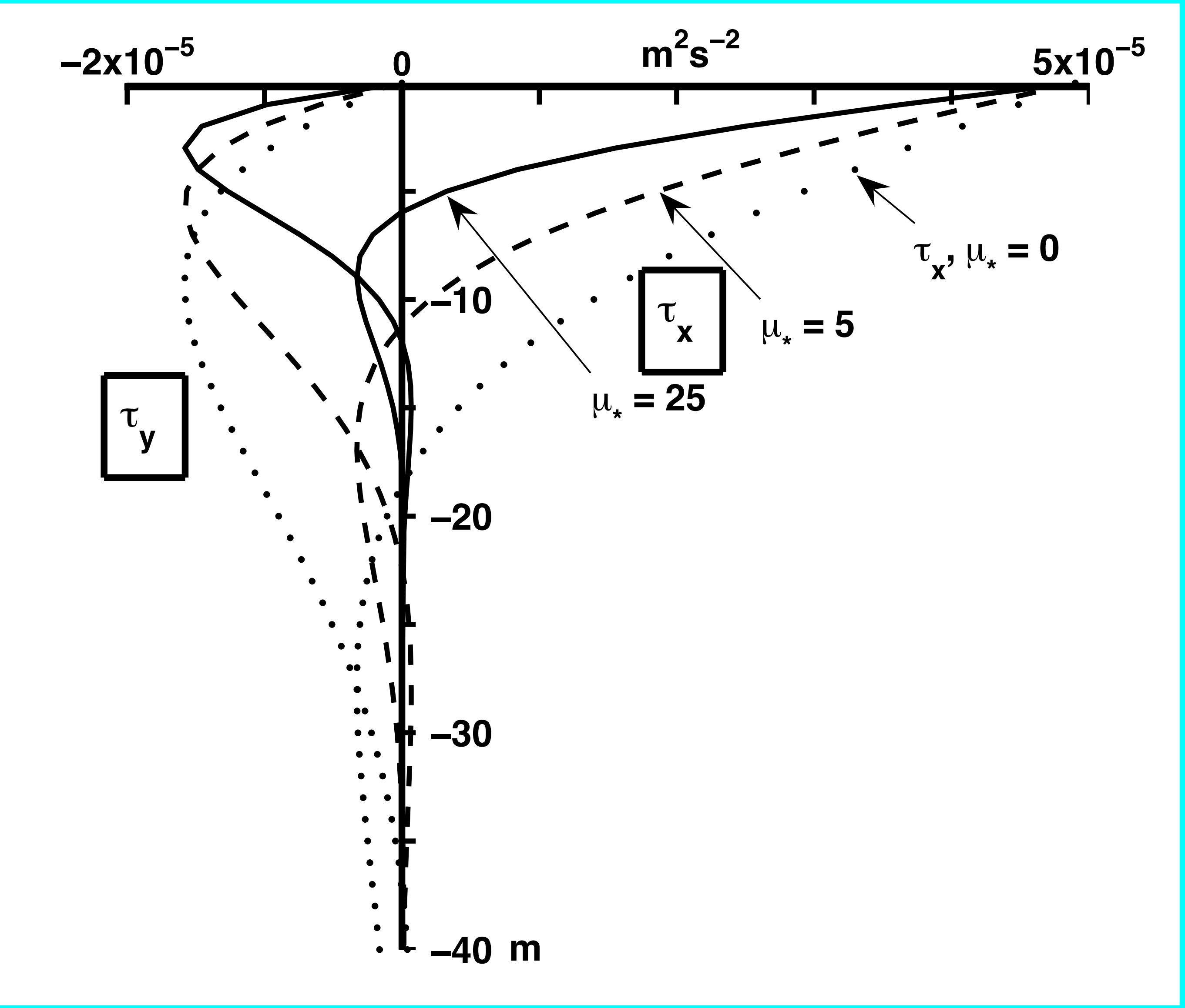

McPhee, M. G, 1981: An analytic similarity theory for the planetary boundary layer stabilized by surface buoyancy, Boundary-Layer Meterol., 21, 325-339.

Stratification (continued)

The impact of rapid melting is to reduce the turbulent length scale, and increase the velocity scale. It increases both *A* and *B*, which reduces the effective drag and increases the turning angle.

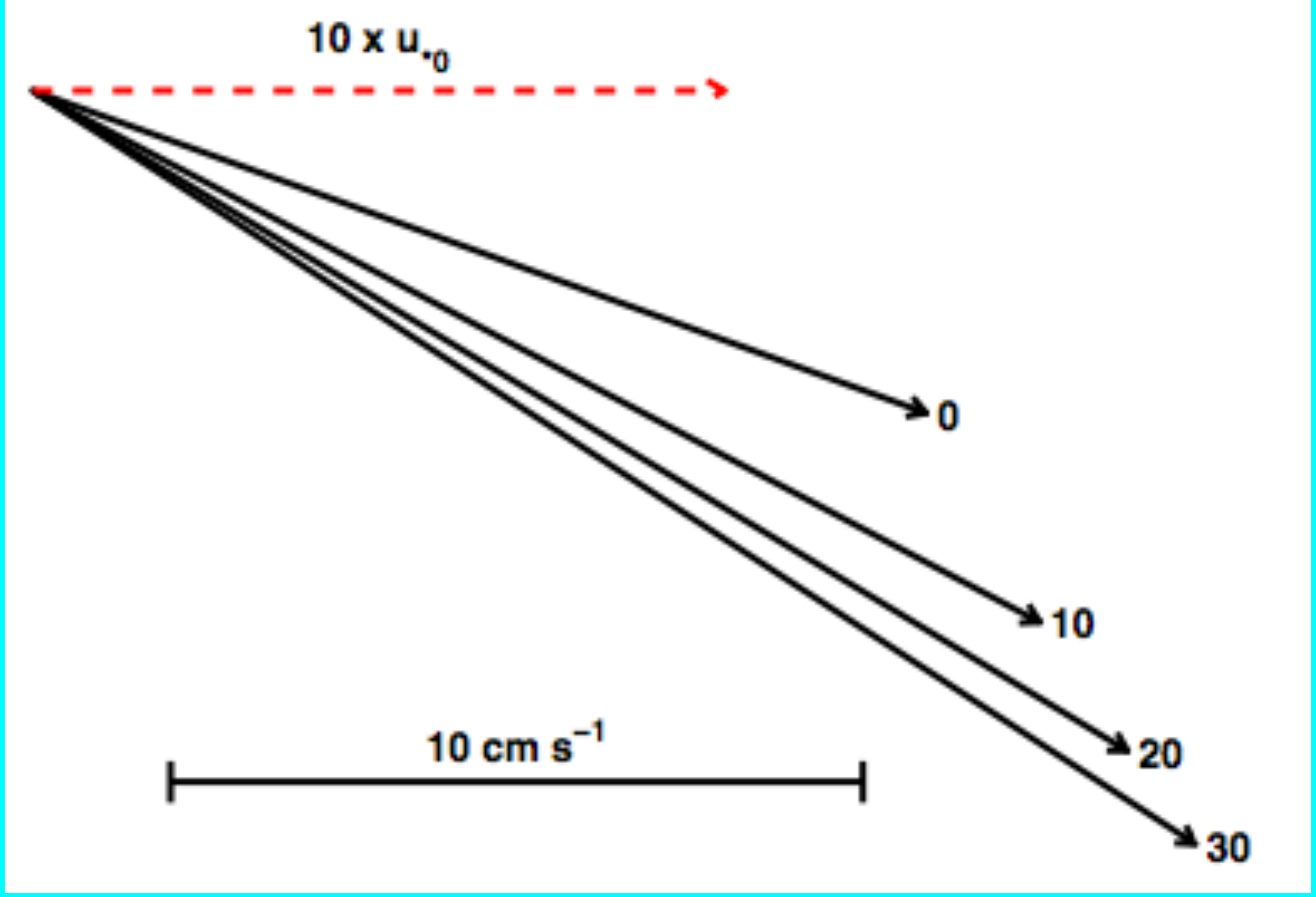

Example for:

$u_{*0} = 0.01\ \mathrm{m\ s^{-1}}$

$z_0 = 0.05\ \mathrm{m}$

and melt rate ranging from 0 to 30 cm/day

The rapidly melting ice (water about 2^{o}C) drifts about 6.5 km farther in a day.


Approaching band from the
north, looking east

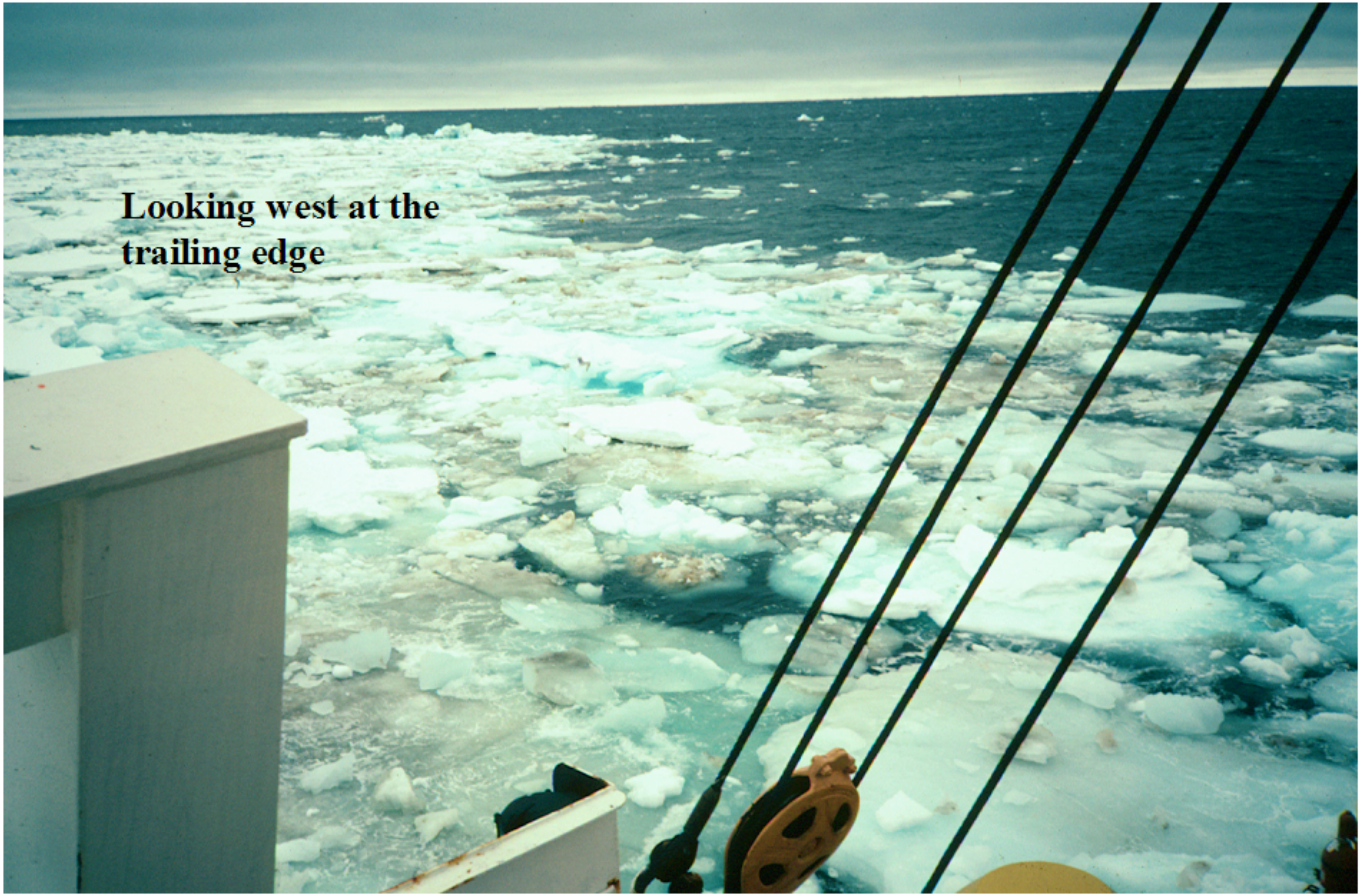
Looking west at the
trailing edge

Stratification: Shallow Pycnoclines

Stratification: Shallow Pycnoclines

In the western Arctic, there has been a remarkable increase in freshwater content over the past decade. This tends to stratify the water column closer to the surface, so the depth of the mixed layer adds a 4th length scale to the IOBL turbulence.

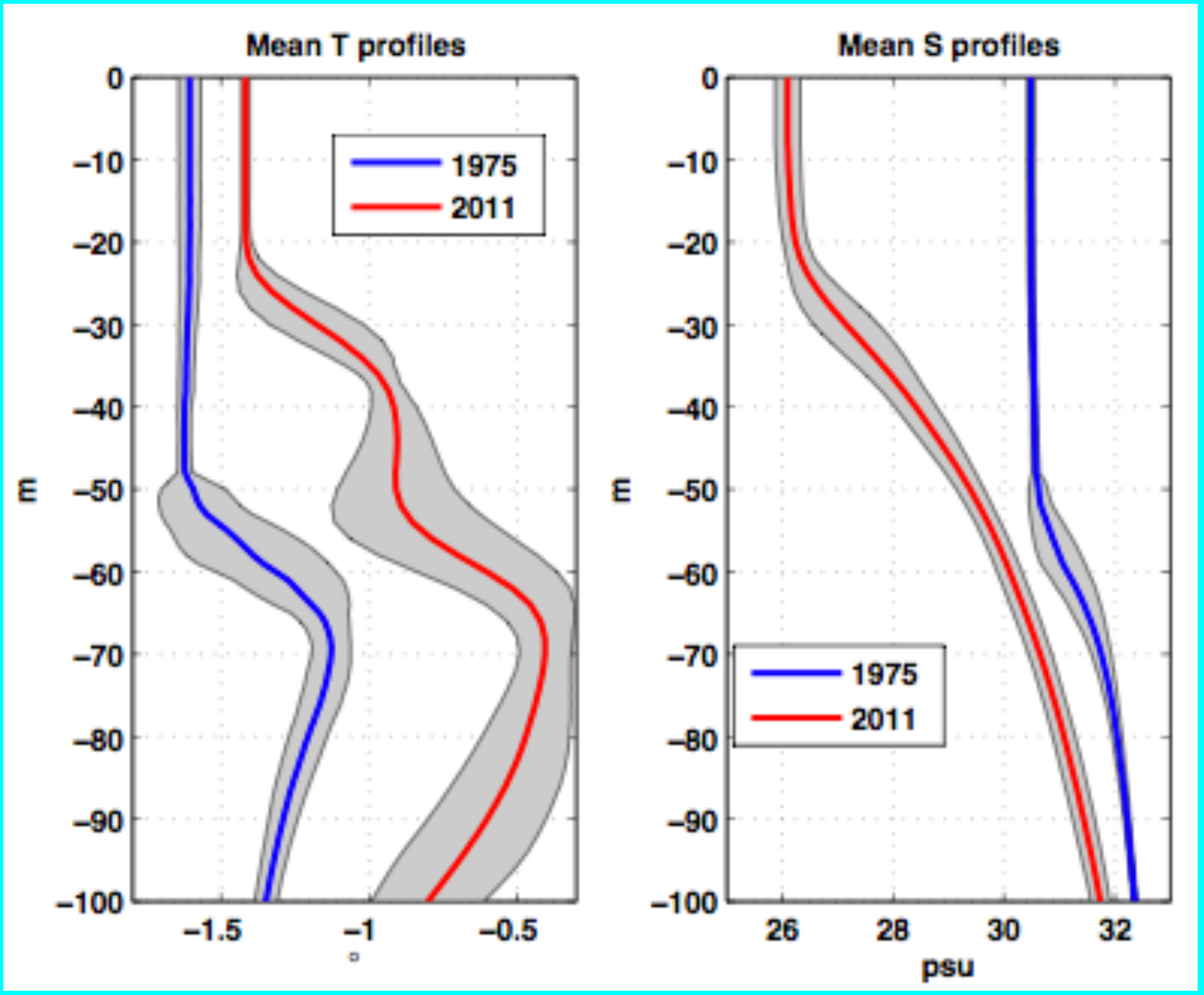

To address this part of the problem requires treatment of fluxes in the upper part of the pycnocline, which requires rudimentary numerical modeling.

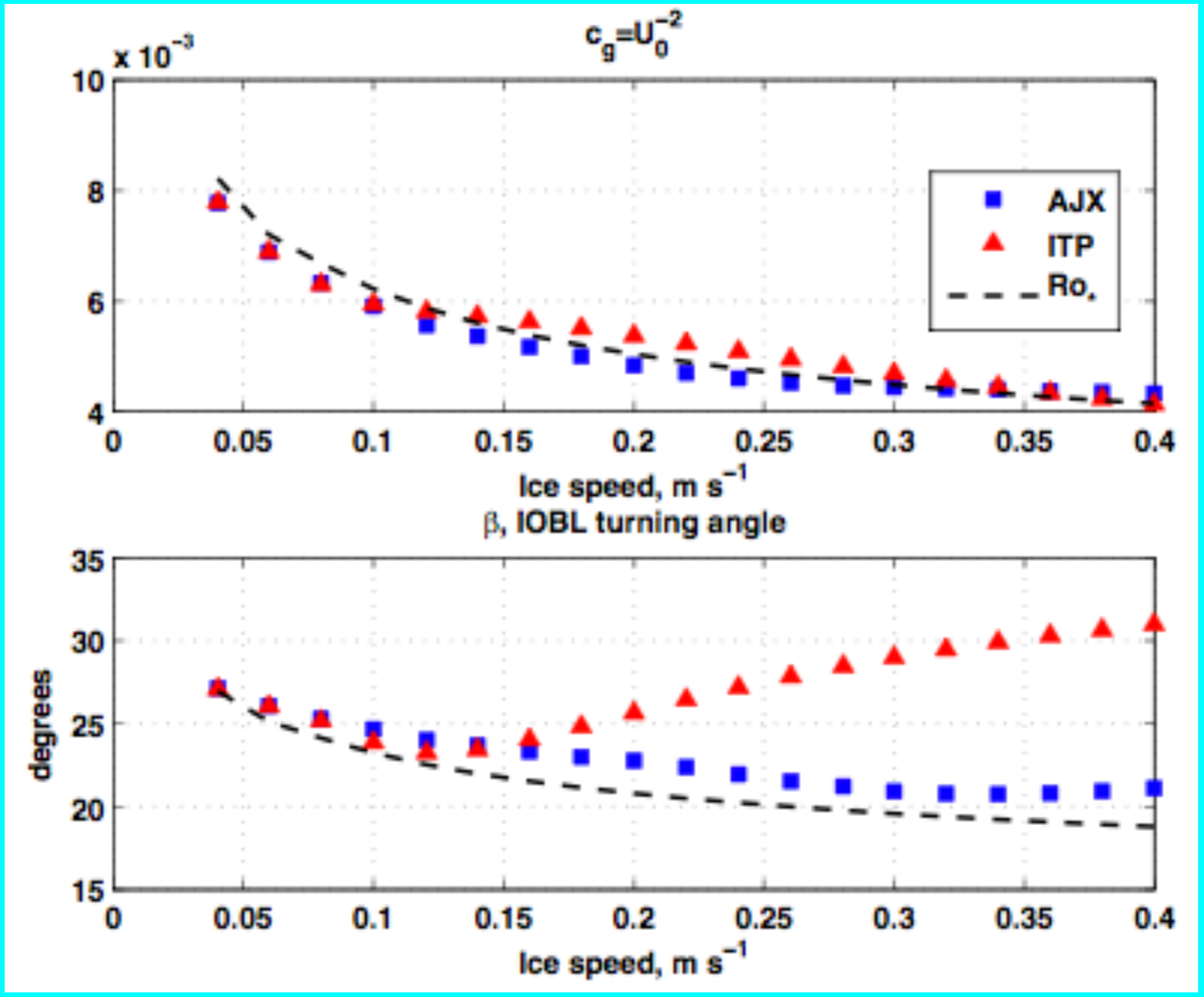

A first-order turbulent closure model I call *steady local turbulence closure* (SLTC) uses the same similarity principles as the 1981 similarity theory, but considers stratification in the outer part of the IOBL.

AIO, Ch 9

Statically Unstable Buoyancy Flux

Statically Unstable Buoyancy Flux

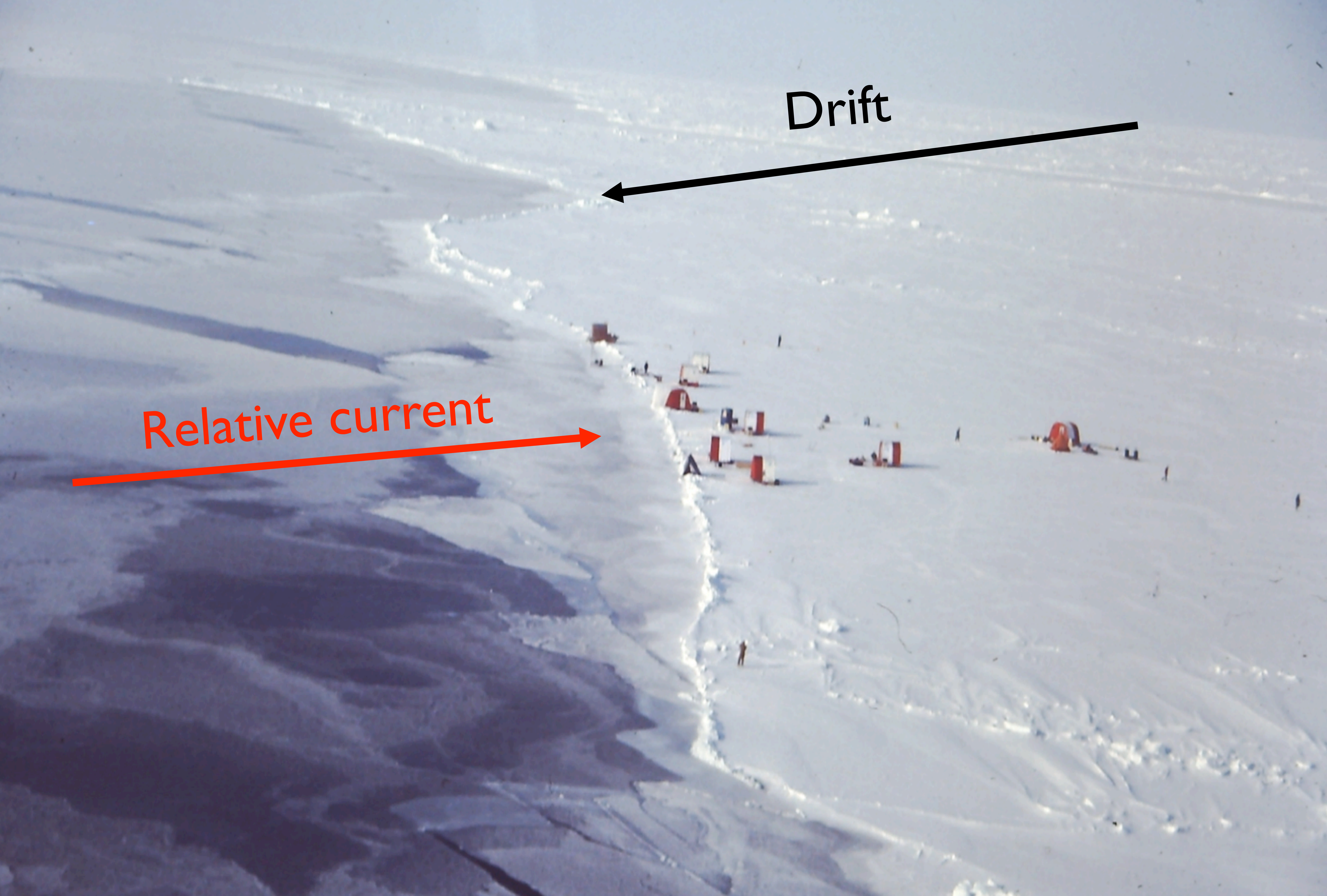

Statically Unstable Buoyancy Flux

Estimates of λ from wavenumber peaks in *w* spectra at the edge of a freezing lead during the 1992 LEADEX project. During this time the average buoyancy flux was:

$$\langle w'b' \rangle = -7.8\times10^{-8}\ \mathrm{m^2 s^{-3}}$$

AIO, section 5.3

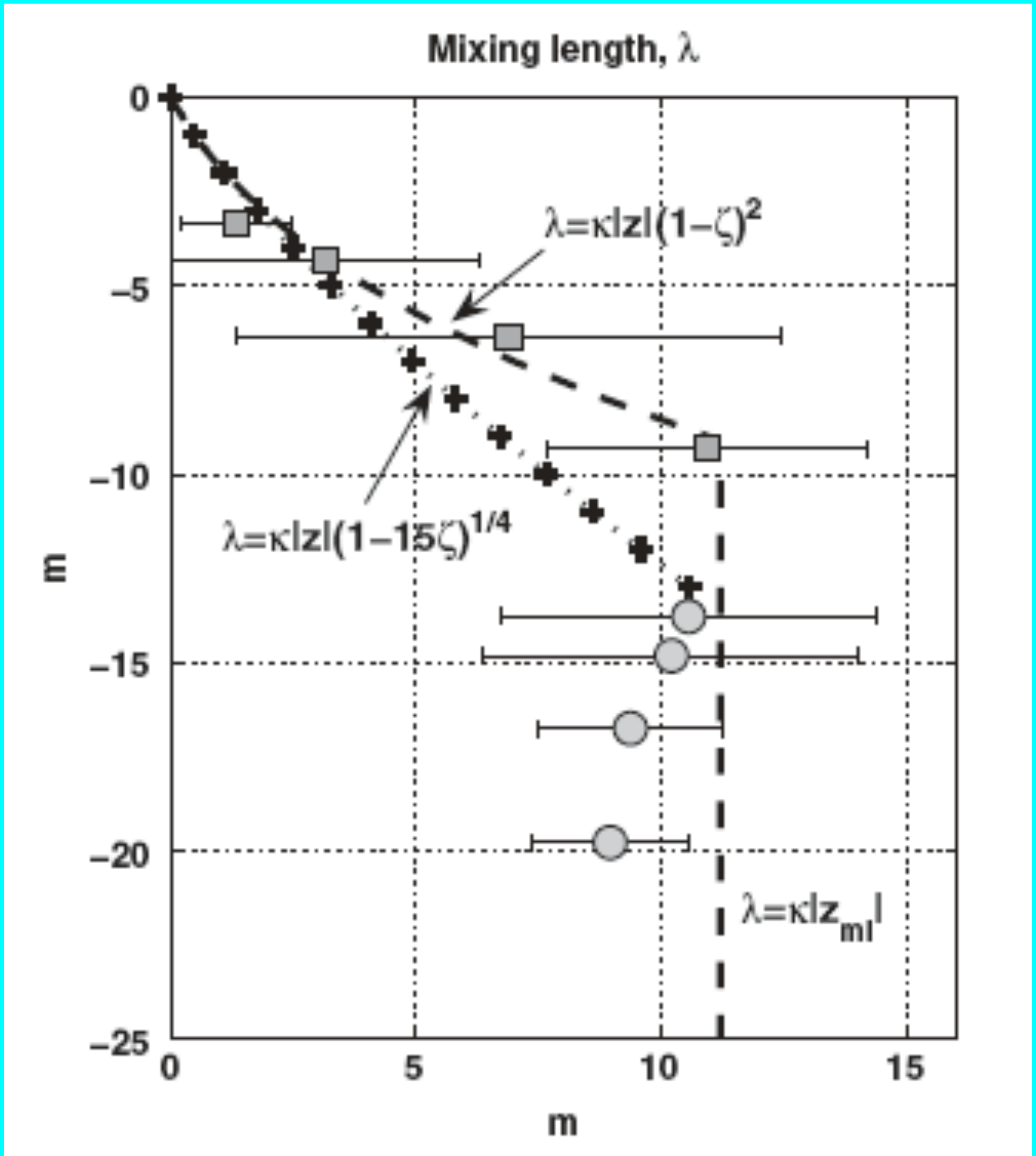

McPhee and Stanton, 1996, *J. Geophys. Res.*, *101*, 6409-6428.

Neutral (no interface buoyancy flux) OBL

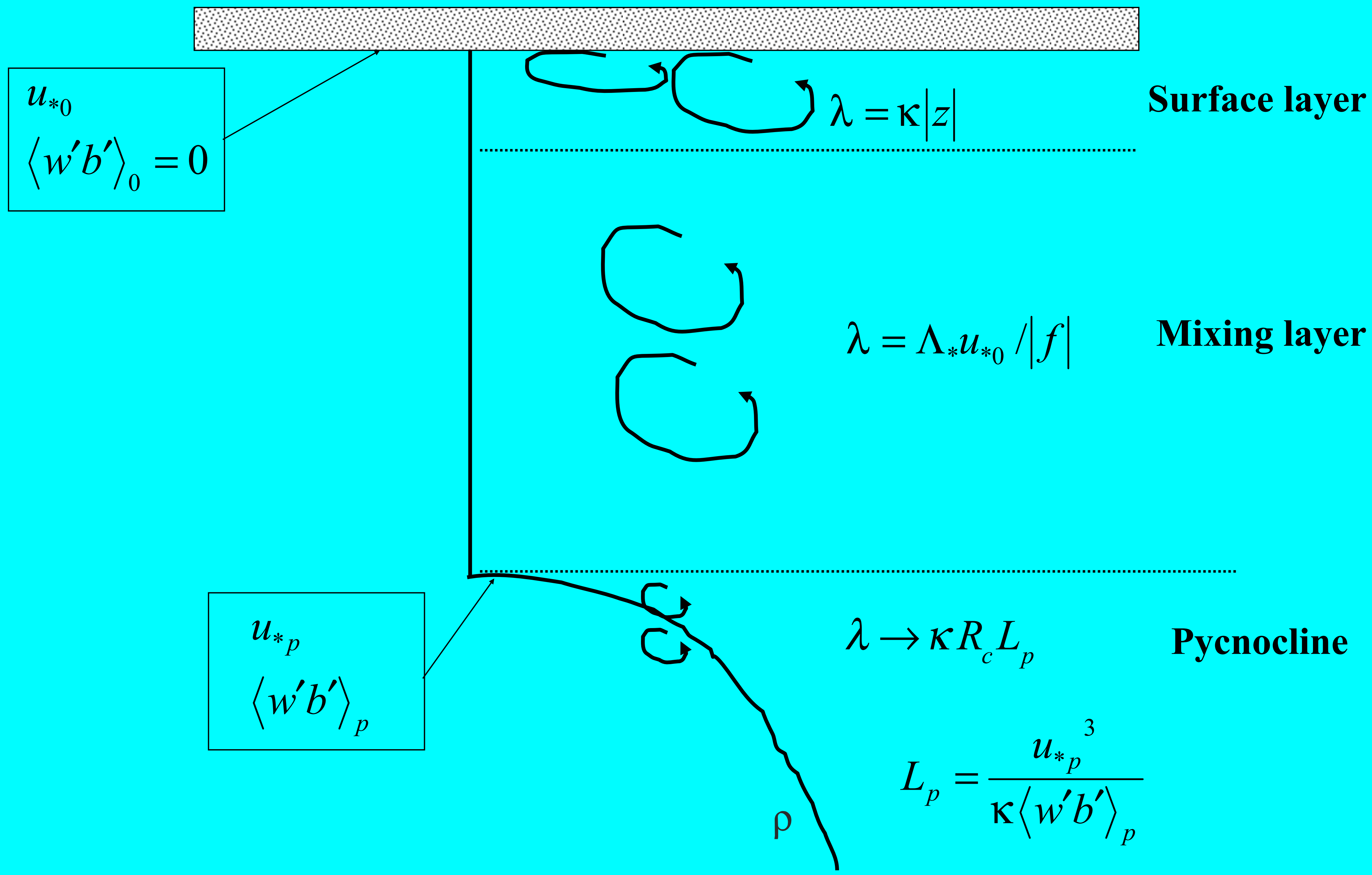

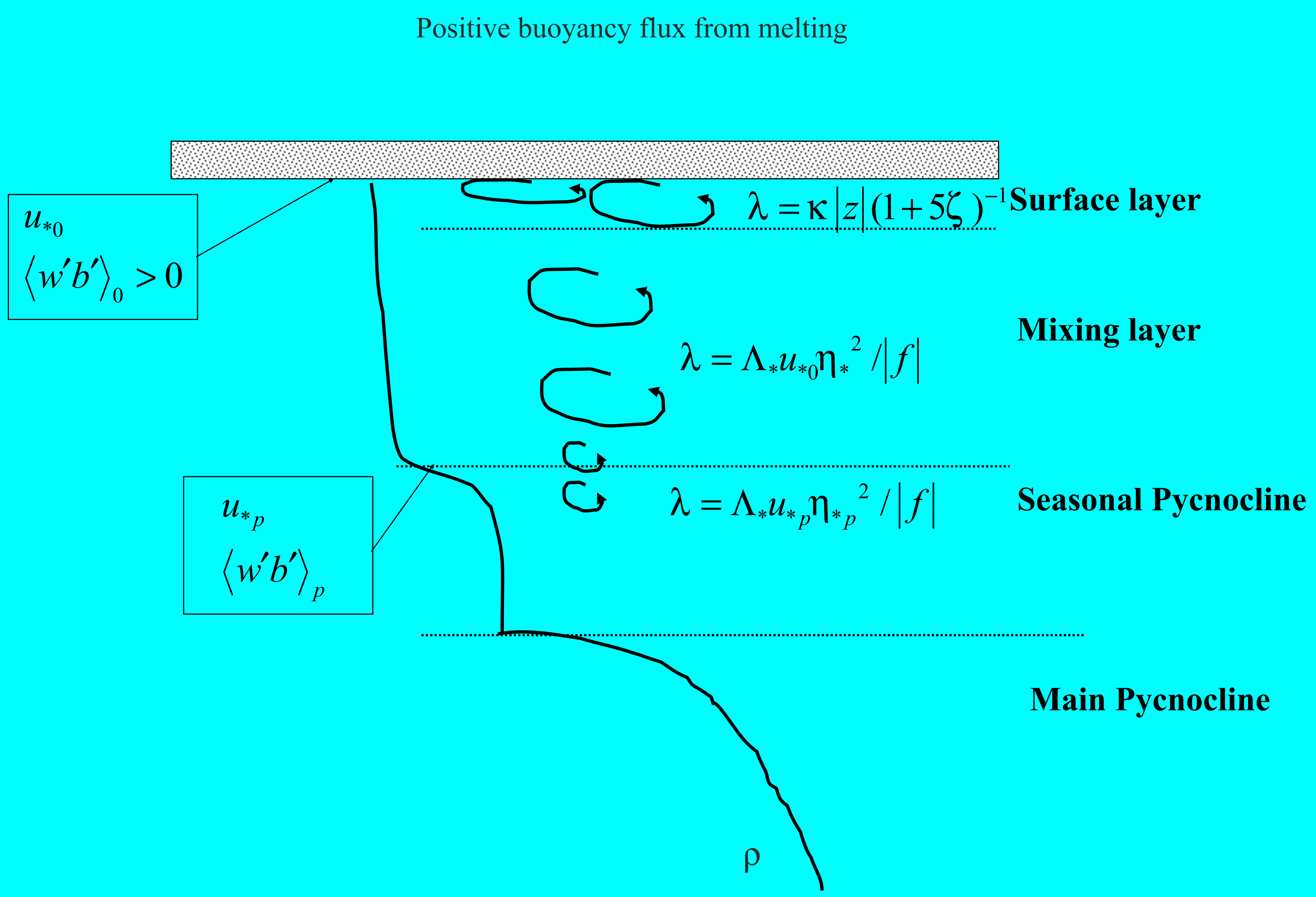

Positive buoyancy flux from melting
u_{*0}
$\langle w'b' \rangle_0 > 0$
$\lambda = \kappa |z| (1+5\zeta)^{-1}$
Surface layer
Mixing layer
$\lambda = \Lambda_* u_{*0} \eta_*^{\,2} / |f|$
Seasonal Pycnocline
u_{*p}
$\langle w'b' \rangle_p$
$\lambda = \Lambda_* u_{*p} \eta_{*p}^{\,2} / |f|$
Main Pycnocline
ρ

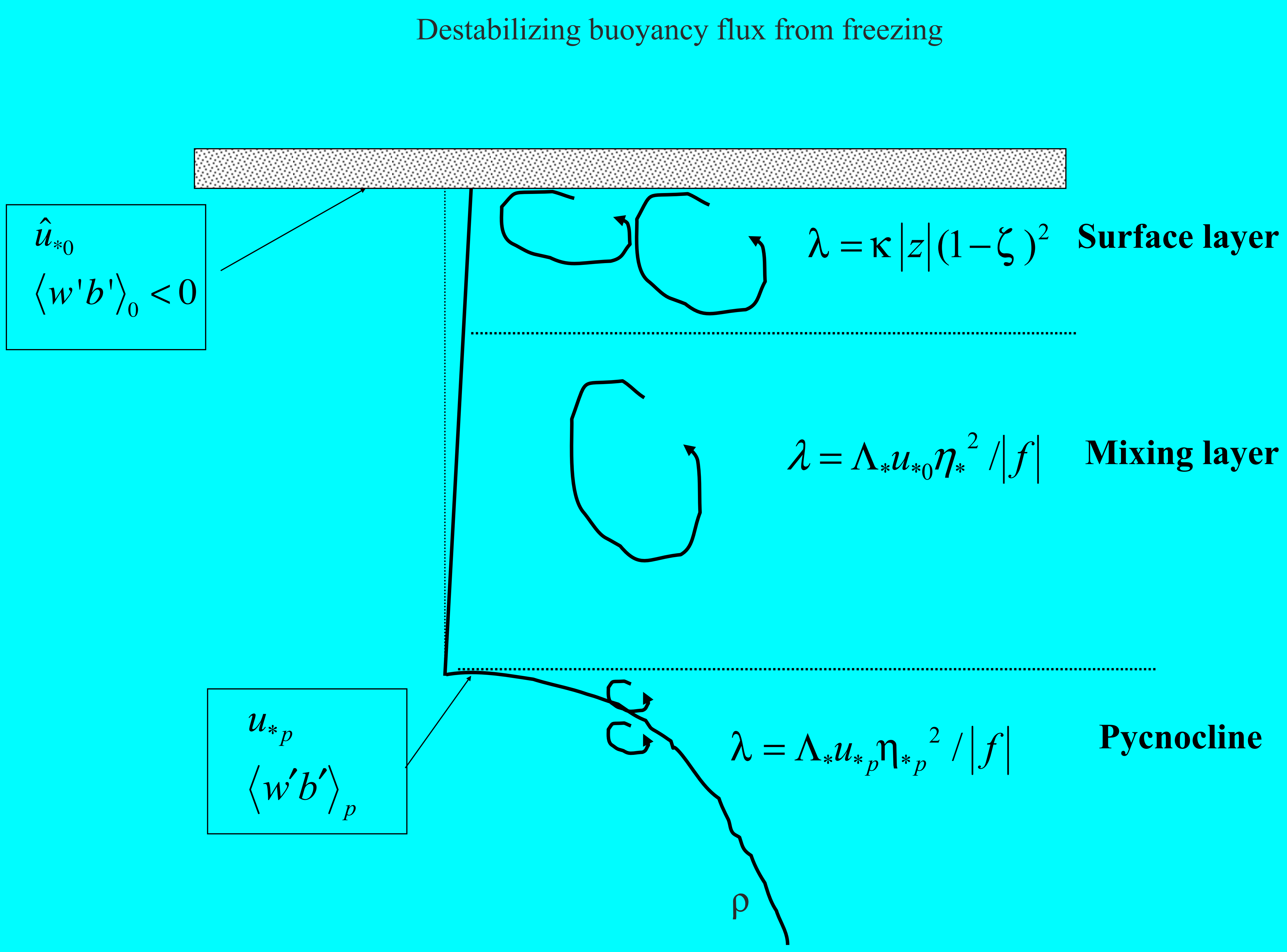
Destabilizing buoyancy flux from freezing
$\hat{u}_{*0}$
$\langle w'b' \rangle_0 < 0$
$\lambda = \kappa |z| (1-\zeta)^2$
Surface layer
$\lambda = \Lambda_* u_{*0} \eta_*^{\ 2} / |f|$
Mixing layer
u_{*p}
$\langle w'b' \rangle_p$
$\lambda = \Lambda_* u_{*p} \eta_{*p}^{\ 2} / |f|$
Pycnocline
ρ

Geostrophic Currents

Geostrophic Currents

Geopotential Anomaly: $\Phi'(p) = -\int_0^p \delta \, dp'$ units: $m^2 s^{-2}$

$\delta = \rho(T,S,p)^{-1} - \rho(0,35,p)^{-1}$ is specific volume anomaly

Dynamic height is $DH = \dfrac{-\Phi'}{g}$ units: dyn-m

Geostrophic Currents

Geopotential Anomaly: $\Phi'(p) = -\int_0^p \delta \, dp'$ units: $m^2 s^{-2}$

$\delta = \rho(T, S, p)^{-1} - \rho(0, 35, p)^{-1}$ is specific volume anomaly

Dynamic height is $DH = \dfrac{-\Phi'}{g}$ units: dyn-m

If flow is small at some reference pressure surface, p, then velocity at the surface ($p = 0$) due to horizontal density gradients above p is given by:

$$f\boldsymbol{k} \times \boldsymbol{v}_g = -\nabla \Phi'(p)$$

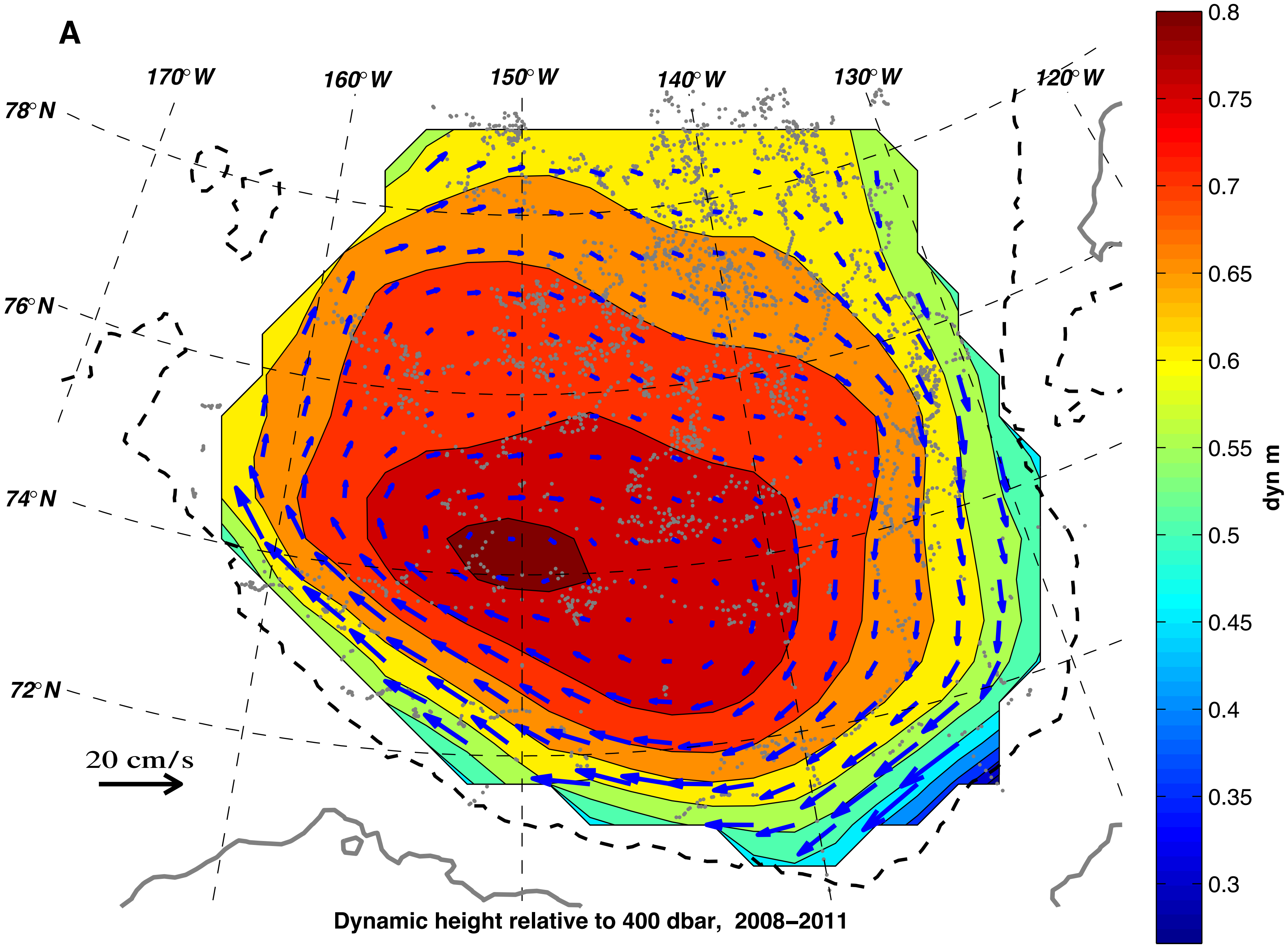

Dynamic height relative to 400 dbar, 2008–2011

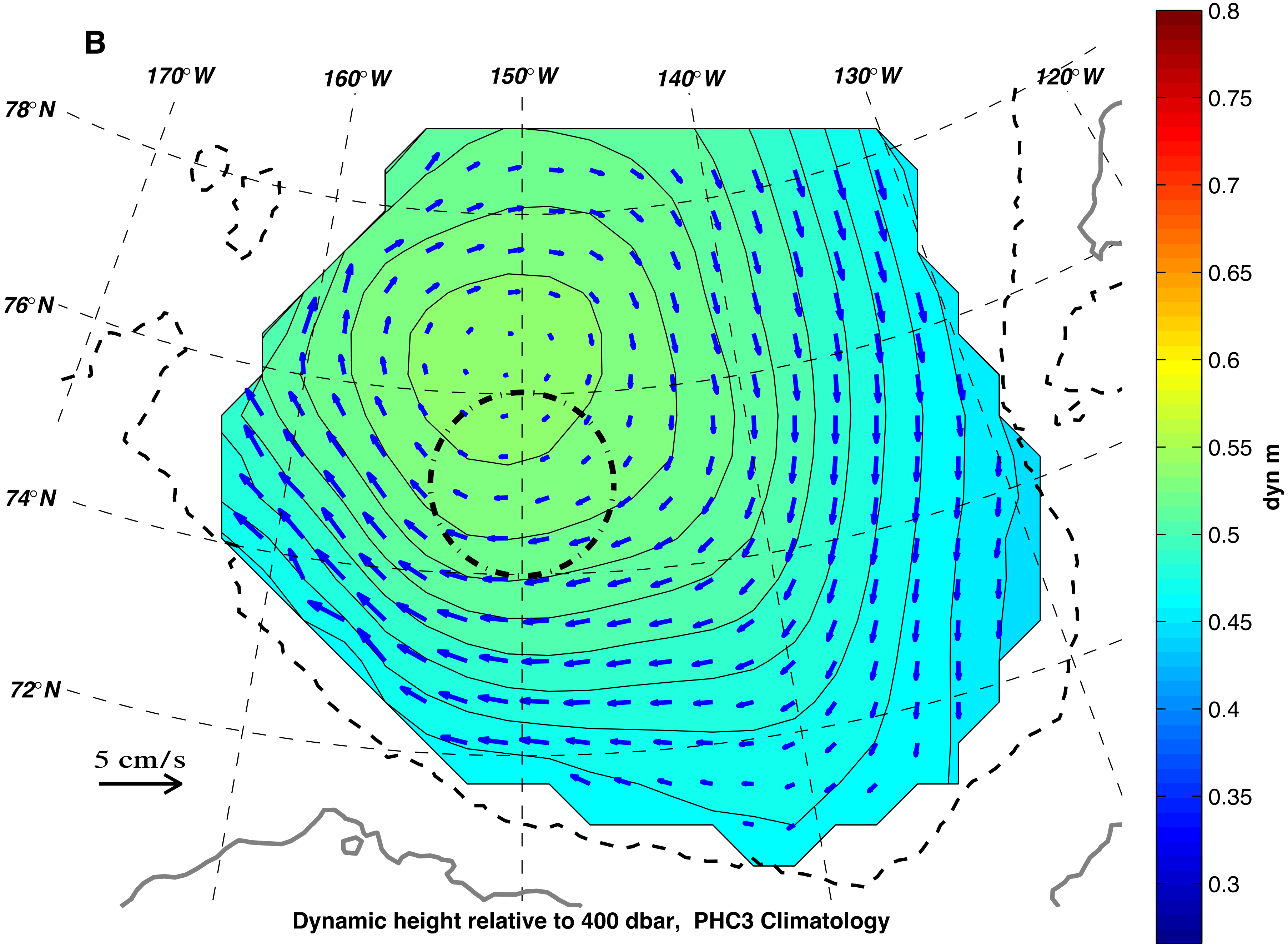

Dynamic height relative to 400 dbar, PHC3 Climatology

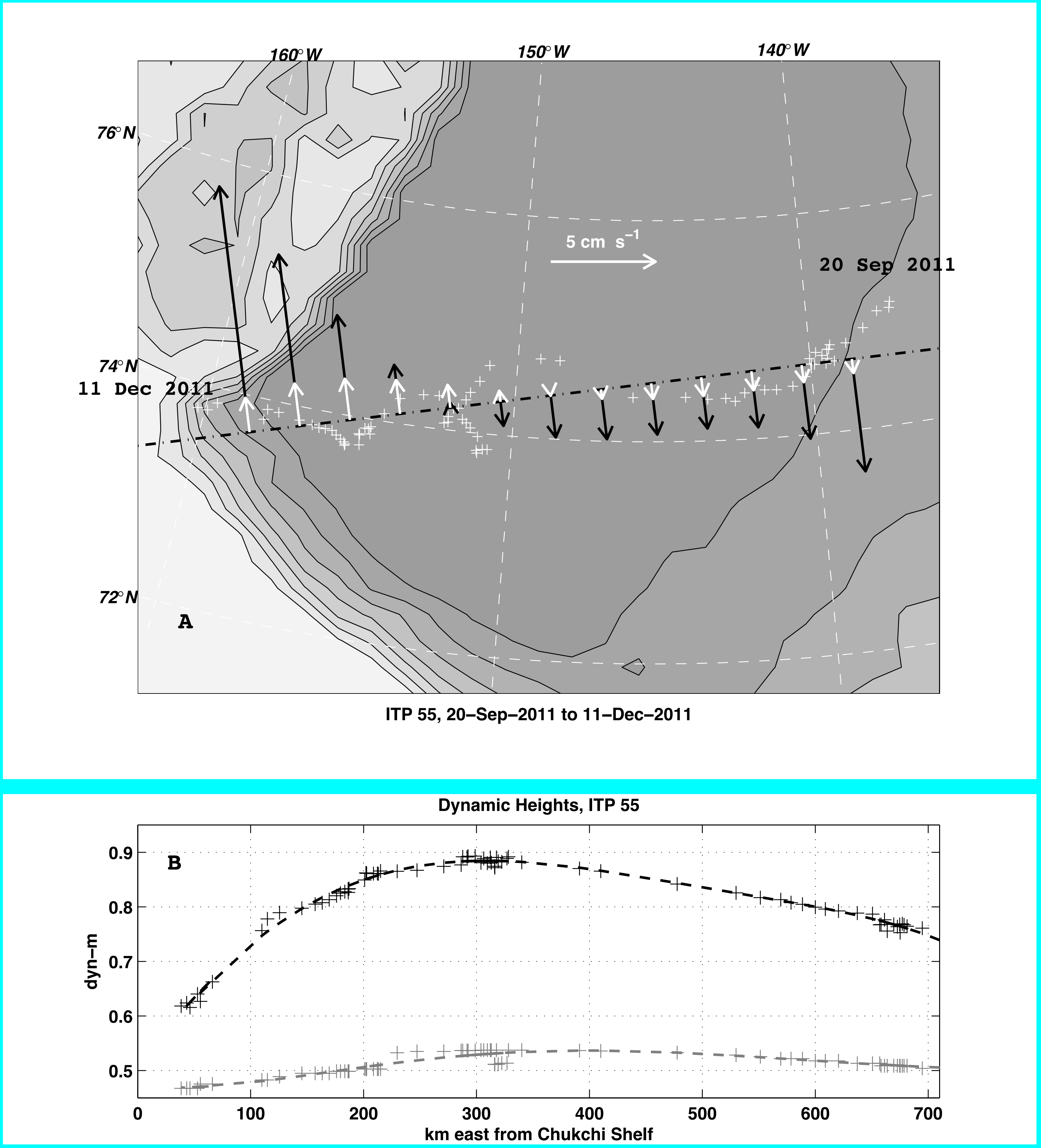
160° W
150° W
140° W
76° N
74° N
72° N
5 cm s^{-1}
20 Sep 2011
11 Dec 2011
A
ITP 55, 20–Sep–2011 to 11–Dec–2011
Dynamic Heights, ITP 55
B
dyn–m
0.9
0.8
0.7
0.6
0.5
0
100
200
300
400
500
600
700
km east from Chukchi Shelf


A
76° N
160° W
150° W
140° W
ITP 55 (2011)
Free–drift trajectory
20–Sep–2011
75° N
74° N
10–Dec–2011
100 km

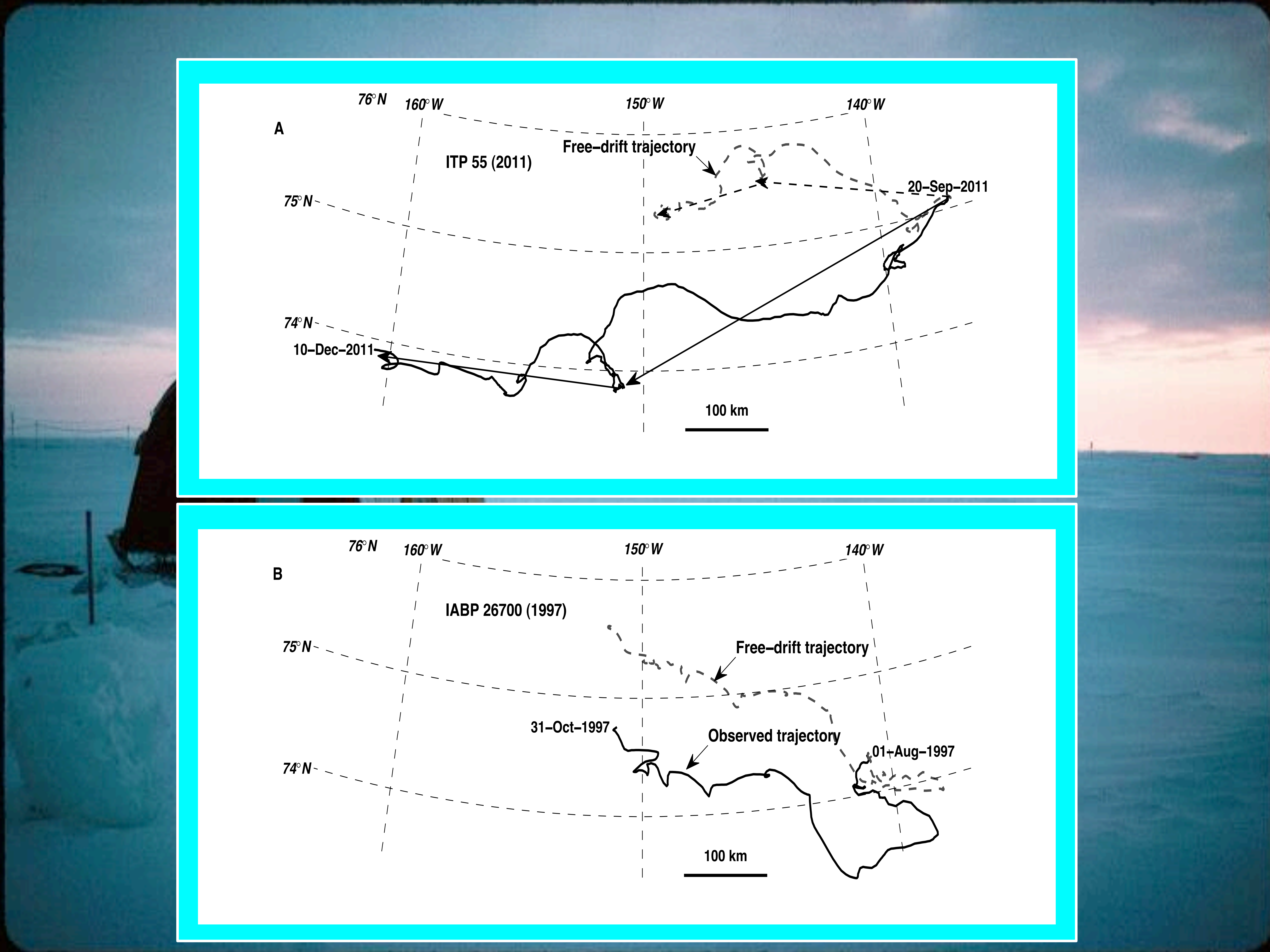
A
76° N
160° W
150° W
140° W
ITP 55 (2011)
Free–drift trajectory
75° N
20–Sep–2011
74° N
10–Dec–2011
100 km
B
76° N
160° W
150° W
140° W
IABP 26700 (1997)
75° N
Free–drift trajectory
31–Oct–1997
Observed trajectory
01–Aug–1997
74° N
100 km

Calculate the annual average of dynamic height near the center of the traditional Beaufort Gyre from 2003 to 2011.

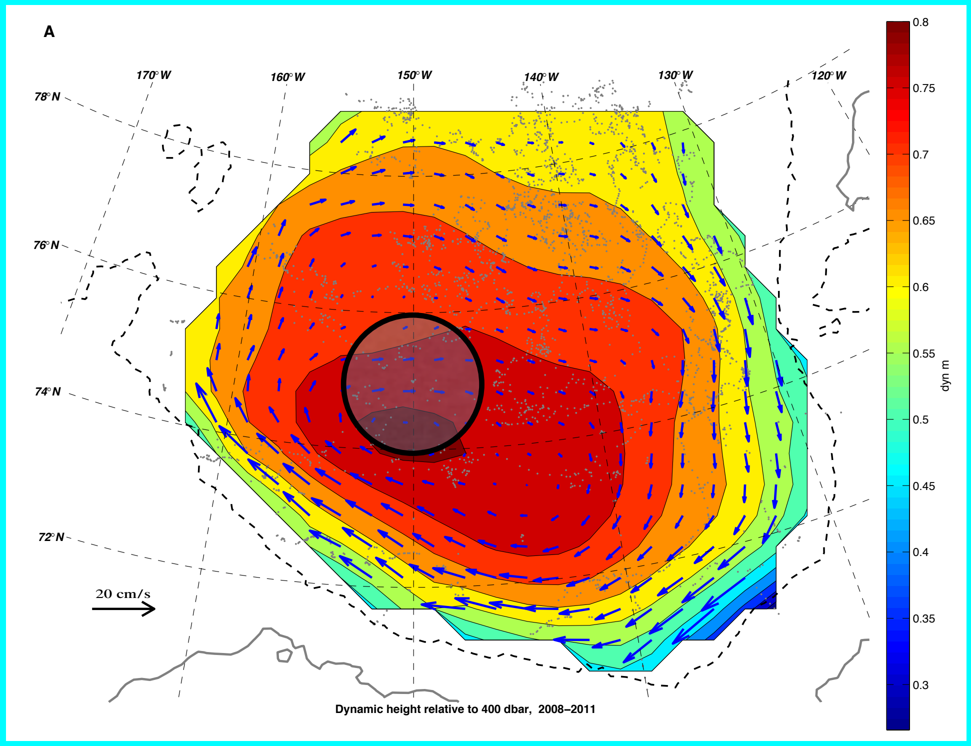

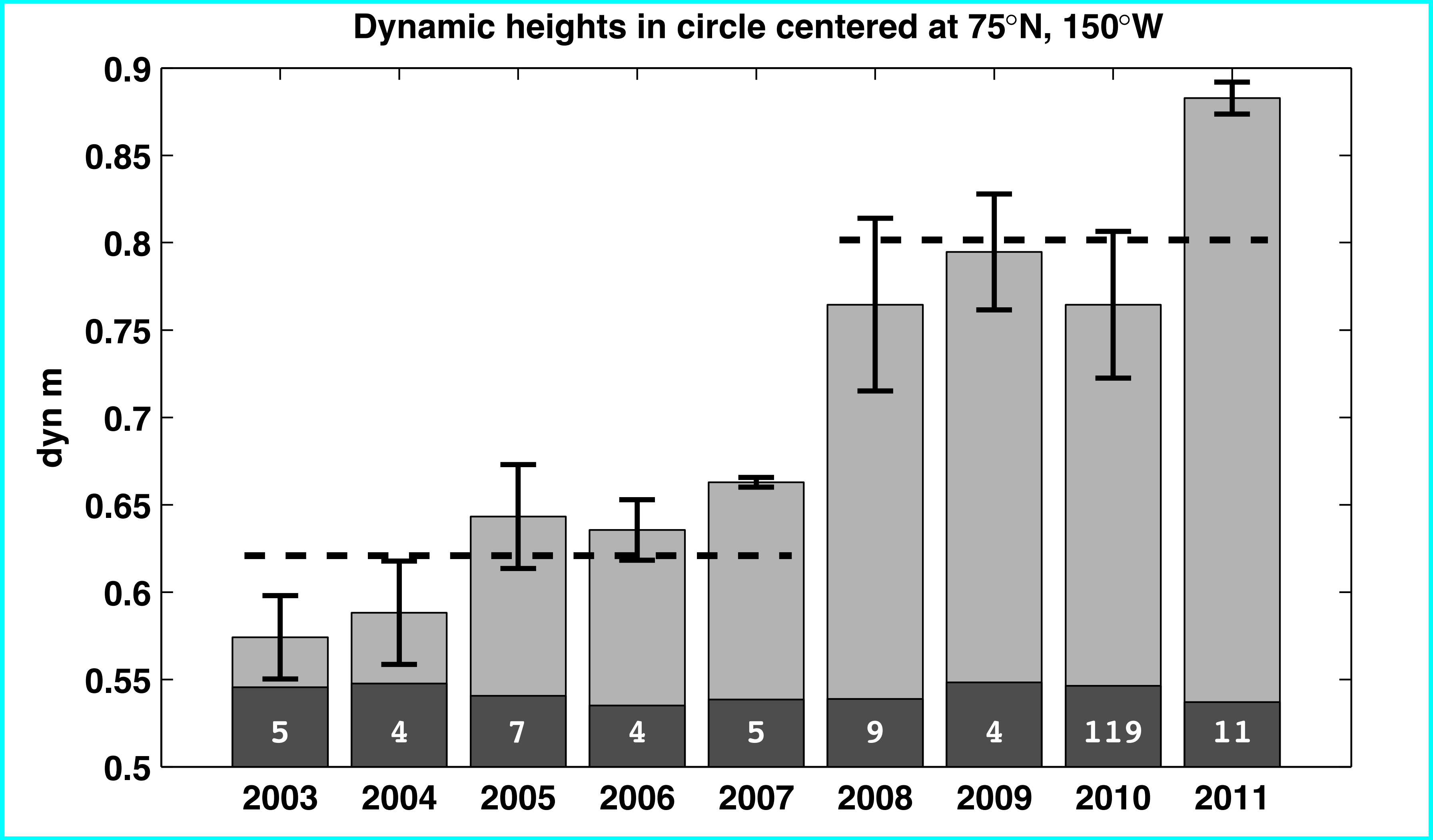

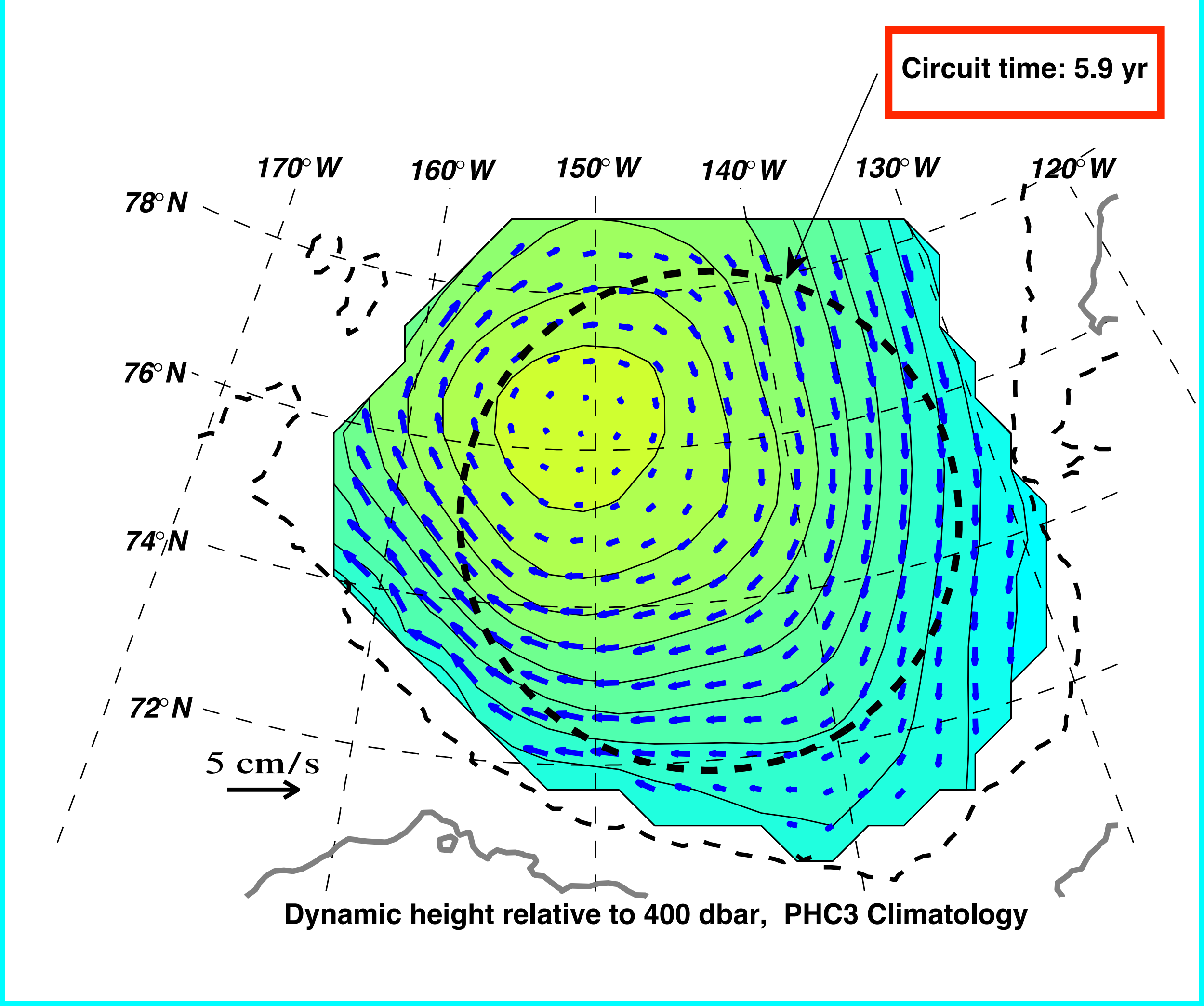
Circuit time: 5.9 yr
170° W
160° W
150° W
140° W
130° W
120° W
78° N
76° N
74° N
72° N
5 cm/s
Dynamic height relative to 400 dbar, PHC3 Climatology

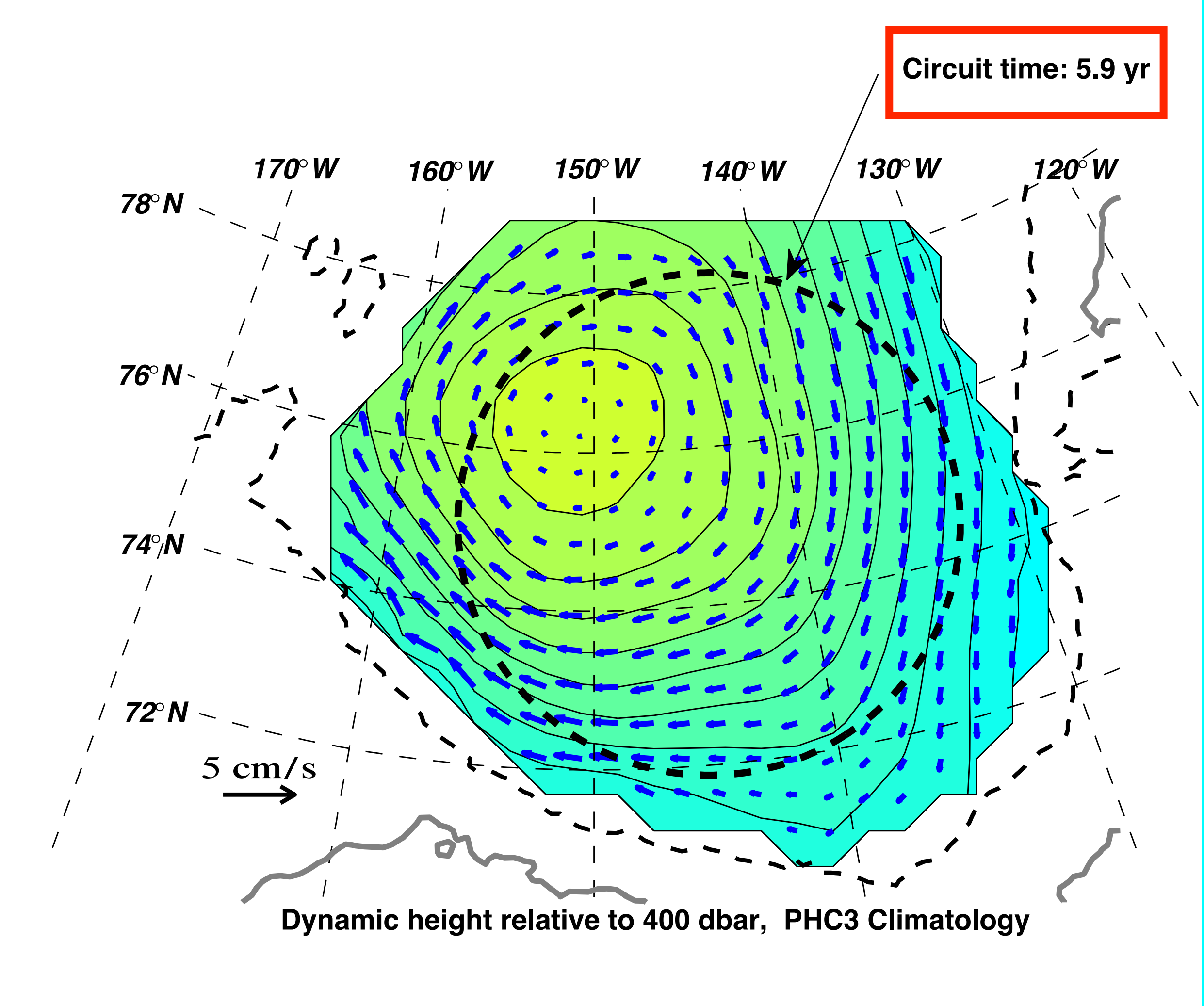
Circuit time: 5.9 yr
170° W
160° W
150° W
140° W
130° W
120° W
78° N
76° N
74° N
72° N
5 cm/s
Dynamic height relative to 400 dbar, PHC3 Climatology

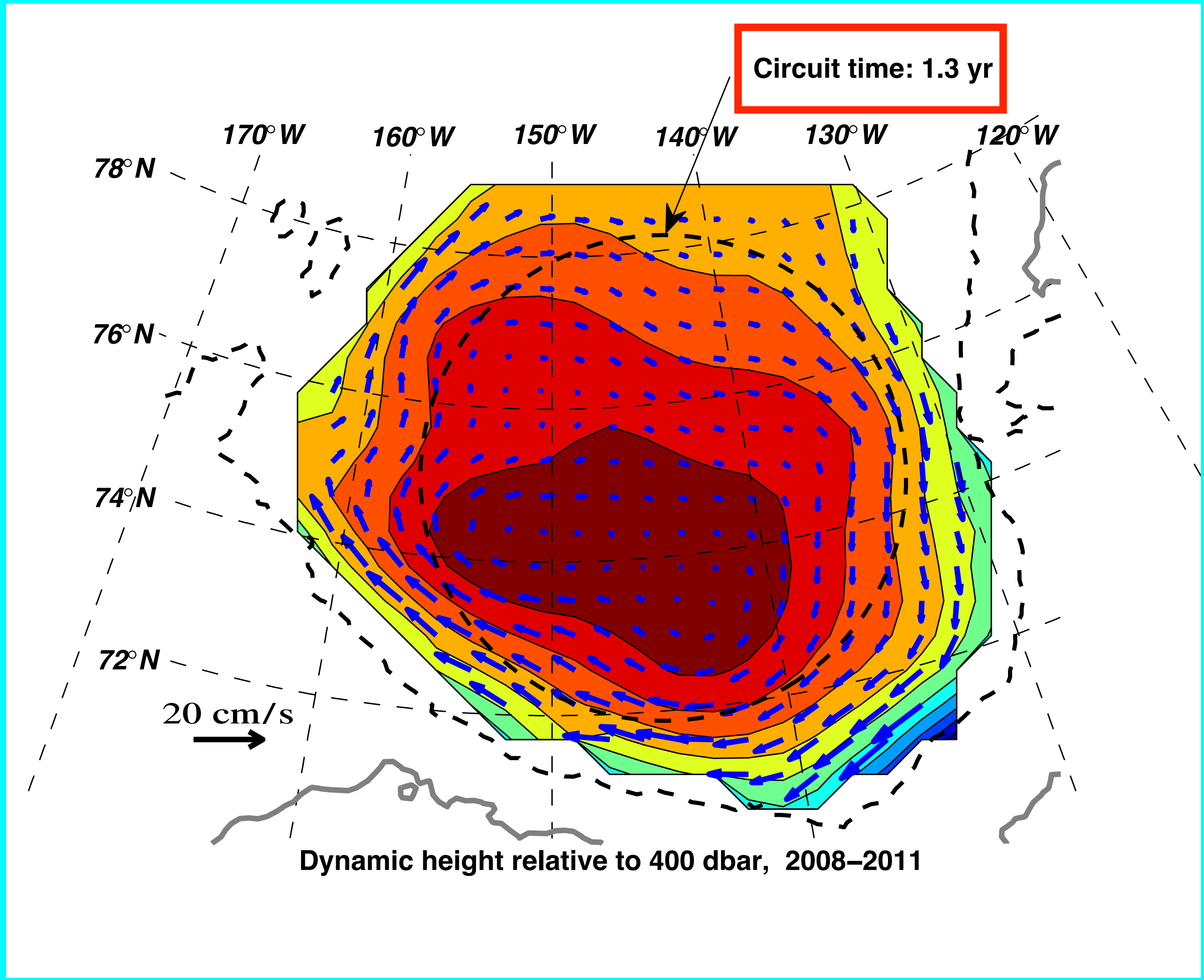
Circuit time: 1.3 yr
170° W
160° W
150° W
140° W
130° W
120° W
78° N
76° N
74° N
72° N
20 cm/s
Dynamic height relative to 400 dbar, 2008–2011

Ekman Pumping

Ekman Pumping

$$if\int_{z_{bl}}^{0}\boldsymbol{u}\,dz = if\boldsymbol{M} = \boldsymbol{\tau}_0$$

$$\nabla\cdot\boldsymbol{M} = -\int_{z_{bl}}^{0}\frac{\partial w}{\partial z}\,dz = w_{pyc} = \frac{1}{f}\nabla\times\boldsymbol{\tau}_0$$

Ekman Pumping

$$if\int_{z_{bl}}^{0}\boldsymbol{u}\,dz = if\boldsymbol{M} = \boldsymbol{\tau}_0$$

$$\nabla\cdot\boldsymbol{M} = -\int_{z_{bl}}^{0}\frac{\partial w}{\partial z}dz = w_{pyc} = \frac{1}{f}\nabla\times\boldsymbol{\tau}_0$$

τ_0 is the stress exerted on the ocean surface, modified by ice.
In late summer, ice internal ice forces are typically small and the force balance is approximately

$$\hat{\boldsymbol{\tau}}_0 \approx \hat{\boldsymbol{\tau}}_a - ifd_{\mathrm{ice}}\hat{V}_{\mathrm{wd}}$$

where $\hat{\boldsymbol{\tau}}_a$ is wind stress divided by water density, d_{ice} is ice draft,

and $\hat{V}_{\mathrm{wd}}$ is the wind driven component of ice velocity

For each year of the NCEP-CFSR record, take the daily average wind stress at each grid point in the 1-deg radius circle centered at 75N, 135W, adjust for ice Coriolis force when present, then integrate w_{pyc} over the Aug-Sep-Oct period to get a measure of pycnocline displacement due to Ekman pumping.

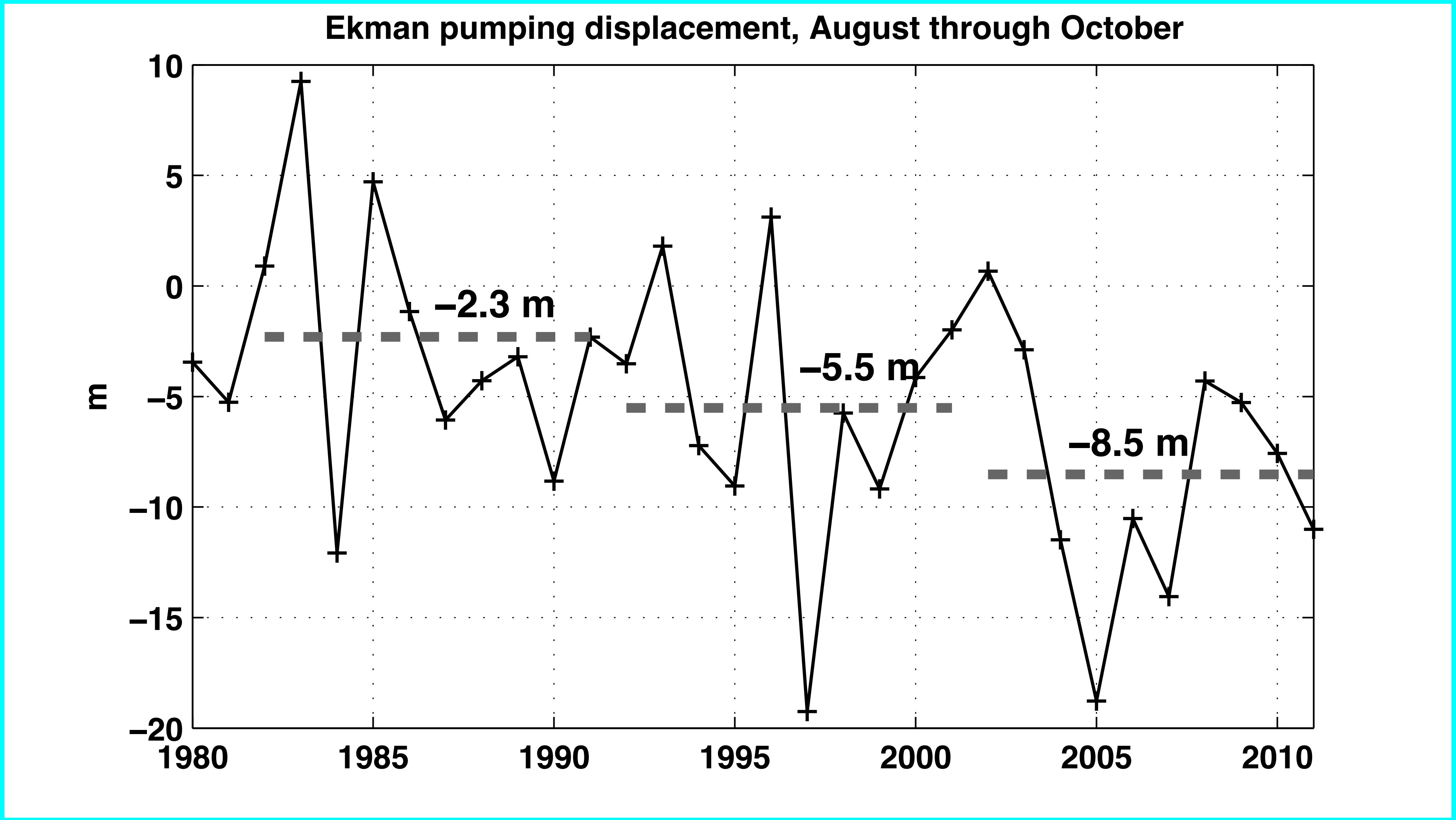

In the first decade of the NCEP-CFSR reconstruction, late summer downwelling occurred below about 75°N, with upwelling in the northern part of the Canada Basin. Average Sep ice coverage was extensive.

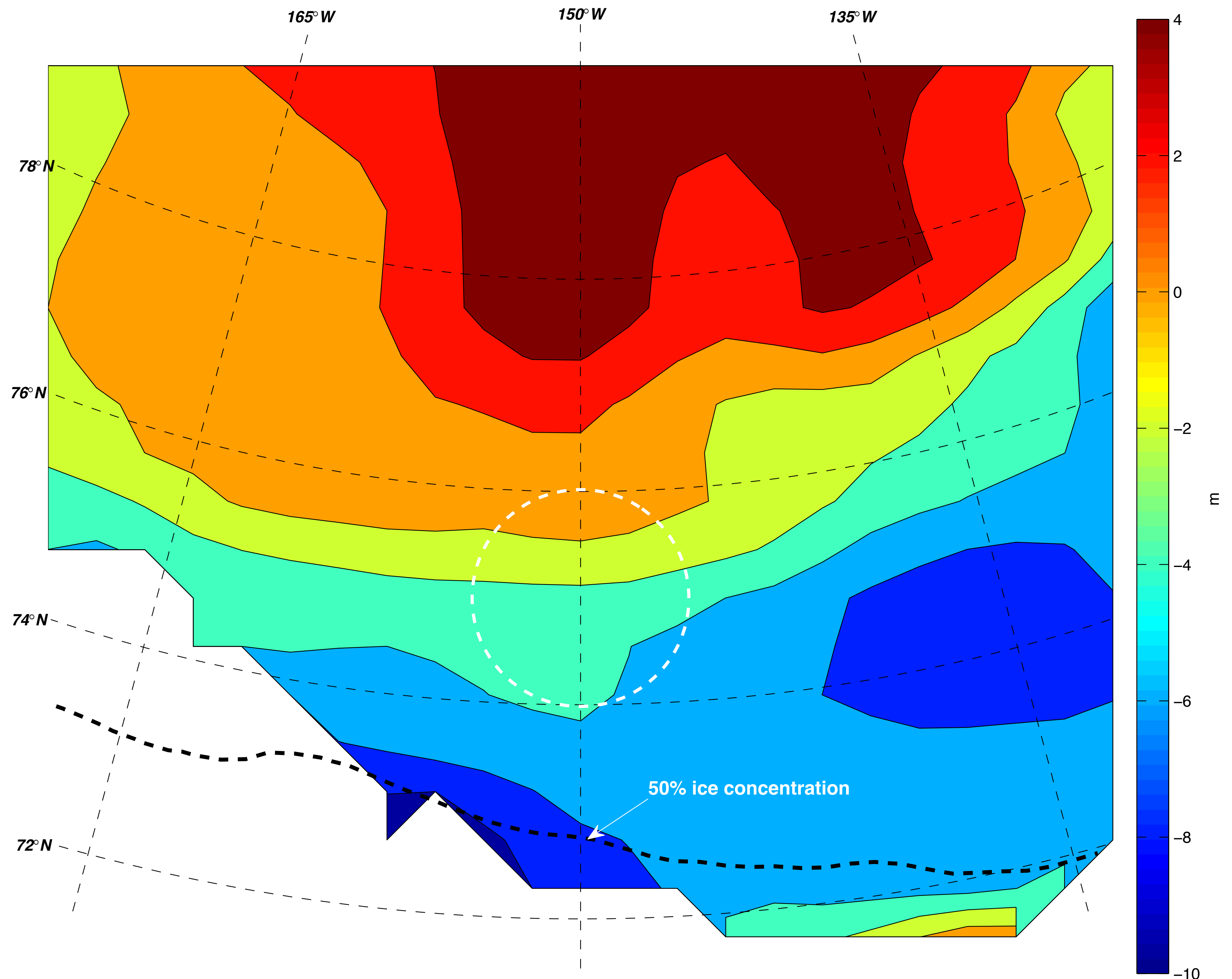

Average ASO Ekman displacement, 1980–1989

In the most recent decade, late summer downwelling occupies the entire Basin. One implication is that the upper ocean in the Canada Basin is a heat *source* rather than sink for the deeper ocean.

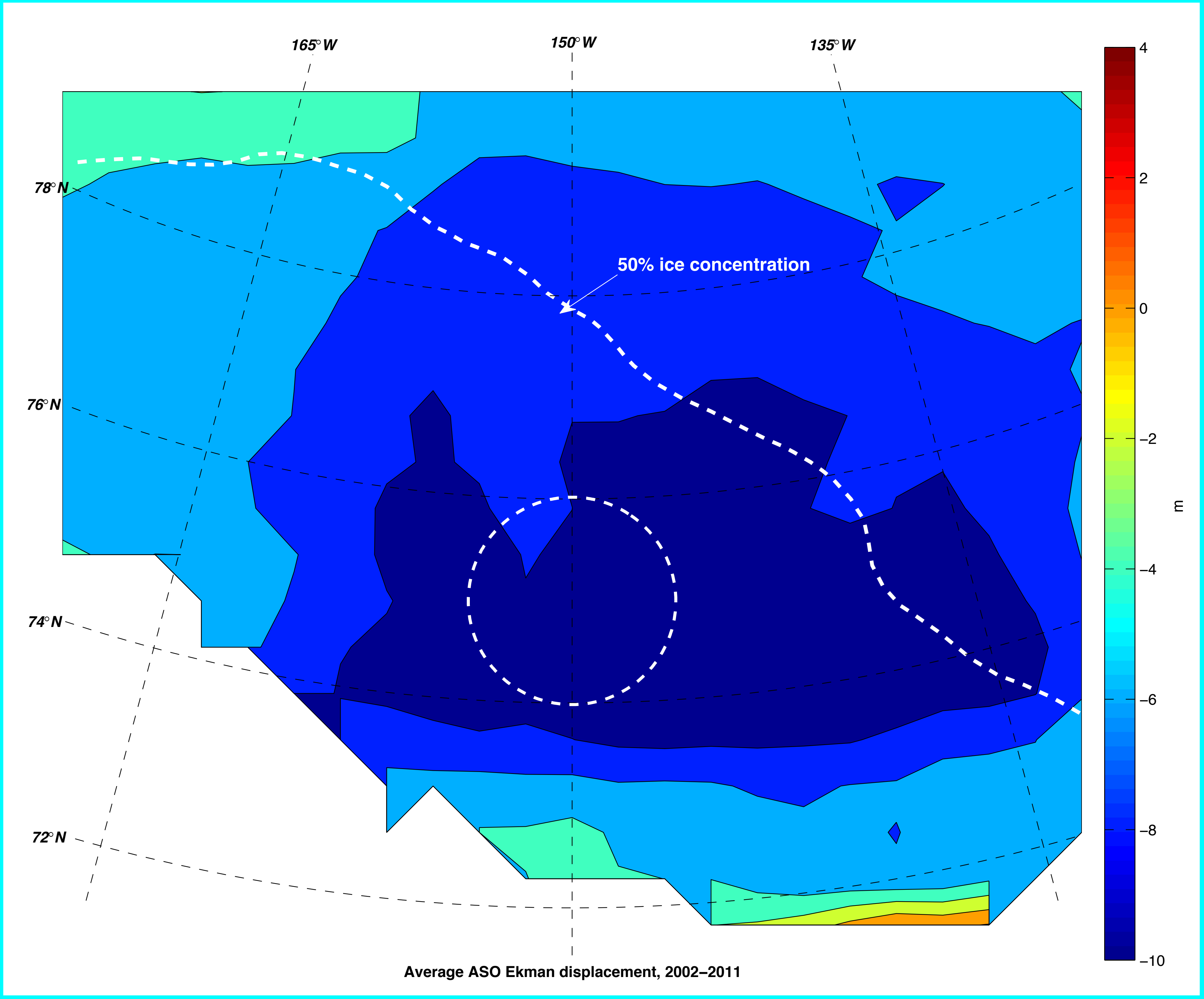

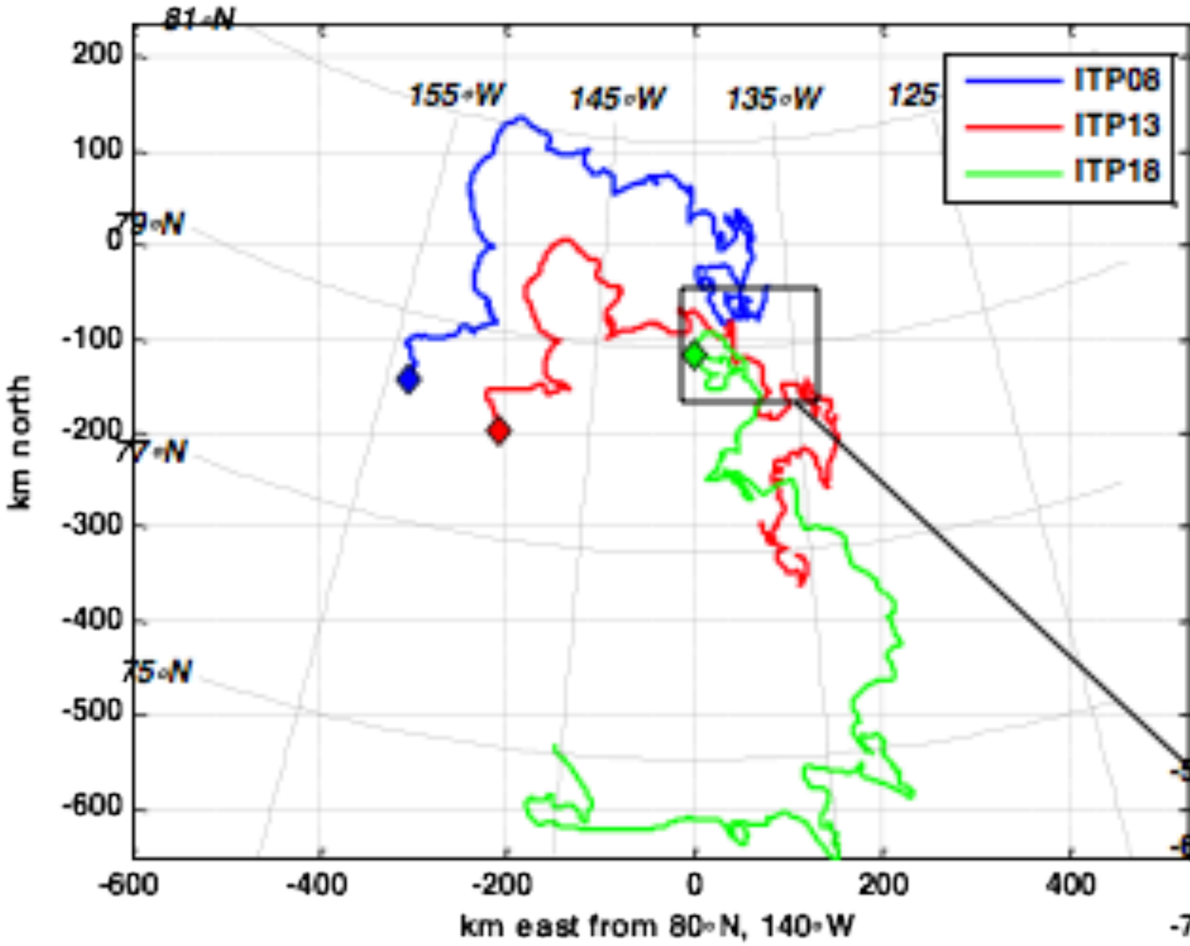

Trajectories of three ITPs in the Canada Basin in 2007 & 2008. There are three periods when separate buoys traversed the same region.

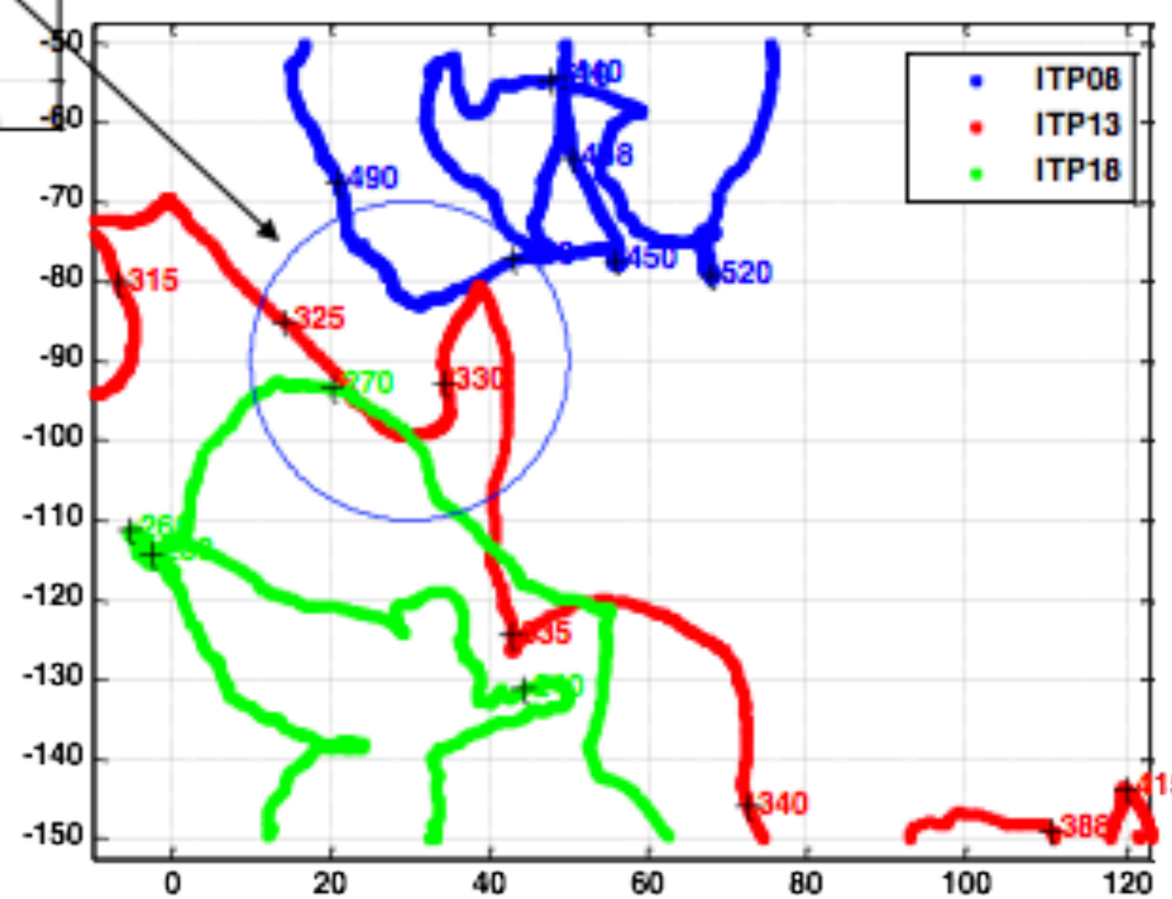

Look at changes the ITPs were within the 20-km radius circle at different times (shown in days of 2007)

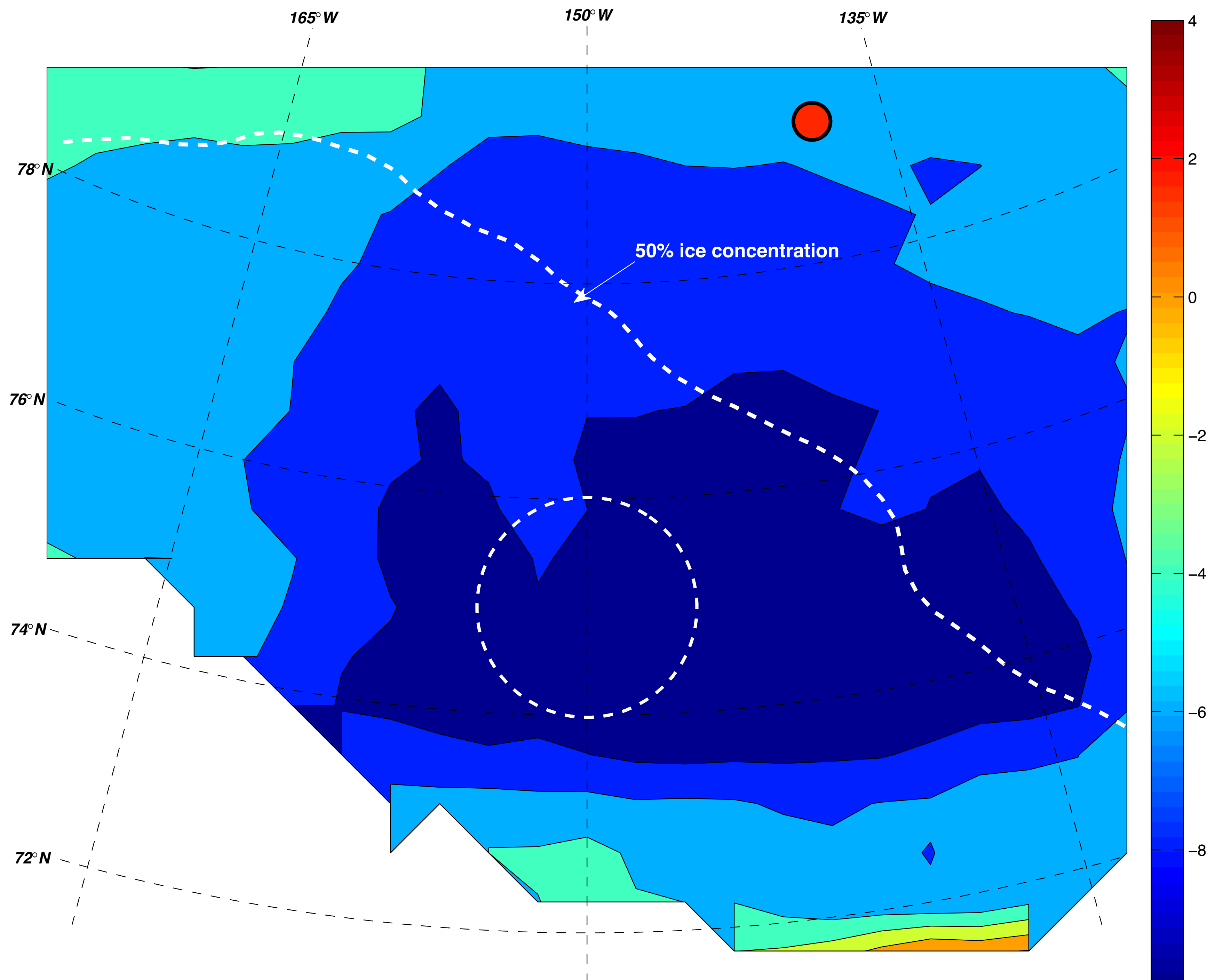

Average ASO Ekman displacement, 2002–2011

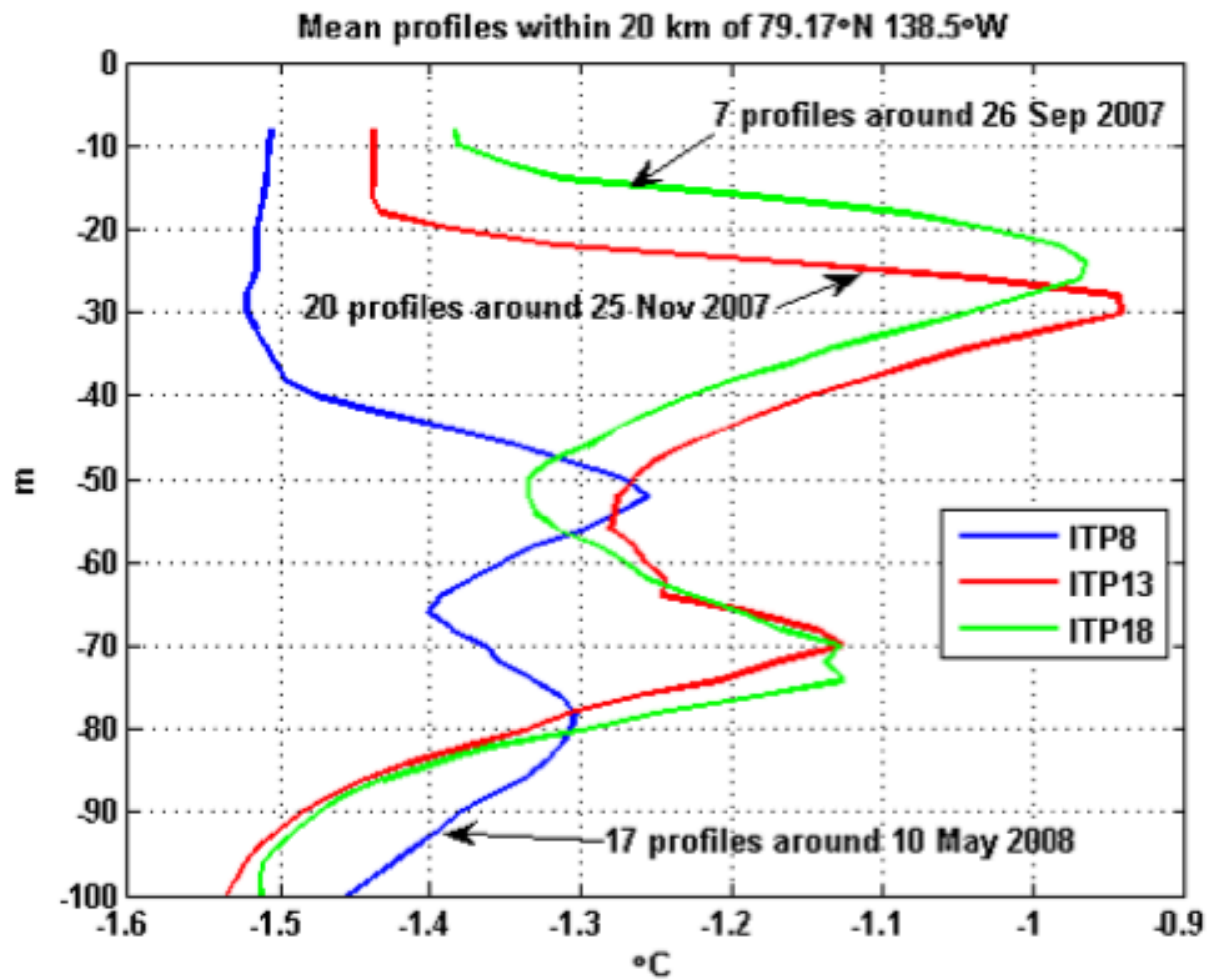

The downward displacement of the upper temperature maximum corresponds to an Ekman pumping velocity of about 3.5 meters per month.


Implications

Implications

Currents on the periphery of the Beaufort Gyre have increased dramatically (5-6 x) in the past few years, particularly just offshore of the Beaufort and Chukchi shelves.

Implications

Currents on the periphery of the Beaufort Gyre have increased dramatically (5-6 x) in the past few years, particularly just offshore of the Beaufort and Chukchi shelves.

The stronger currents may be preventing thick, multiyear ice advected southward on the eastern side of the BG from reaching its interior.

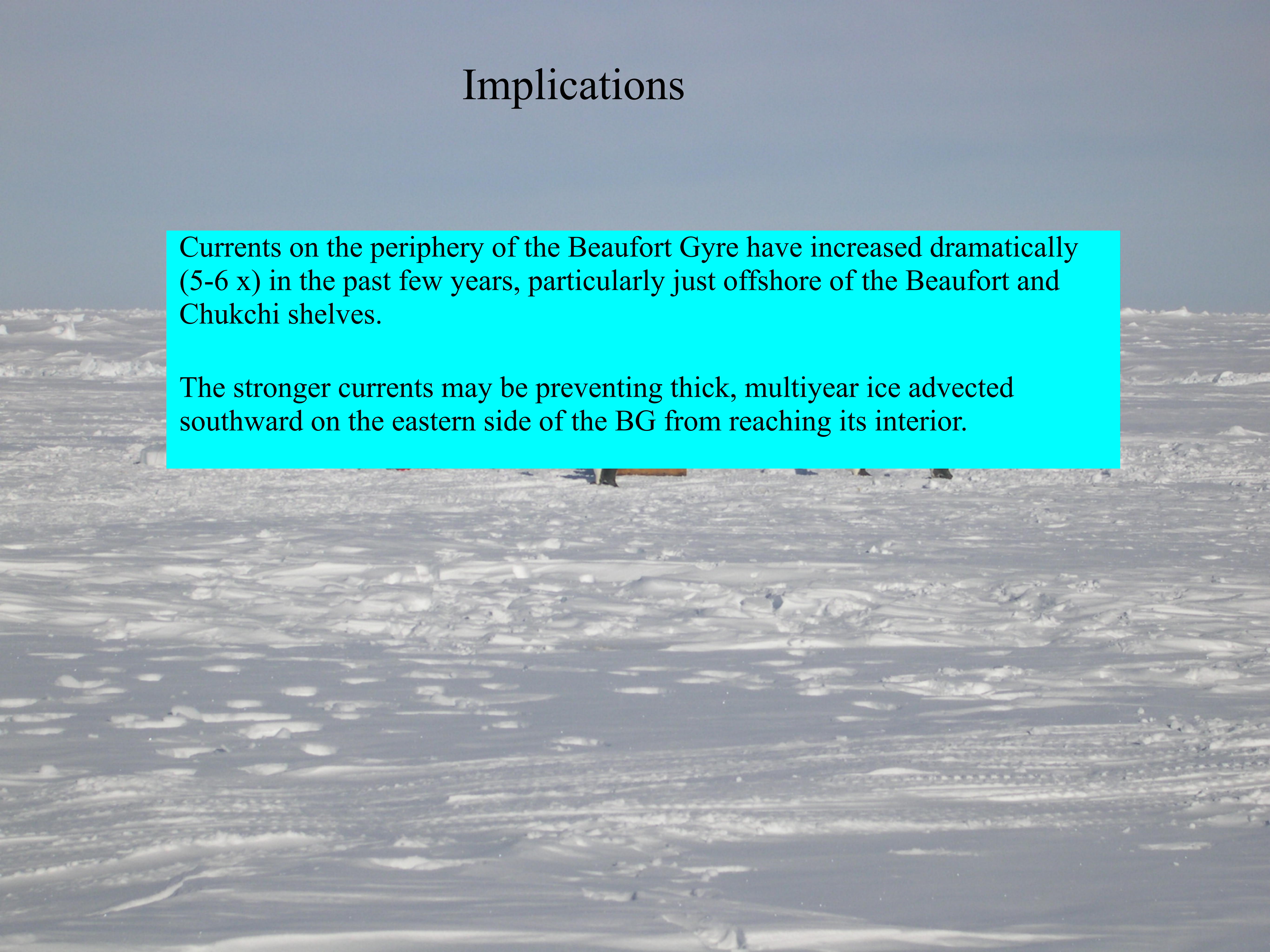

Implications

Currents on the periphery of the Beaufort Gyre have increased dramatically (5-6 x) in the past few years, particularly just offshore of the Beaufort and Chukchi shelves.

The stronger currents may be preventing thick, multiyear ice advected southward on the eastern side of the BG from reaching its interior.

During summer, increased temperature contrast between more open water in the west and southward advection of compact ice in the east may be enhancing late summer anticyclonic atmospheric conditions (and Ekman pumping).

Implications

Currents on the periphery of the Beaufort Gyre have increased dramatically (5-6 x) in the past few years, particularly just offshore of the Beaufort and Chukchi shelves.

The stronger currents may be preventing thick, multiyear ice advected southward on the eastern side of the BG from reaching its interior.

During summer, increased temperature contrast between more open water in the west and southward advection of compact ice in the east may be enhancing late summer anticyclonic atmospheric conditions (and Ekman pumping).

Thus a positive feedback may be at play between convergence of seasonally available fresh water from melting and runoff, and early removal of ice in the western Beaufort Gyre.

Discussion...